Investigating the Re-initiation of Segmentation with Temporally Restricted RNAi in *Tribolium castaneum*

Dissertation
For the award of the degree
"*Doctor rerum naturalium*"
Division of Mathematics and Natural Sciences
of the Georg-August-Universität Göttingen

within the doctoral program Genes & Development
of the Georg-August University School of Science (GAUSS)

submitted by

Felix Kaufholz

from Göttingen, Germany

Göttingen 2020

Thesis Committee

Prof. Dr. Gregor Bucher (advisor)
(University of Göttingen, Johann-Friedrich-Blumenbach Institute for Zoology and Anthropology, Dept. “Evolutionary Developmental Genetics”)

Prof. Dr. Jörg Großhans
(University of Marburg, Abt. “Entwicklungsgenetik und Zellbiologie der Tiere“)

Prof. Dr. Gregor Eichele
(Max-Planck-Institute for Biophysical Chemistry, Dept. “Genes and Behaviour”)

Members of the Examination Board

First reviewer: **Prof. Dr. Gregor Bucher**
(University of Göttingen, Johann-Friedrich-Blumenbach Institute for Zoology and Anthropology, Dept. “Evolutionary Developmental Genetics”)

Second Reviewer: **Prof. Dr. Jörg Großhans**
(University of Marburg, Abt. “Entwicklungsgenetik und Zellbiologie der Tiere”)

Further Members of the Examination Board

Prof. Dr. Christoph Bleidorn
(University of Göttingen, Johann-Friedrich-Blumenbach Institute for Zoology and Anthropology, Dept. “Animal Evolution and Biodiversity”)

Prof. Dr. Gregor Eichele
(Max-Planck-Institute for Biophysical Chemistry, Dept. “Genes and Behaviour”)

Prof. Dr. Daniel Jackson
(University of Göttingen, Geoscience Centre, Dept. “Evolution of the Metazoa”)

Dr. Nico Posnien
(University of Göttingen, Johann-Friedrich-Blumenbach Institute for Zoology and Anthropology, Dept. “Developmental Biology”)

Date of Submission: 2020/05/25
Date of Oral Examination: 2020/07/06

Declaration

I hereby declare that the doctoral thesis entitled

"Investigating the Re-initiation of Segmentation with Temporally Restricted RNAi in *Tribolium castaneum*"

has been written independently and with no other sources and aids than referenced

Göttingen, May 25th 2020 _____

Felix Kaufholz

Für Natascha und Reya.
Für meine Eltern.

Danksagung

An dieser Stelle möchte ich die Gelegenheit nutzen mich bei all den Menschen zu bedanken, dich mich innerhalb der letzten 3½ Jahre unterstützt haben.

An vorderster Stelle möchte ich mich natürlich bei Gregor Bucher bedanken. Seit ich ihn im Invertebraten-Praktikum während des DNB-Masters (anno datio 2015?) auf eine Laborrotation angesprochen habe, hat er mich wissenschaftlich und später auch privat stets unterstützt. Er hat mir, mit hoffentlich bleibenden Folgen, wissenschaftliches Arbeiten (noch) nähergebracht. Er war ein stets loyaler, wissenschaftlicher Betreuer, der aber auch nicht davor zurückgeschreckt ist, mir ein, zwei Mal deutlich zu sagen, was Sache ist. Während gesundheitlich eher durchwachsenen Zeiten hat er sich nie in meinen Weg gestellt, sondern stattdessen viel dafür getan, dass es mir und damit auch meiner Arbeit besser geht. Und auch wenn ich es im Gegensatz zu vielen anderen nie voll ausgenutzt habe: er war immer für eine Diskussion über Politik, dies und das, und alles andere auch zu haben. Vielen Dank dafür!

Weiterer, vor allem wissenschaftlicher Dank geht an die beiden weiteren Mitglieder meines Thesis Committees: Prof. Dr. Großhans und Prof. Dr. Eichele. Die beiden haben selbst aus dem manchmal aus mir hervorsprudelnden Ergebnis-Wust immer noch verstehen können was ich ihnen mitteilen wollte. Auch haben sie Gregor und mich ein-, zweimal an der richtigen Stelle gebremst und unsere Aufmerksamkeit in die richtige Richtung gelenkt. Dafür mein aufrichtiger Dank!

Weiterer Dank geht an die PIs der Abteilung Entwicklungsbiologie: Ernst, Nico, Sigrid, Gerd, anfangs noch Niko und später dann Ufuk. Ihr habt oftmals zur richtigen Zeit die richtige Frage gestellt und dabei teilweise den Finger schön in die Wunde gelegt, so wie es halt manchmal sein muss. Und dennoch (oder gerade deswegen?) habe ich meine Zeit in der Abteilung Entwicklungsbiologie genossen.

Und wenn ich schon mal bei der Abteilung bin: weiterer Dank geht natürlich und vor allem an Labor 3. Hier wurde ich mit offenen Armen als „kleiner doofer Student“ aufgenommen und habe sehr viel lernen dürfen. Sowohl wissenschaftlich als auch menschlich. Daher vielen Dank an Janna, Magdalena, Salim, Salim, Max, Vera, Bicheng, Yonggang, Marita, Dominik, Jürgen, Dani und besonderer Dank an Claudia und Elke. Sehr dankbar bin ich auch Peter, der die Ehre (oder sowas) hatte mir *Tribolium* als Modellorganismus näher zu

bringen. Und mit dem ich mich die ganze Zeit über hervorragend verstanden habe: Danke für die Biere und interessanten Unterhaltungen! Weiterer Dank geht an meine Studenten, denen sowohl ich (hoffentlich) als auch sie mir etwas beigebracht haben. Danke an Rachel, Anka, Susanne, Julia und (nochmal) Dominik.
Außerdem natürlich vielen und herzlichen Dank an alle anderen Mitglieder der Abteilung. Egal ob Bachelor- oder Masterstudent, Doktorand, Postdoc, im Sekretariat oder TA: Vielen, vielen Dank. War sehr schön mit euch.
Und dann gab es natürlich noch die Leute aus dem Labor, die weitaus mehr geworden sind. Danke daher an Felix, für so ziemlich alles und vor allem dafür, dass du immer wieder gezeigt hast, dass es ein Leben neben dem Labor gibt. Und natürlich dafür, dass du mir quasi Natascha vorgestellt hast, die ich zwar schon vorher kannte, aber immer Angst vor ihr hatte. Und wir wissen ja wie das ganze geendet ist.

Aber da es noch mehr als nur Labor gibt, gibt es noch viele weitere und vor allem wichtige Leute denen ich von Herzen danken will.
An vorderster Stelle meiner Familie, die mich stets emotional (und am Anfang des Studiums auch finanziell und kulinarisch) unterstützt hat. Danke Mama und Papa, danke Sophia und Charlotte.
Unendlich viel Dank an Natascha und Reya. Ihr beiden seid mein Ein und Alles und ohne eure Unterstützung bin ich mir sicher, dass ich das nicht durchgestanden hätte. Und Danke dafür, dass Natascha die komplette Arbeit zwei Mal Korrektur gelesen hat!

Weiterer Dank an alle meine Freunde, die es immer wieder ertragen haben, dass ich über Wissenschaft und Käfer geredet habe, wenn wir doch eigentlich was ganz anderes machen wollten. Vor allem Runge, Lisa und Xaver. Ob es nun UFC-Sonntage oder „kurze“ Kneipengänge waren: ihr habt einen großen Teil dazu beigetragen, dass ich Ich bin und auch geblieben bin. Danke auch an Felix L. und Johann und Markus fürs zuhören und einfach mal über was anderes reden!

Am Ende möchte ich mich noch bei mir selbst bedanken: Fürs ewige in-Frage-stellen und Steine-in-den-Weg-legen. Hab es aber ja doch irgendwie geschafft (Kaufholz, 2020).

Contents

List of Figures

List of Tables

1 Summary

Much of the success of arthropods is attributed to their body's segmentation. Segmentation provides various opportunities for nature to evolve new structures without greatly impacting overall fitness of the animal. Most knowledge about the development of segmentation comes from the vinegar fly, *Drosophila melanogaster*. *Drosophila* has a derived long-germ embryogenesis with simultaneous segmentation. Short-germ embryogenesis or sequential segmentation as in the red flour beetle, *Tribolium castaneum*, however, is regarded as a more ancestral state of segmentation. Much less is known about the genetic processes underlying this sequential segmentation. Recently, a segmentation clock was identified in *Tribolium*. This clock utilizes oscillatory expression of the primary pair-rule genes (pPRGs) to pattern the body axis during both the static blastoderm and the elongating germband. The segmentation clock receives input from the upstream "posterior signaling center" and *Tc-caudal* (*Tc-cad*). Downstream of the segmentation clock, the secondary PRGs and the segment polarity genes interpret the pPRG input and provide further positional information along the AP axis. Studies in *Tribolium* revealed great insights into the molecular mechanism of sequential segmentation. However, most of these findings are based on RNAi leading to the permanent knockdown of gene function. Thus, they are not suited for studying gene interactions at later stages of the dynamic process of segmentation and the segmentation clock. I utilized a Viral Suppressors of RNAi (VSR) as a novel tool to temporally restrict RNAi in Tribolium. This novel tool, hsVSR (heat shock VSR), allowed me to investigate the segmentation processes in more depth. Specifically, I aimed to answer the question whether RNAi-induced breakdown of segmentation is irreversible or if re-initiation of segmentation is possible. With proof-of-concept experiments, I

confirmed the functionality and specificity of the hsVSR system to investigate segmentation. I could then show that a rescue of segmentation after RNAi-mediated breakdown is possible by re-initiating the segmentation clock itself. However, rescue of segmentation by inhibiting RNAi of upstream factors of the segmentation clock was not possible. Once the “posterior signaling center” is lost, it cannot re-initiate. Additionally, a possible negative autoregulation of the pPRG *Tc-even-skipped* was uncovered. Taken together, I showed the functionality of the hsVSR system during segmentation. I identified the level at which RNAi inhibition can rescue segmentation within the segmentation process and provided molecular evidence for the nature of the rescue.

2 Introduction

2.1 Segmentation

One of the most obvious and simultaneously striking features of arthropods is their body segmentation, the subdivision of the anteroposterior (AP) body axis into serially repeating yet often morphologically distinct units (Hannibal and Patel, 2013). There are two other big clades of metazoans that show segmentation: the annelids and the vertebrates. In the former, the segmentation is as obvious as it is in the arthropods. In vertebrates, it is less obvious since the initial segmented structure, the somites, are not visible from the outside. The debate about whether or not segmentation is an ancestral feature of the urbilateria is ongoing (Budd, 2001; Clark et al., 2019; Davis and Patel, 1999; Graham et al., 2014; Peel and Akam, 2003). To better understand the evolution of segmentation and its possible origin(s), it is necessary to first understand the genetic and molecular processes governing the segmentation process itself. In vertebrates, quite a bit is known about the underlying mechanisms and signaling controlling segmentation (reviewed in Bénazéraf and Pourquié, 2013; Hubaud and Pourquié, 2014). In insects, most of what we know about segmentation was found out in *Drosophila melanogaster* (henceforth *Drosophila*), the prime arthropod model organism (Akam, 1987; Alberts et al., 2002; Gilbert, 2000). *Drosophila*, however, shows a rather derived mode of embryogenesis (Davis and Patel, 2002; Sander, 1976; Tautz and Sommer, 1995). Studies in other insect and arthropod models, especially in the last decade and a half, revealed quite a level of conservation of embryogenesis and even similarities to vertebrate segmentation, albeit only on a mechanistic level (Choe et al., 2006; Clark and Peel, 2018; Clark et al., 2019; El-Sherif et al., 2012; Paese et al., 2018; Peel and Akam, 2003; Peel et al., 2005; Richmond and Oates, 2012; Sarrazin et al., 2012; Schönauer et al., 2016; Stollewerk et al., 2003).

In the following introduction, I will first give a brief overview of vertebrate segmentation, mainly due to the commonalities in the segmentation mechanism that might be shared between them and arthropods: the segmentation clock. Then, a more in-depth introduction of insect segmentation with a focus on the segmentation process of *Tribolium castaneum* (henceforth *Tribolium*), the red flour beetle is given. This will include the current (and rather new) models to explain *Tribolium* segmentation. This is followed by a paragraph about the appeared conservation of a common segmentation network within arthropods

and possibly beyond, to appreciate the importance of the study of segmentation processes in a diverse range of animals.

2.1.1 Vertebrate segmentation

The segmental unit of vertebrates are the somites. These are blocks of mesodermal tissue derived from the so-called presomitic mesoderm (PSM) that are located on both sides of the neural tube of developing vertebrate embryos. Somites will give rise to, among other things, the vertebrae. The development of this segmental patterning involves a molecular oscillator, the so-called segmentation clock. Its presence was already theoretically predicted with the "clock-and-wavefront" model (Cooke and Zeeman, 1976). Later, also molecular evidence in the form of periodic or oscillating expression of multiple genes linked by intercellular signaling was found (Horikawa et al., 2006; Palmeirim et al., 1997a).
In summary, there are two opposing gradients along the AP (or caudorostral) axis, retinoic acid from anterior and fibroblast growth factor (FGF) and Wnt signaling from posterior. The determination front is basically the intersect of the opposing gradients and travels from anterior towards posterior during axial elongation. Within this field, gene expression of the clock genes oscillates while the frequency of oscillation depends on the gradients. The phase of the oscillation is linked from cell to cell by Delta-Notch signaling. Due to the gradient of the FGF and Wnt signaling, the expression of the segmentation clock genes appears to move along the AP axis from posterior towards anterior. The oscillation slows and finally freezes as it reaches the determination front and there, a new somite boundary (i.e segment border) is formed. The retinoic acid gradient, and with it the determination front moves posterior and the next wave of the segmentation clock oscillation travels long the AP axis towards it. This process is repeated to form consecutive somites along the AP axis (Maroto et al., 2012).

2.1.2 Segmented arthropod body Bauplan

Much of the success of arthropods, both evolutionary and ecologically speaking, is probably due to their segmented body Bauplan. It enables natural selection to tinker with form and function of a single (or in some cases, multiple) segments and their appendages without disturbing the others and decreasing the fitness of the whole organism. The resulting flexibility gave rise to a true plethora of specialized and morphologically divers modes of

sensing, feeding, and locomotion and many more (Davis and Patel, 1999; Grimaldi and Engel, 2005; Hannibal and Patel, 2013; Prpic and Damen, 2008; Tautz, 2004). The Euarthropoda, the "true arthropods" are made up of three extant groups: the Chelicerata (like spiders, mites and scorpions), the Myriapoda (millipedes and centipedes) and the Pancrustacea (crustaceans and insects). The insects, with more than a million described species, are the most numerous among them (Chapman, 2009) and do show a vast number of segmental appendage adaptations. However, the presence of their appendages is mainly limited to the head and thorax segments, while the abdominal segments are (with a few exceptions, like reproductive appendages) appendage-free. Also, the number of body segments within the Insecta is rather stable. It usually consists of at least two pre-gnathal segments (ocular and antennal – the nature of the labrum as either a segment (Schmidt-Ott and Technau, 1992; Schmidt-Ott et al., 1994) or a non-segmental part of the head (Haas et al., 2001; Posnien et al., 2009b) remains disputed), the intercalary segment, three gnathal segments (mandibles, maxillae, labium), three thoracic segments (pro-, meso, and metathorax) and 10-12 abdominal segments. The embryonic development that leads to this stable body plan can, however, vary quite extensively and further be divided into two different modes, long- and short-germ embryogenesis.

2.1.3 Long- vs. short-germ embryogenesis

Among arthropods, *Drosophila* is the best studied model organism. It develops as a long germ embryo, which originally meant that the embryo itself takes up most of the space within the blastoderm, leaving only very little room for extraembryonic tissue (Fig. 2.1A) (Sander, 1976). It also became synonymous for embryos that pattern all their segments more or less at the same time, often before the onset of gastrulation and germband extension/elongation. The mode of long germ embryogenesis is considered a derived mode of development (Davis and Patel, 2002; Peel et al., 2005; Tautz and Sommer, 1995). However, it appears to have evolved multiple times within the insects. A more ancestral and commonly used mode is short-germ embryogenesis (Sander, 1976). According to the older definition[1], short germ embryos only take up a limited (but rather variable) space

[1] Sander (Sander, 1976) and others (Davis and Patel, 2002) have distinguished between, short-, intermediate- and long-germ embryos, often based on both the ratio germband to blastoderm size and mode of segmentation. In recent years, often only a distinction between short- and long-germ embryos is made.

within the whole egg (Davis and Patel, 2002). Short germ insects only pattern a few anterior segments in the blastoderm stage. The more posterior segments are patterned sequentially from anterior to posterior in the germband stage from a segment addition zone (SAZ)[2]. Recently, the terms long- and short-germ embryogenesis to describe modes of segmentation were replaced by "simultaneous" and "sequential" segmentation, respectively, to distinguish them from the previous, more morphological terms (Clark et al., 2019).

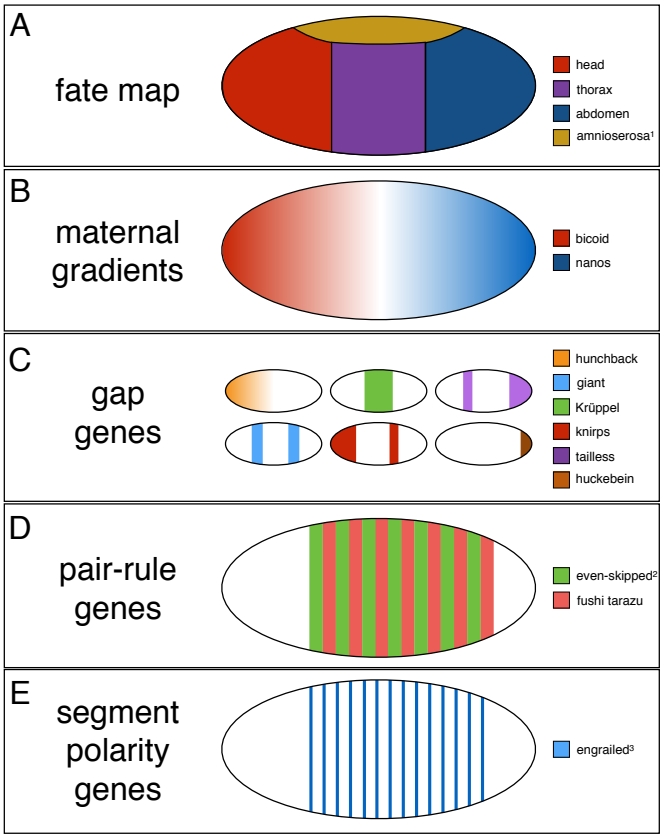

Figure 2.1 – The Drosophila fate map and segmentation cascade

Drosophila develops as a long-germ embryo, therefore the germ Anlagen and primordia for all future body regions are determined during the blastoderm stage (A). The hierarchical and simultaneous segmentation cascade in *Drosophila* starts with maternal gradients from anterior and posterior (exemplified by *bicoid* and *nanos* expression in B). Gap genes expressed in broad and partially overlapping domains spanning multiple segment primordia and are positioned by both maternal gradient and regulations between themselves **(C)**. The gap genes activate the pair-rule genes (primary and secondary) in seven two-segment periodicity stripes (some of which later become segmental; exemplified in the scheme by *even-skipped* and *fushi tarazu* expression) (D). Lastly, the segment polarity genes (exemplified by *engrailed* expression) are activated to define the (para-)segment borders and maintain them (E). (based on Gilbert, 2000; Martin and Kimelman, 2009)

2.1.4 Segmentation in *Drosophila*

Drosophila has contributed widely to the understanding of biological and developmental mechanisms. One of the prime achievements of *Drosophila* research was a saturated screen that identified many of the genes involved in patterning of the *Drosophila* embryo

[2] The previously used term "growth zone" fell out of favor since it implies that growth (i.e. proliferation) plays a dominating role during segmentation and germ band elongation when in reality it is only one of several processes important in elongation and (subsequent) segmentation (Janssen et al., 2010)

(Nüsslein-Volhard and Wieschaus, 1980). Most research into segmentation of insects or even arthropods can be back-traced to this initial publication and its follow-ups.

In broad strokes, the *Drosophila* genetic cascade controlling its simultaneous segmentation can be subdivided into four more or less hierarchical levels: (1) the maternal effect genes, (2) the gap genes, (3) the pair-rule genes (PRGs) and (4) the segment polarity genes (Fig. 2.1B-E). The Hox genes are required for segment identity and not involved in the segmentation process per se. This cascade and its molecular components are text-book knowledge and reviewed in more depth elsewhere (Akam, 1987; Alberts et al., 2002; Gilbert, 2000). I will therefore only give a brief overview of the segmentation cascade and some exemplary genes involved to highlight its hierarchical organisation.

Gradients of maternal effect genes set up the AP axis with gene product gradients from both the anterior and posterior poles of the embryo (classified as the “anterior system”, the “posterior system” and the “terminal system”; Fig. 2.1B). The anterior system relies on *bicoid* (*bcd*) while the posterior system is defined by *nanos* (*nos*). *Bicoid* is responsible for the first body axis symmetry break and both instructive for anterior fates while blocking the translation of *caudal* (*cad*), another maternal factor. *Nanos*, together with *cad* is determining posterior (abdominal) fates. Maternal Torso signaling and the resulting MAPK/ERK signaling gradients determine terminal structures.

On the next level, the gap genes (e.g. *hunchback* (*hb*), *Krüppel* (*Kr*), *knirps* (*kni*)) are activated via thresholds and combinations of the maternal gradients in broad and often overlapping expression domains along the AP axis. Their mutual interactions refine their patterns (Fig. 2.1C). The gap gene further subdivide the three fates (head, thorax, abdomen) by regulating both Hox genes and the expression of the pair-rule genes.

The pair-rule genes (PRGs) can be subdivided into two groups, the earlier expressed primary (e.g. *even-skipped* (*eve*), *fushi tarazu* (*ftz*)) and later expressed secondary PRGs (e.g. *paired* (*prd*)). They are expressed via certain combinations of activation and repression by the gap genes via stripe-specific enhancers along the AP axis in a two-segment periodicity. Later cross-regulation among themselves via zebra elements refines their pattern. The PRGs expression is the first indication of the metameric body plan of *Drosophila*. Some PRG later transition into a segmental periodicity.

Lastly, the segment polarity genes interpret the pair-rule gene expression and define (para-)segmental borders as well as maintain them.

2.1.5 Segmentation in *Tribolium*

Although most genetic studies were performed in *Drosophila*, its simultaneous segmentation probably represents a derived mode of segmentation. The question how similar the genetic basis of the different modes of segmentation is, requires studies in more insect species, especially with examples from the more conserved sequential segmentation mode (i.e. short-germ embryogenesis).

Tribolium castaneum, the red flour beetle shows such a sequential segmentation. In the last 20 years, it has emerged as a sophisticated model organism for the study of evolution and development that is second only to *Drosophila* in terms of functional genetic tools (Brown et al., 2009; Schröder et al., 2008). *Tribolium* segmentation can generally be divided into two stages: the blastoderm and the germband stages. During the blastoderm stage roughly ⅓ of the anterior and dorsal tissue become extraembryonic tissue primordia. The ventral-posterior ⅔ of the blastoderm are the germ anlagen (Fig. 2.2A, left-most panel) (Benton, 2018). The head and thorax are (pre-)patterned during this stage, at least on the level of the pPRGs (El-Sherif et al., 2012). The second stage is the germband stage. The germband forms during gastrulation by extensive cell movements (Benton, 2018). During this stage, the germband elongates and the abdominal segments are patterned progressively from a posterior SAZ (El-Sherif et al., 2012; El-Sherif et al., 2015; Sarrazin et al., 2012). This progressive elongation of the germband makes it obvious that (more or less) static expression domains like those found in *Drosophila* blastoderm could not pattern the complete body axis of Tribolium (or any other sequential segmenting insect for that matter). It was therefore assumed that the blastoderm could be patterned similar to the *Drosophila* blastoderm via a hierarchical segmentation cascade while the elongating germband might be segmented using similar mechanisms as in vertebrates (i.e. a segmentation clock) (Peel et al., 2005). However, already during the blastoderm stage of *Tribolium* embryos, a segmentation clock consisting of the pPRGs can be found with pair-rule stripes moving from posterior to anterior. This segmentation clock patterns the head and thoracic segments (Choe et al., 2006; El-Sherif et al., 2012; Schröder et al., 1999). In the germband, the same segmentation clock continues to segment the body axis from the posterior SAZ (El-Sherif et al., 2012; Sarrazin et al., 2012). Secondary pair-rule genes (sPRGs) are expressed later from the anterior SAZ (Choe and Brown, 2007; Clark and Peel, 2018; Davis et al., 2001). The expression of both pPRGs and sPRGs is transient and will fade in the

more anterior (i.e. older) segments (Choe and Brown, 2007; Choe et al., 2006; Clark and Peel, 2018). Ultimately, the segment polarity genes are expressed to define and maintain the (para-)segment boundaries (Brown et al., 1994; Choe and Brown, 2009; Davis et al., 2001; Nagy and Carroll, 1994).

Since one of the central components of segmentation in *Tribolium* is the segmentation clock, in the following paragraphs, I will provide a more detailed overview of the patterning events upstream of the clock, the mechanisms of the segmentation clock itself, and patterning downstream of the clock. After that, I will give an overview of the current models that try to explain sequential segmentation.

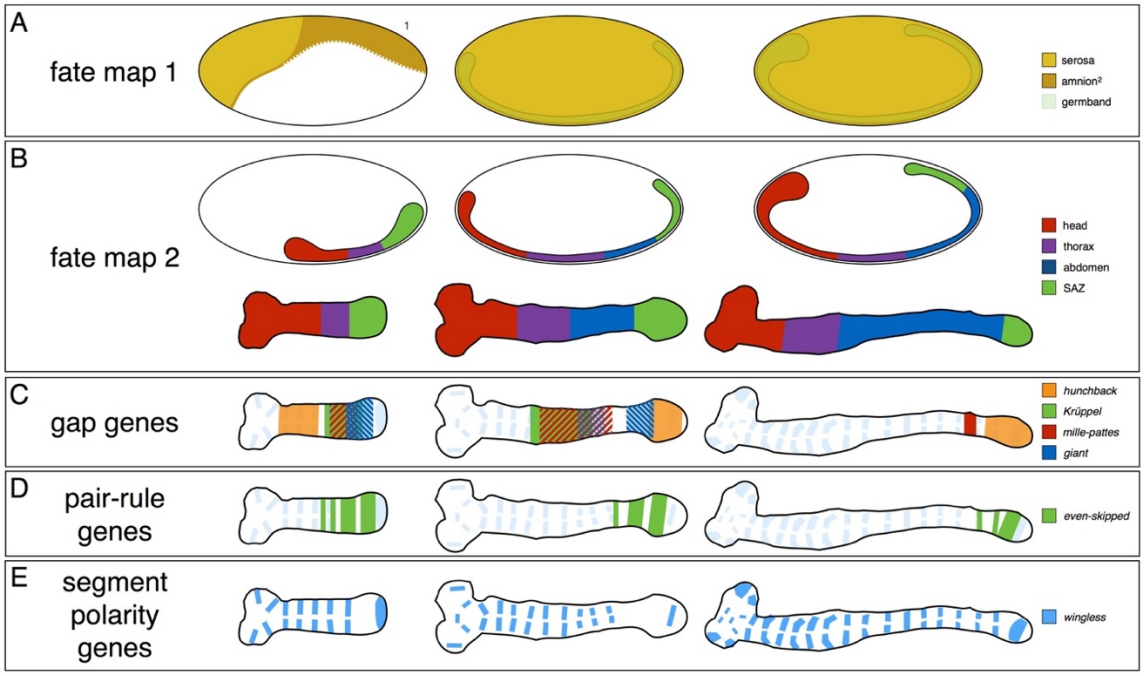

Figure 2.2 – The Tribolium fate maps and axis patterning gene expressions

(A) In contrast to *Drosophila*, in *Tribolium* roughly the anterior and dorsal 1/3 of blastoderm tissue are extraembryonic tissue primordia (amnion and serosa). The former will completely cover the embryo during germband elongation. **(B)** In the sequential segmentation process in *Tribolium*, only head and thorax are patterned during the blastoderm stage. After gastrulation the germband has a posterior segment addition zone (SAZ) from which segments are added progressively during germband elongation. **(C)** During germband elongation, gap genes are expressed in a specific anterior-to-posterior cascade and have no (known) influence on pair-rule gene expression. **(D)** Pair-rule gene (PRG) expression (exemplified by the primary PRG *Tc-even-skipped*) is independent of gap gene expression and emerges from the SAZ, initially in a two-segment periodicity, and later splits into segmental stripes. Primary and secondary PRGs are expressed transiently and activate the segment polarity genes. **(E)** Segment polarity genes (exemplified by Tc-wingless expression) emerge progressively due to activation from the PRGs and define and later maintain the segment boundaries, resulting in a segmented germband. (based on Benton, 2018; Boos et al., 2018; Choe et al., 2006; Martin and Kimelman, 2009; Bucher (unpubl.))

2.1.5.1 Patterning upstream of the segmentation clock

One of the most important early developmental steps is breaking the symmetry of the egg. For this first, important step during embryonic development *Tribolium* is not different from many other metazoans because posterior Wnt signaling is required for this symmetry break (Ansari et al., 2018; Bolognesi et al., 2008b; Martin and Kimelman, 2009). Hand in hand with posterior Wnt signaling goes the expression of *Tc-cad*, forming a gradient from the posterior pole (Copf et al., 2004; Schulz et al., 1998; Schulz et al., 1998). At the anterior pole of the *Tribolium* egg and blastoderm, the Wnt antagonist *Tc-axin* is counteracting the posterior Wnt signaling allowing the expression of anterior fate genes (Fu et al., 2012). Disruptions of these gradients can have drastic consequences for the embryo, like loss of anterior structures in the case of *Tc-axin* (Fu et al., 2012) or axis duplication (Ansari et al., 2018). Posterior Wnt signaling further acts as a "posterior signaling center" for patterning (Oberhofer et al., 2014). *Tc-Wnt8/D*, together with *Tc-wg*, is specifically expressed in the posterior of both blastoderm and germband stage embryos (Bolognesi et al., 2008b). Both *Tc-Wnt8/D* and *Tc-arrow* (*Tc-arr*, a Wnt co-receptor) are necessary for segmentation of the abdomen. Parental RNA interference (pRNAi) of these two Wnt signaling components results in loss of posterior segments in germbands while the head and thorax segments are patterned normally (Bolognesi et al., 2009). However, already established segment polarity stripes fade away during further germband development indicating the loss of segment boundary maintenance function. In cuticles, however, all visible segmentation is lost, most likely since the retraction of the germband is misregulated, possibly due to the (later) loss of segment boundary maintenance (Bolognesi et al., 2008b). Wnt signaling also shows an influence on *Tc-cad* expression (Ansari et al., 2018; Beermann et al., 2011; Oberhofer et al., 2014), which itself influences the expression of both gap and primary pair-rule genes (El-Sherif et al., 2015; Zhu et al., 2017)

Similar to *Drosophila*, the terminal system in *Tribolium* also depends on the Torso signaling (Schoppmeier and Schröder, 2005; Schröder et al., 2000). In *Tribolium* posterior Torso signaling is required for the establishment of the SAZ and therefore posterior segmentation of the germband. It also showed influence of the expression of a gap gene (Schoppmeier and Schröder, 2005).

In stark contrast to *Drosophila*, *Tribolium* pPRGs expression and regulation is probably independent from the gap genes (Marques-Souza et al., 2008). It was even shown that the

gap gene *Tc-knirps* is regulated by the pair-rule gene *Tc-even-skipped* (*Tc-eve*) (Peel et al., 2013). I will not detail the gap gene expressions and current models on their regulation in *Tribolium* since they appear to be less involved in segmentation per se, but rather involved in providing segment identity via the Hox genes. However, one needs to keep in mind that knockdown of the gap genes lead to breakdown of segmentation (either directly or due to halted germband elongation), which is not yet fully understood (Bucher and Klingler, 2004; Cerny et al., 2005; Marques-Souza et al., 2008; Peel et al., 2013; Schröder, 2003).

2.1.5.2 The segmentation clock

One major developmental difference between segmentation in *Drosophila* and *Tribolium* is the presence of a segmentation clock in the latter. In *Tribolium* this clock is necessary for the formation of all gnathal, thoracic and abdominal body segments. While the genes involved in this insect segmentation clock are different from the vertebrate segmentation clock genes, both clocks have converged on using a similar principle, based on a "clock-and-wavefront" system (Cooke and Zeeman, 1976). This system involves (cell-autonomous) oscillating gene expression in an elongating tissue and a traveling wavefront to arrest the oscillation of the clock. This results in repetitive structures along the elongation axis. In *Tribolium*, the oscillating segmentation clock genes are the primary pair-rule genes[3] *Tc-even-skipped* (*Tc-eve*), *Tc-runt* (*Tc-run*), and *Tc-odd-skipped* (*Tc-odd*). Their involvement and necessity for segmentation was shown repeatedly (this work; Choe et al., 2006; El-Sherif et al., 2012; Sarrazin et al., 2012). However, the exact regulatory relationship between the pPRGs (e.g. activation- vs. repression-based) is still discussed (Choe et al., 2006; Clark, 2017; Clark et al., 2019). In *Drosophila* mutants of the pPRGs *eve*, *run* and *odd* are missing half their segments (i.e. every other segment, the "classic" pair-rule gene phenotype). In contrast, parental RNAi knockdown of the pPRGs in *Tribolium* leads to a complete breakdown of segmentation and results in offspring cuticles missing all (in the case of *Tc-eve*) or almost all (in the case of *Tc-run* and *Tc-odd*) segments beyond the pre-gnathum (Choe et al., 2006). The segmentation clock is active in both the posterior of the

[3] The use of the term "pair-rule gene" (PRG) might lead to confusion here. The terms originate from *Drosophila*, where the function of this group of genes was deduced from their mutant phenotypes ("classic" PRG phenotype) (Nüsslein-Volhard and Wieschaus, 1980). This phenotype was caused by their two-segment periodicity expression pattern and the specific loss of structures within this domain. The use of the term "pair-rule gene" in other insects is now mainly based on their two-segment periodicity expression and NOT on their RNAi or mutant phenotype.

blastoderm and in the posterior SAZ in the germband (El-Sherif et al., 2012; Sarrazin et al., 2012). The spatiotemporal dynamics of the clock in both the blastoderm and germband are probably regulated by *Tc-cad* (Ezzat El-Sherif, personal communication; El-Sherif et al., 2015). Segmentation by the segmentation clock is a reiterating process along the AP axis in both the blastoderm and germband. It receives a more or less static posterior input from the "posterior signaling center" via Wnt signaling and *Tc-cad* and has a transient output in the form of pPRG stripes.

2.1.5.3 Patterning downstream of the segmentation clock

The dynamics of the segmentation clock lead to the expression of the pPRGs *Tc-eve*, *Tc-run*, and *Tc-odd* in an initial two-segment periodicity, emerging from the posterior SAZ, along the body axis (Choe et al., 2006; El-Sherif et al., 2012; Patel et al., 1994; Sarrazin et al., 2012). This pattern later resolves into a segmental periodicity probably due to the expression of timing factors (Clark and Peel, 2018). Additionally, a second striped expression pattern consisting of the secondary pair-rule genes (sPRGs) *Tc-paired* (*Tc-prd*) and *Tc-sloppy-paired* (*Tc-slp*) emerges from the anterior SAZ. Both *Tc-prd* and *Tc-slp* are initially also expressed in a two-segment periodicity, but split into segmental stripes with alternating expression intensity during further germband elongation (according to Choe and Brown, 2007). The sPRG expression is controlled by both the pPRGs and the timing factors (Choe and Brown, 2007; Choe et al., 2006; Clark and Peel, 2018) More interestingly, RNAi knock-down of both *Tc-prd* or *Tc-slp* result in classic pair-rule gene phenotypes with every other segments missing (Choe and Brown, 2007), comparable to PRG phenotypes in *Drosophila*. A combination of primary and the secondary PRGs is then responsible for the expression of the segment polarity genes, that determine and maintain the final (para-)segment borders (Choe and Brown, 2007; Choe et al., 2006).

2.1.6 Same genes, different mechanisms (?), same output

As described so far, and from a mechanistical point of view, segmentation between *Drosophila* and *Tribolium* appears to be rather different. In *Drosophila*, all segments are patterned during the blastoderm stage and more or less simultaneously. In *Tribolium*, only the head and thorax are progressively patterned during the blastoderm stage and not all at once. In addition, the posterior segments are pattered in the germband, also in a

progressive fashion from a SAZ. The use of a segmentation clock patterning system in *Tribolium* further distinguishes it from *Drosophila* patterning and actually makes *Tribolium* segmentation, at least in this particular aspect, more similar to vertebrate somite segmentation. Interestingly, despite all these remarkable mechanistic differences, the same set of genes acts as key players controlling germband patterning and segmentation in both species. In accordance, two recently published models suggest that there are indeed more similarities between *Drosophila* and *Tribolium* segmentation than originally thought.

These two, largely complementary, hypothetical models are primarily concerned with the evolvability of short- into long-germ patterning and vise-versa. They are both based on the more general "clock-and-wavefront" model (Cooke and Zeeman, 1976), that was originally proposed in the context of vertebrate somitogenesis.

The "speed regulator model" (Zhu et al., 2017) was originally proposed to explain patterning in both blastoderm-like and germband-like tissues by a posterior "speed regulator" molecule and was mainly tested with the *Tribolium* gap gene cascade. Its mechanism, however, is also applicable to the segmentation clock and the pPRGs (Ezzat El-Sherif, pers. communication; Zhu et al., 2017). The as of yet unnamed "segmentation by timing factors model" (Clark et al., 2019) tries to answer the evolution from a "sequential" segmentation towards "simultaneous" segmentation. This model could show that the key mechanisms of PRG expression and regulation are largely conserved between *Drosophila* and *Tribolium* and orchestrated by a conserved set of "timing factors"(Clark, 2017; Clark and Akam, 2016; Clark and Peel, 2018). In the following few paragraphs I will give a brief introduction of each model and point out the information most relevant for this work.

1. Speed Regulator model

In the "speed regulator model", the concentration of the speed regulator molecule has influence on the oscillation of the clock (Fig. 2.3A and B). In the blastoderm, the speed regulator molecule forms a gradient along the AP axis (Fig. 2.3C, "Blastoderm"; Fig. 2.4, "Blastoderm"). Because of this gradient, cells in the posterior will oscillate faster than those in the anterior, resulting in a wave-like expression pattern of the pPRGs towards anterior along the AP axis (Fig. 2.3C, "Blastoderm"; Fig. 2.4, "Blastoderm"). These particular

expression waves were indeed observed for *Tc-eve* in the blastoderm (El-Sherif et al., 2012). In the germband, the "speed regulator" molecule does not form a gradient but a stable expression domain in the posterior (Fig. 2.3 C, "Germband"; Fig. 2.4, "Germband"). Therefore, the clock in this posterior domain is oscillating at a constant speed. The phase of the clock (i.e. the expressed pPRG) starts to freeze upon leaving the posterior domain due to axial elongation. *Tc-cad* was predicted to be this posterior speed regulator because it on the one hand, shows compatible expression in the *Tribolium* germband (Copf et al., 2004; Schulz et al., 1998) and on the other hand it has a fitting influence on the spatiotemporal expression of the pPRGs (Ezzat El-Sherif, personal comm.; El-Sherif et al., 2015) and the gap gene cascade (Zhu et al., 2017).

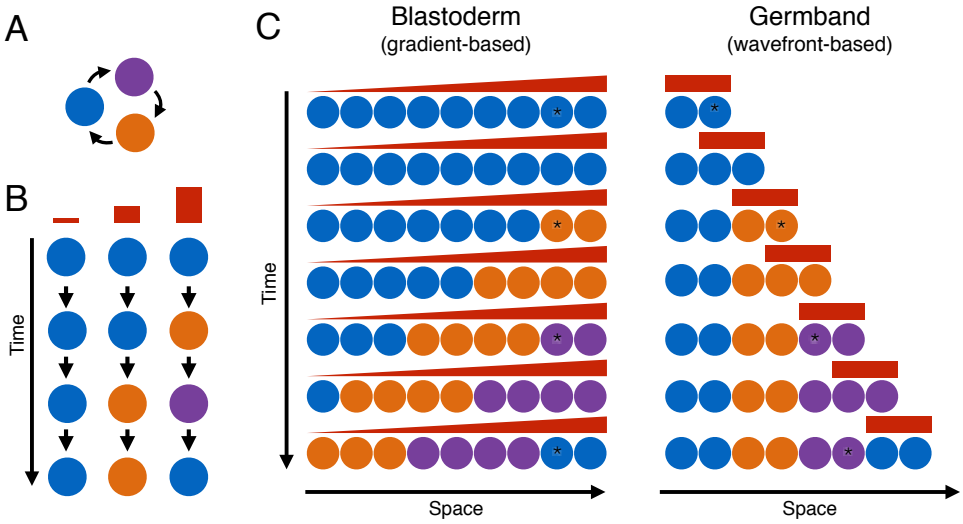

Figure 2.3 – The "speed regulator" model I

The speed regulator model describes patterning along both a fixed (blastoderm-like) and an elongating (germband-like) tissue axis. **(A)** The basis of this model is a genetic network that enables a cell to express genes in a cascade and transition from one state to the next (in the case of the pPRGS, oscillation of three factors). **(B)** The oscillation speed is dependent on the concentration of the speed regulator molecule, with little to no molecule leads to no oscillation while high concentrations lead to fast oscillation. **(C)** In the blastoderm, the speed regulator forms a gradient, so cells in the posterior oscillate faster than cells more anterior. This differences in oscillation speed in each cell along the AP axis forms waves of gene expression propagating from posterior to anterior, patterning the blastoderm. In the germband, the speed regulator molecule does not form a gradient but is restricted to a posterior domain. Cells in this domain will oscillate and transition from one state to the next (see A) with a constant speed, but will arrest in a specific state upon leaving the posterior speed regulator domain due to axial elongation. The posterior shift of the posterior domain is relative to the rest of the germband. The asterisk marks a hypothetical cell during both blastoderm and germband patterning, see text more for details. Note: the arrows in (A) are only indented to show progression from one state to the next (i.e. oscillation) and do not represent a regulatory relationship. (modified from Zhu et al., 2017).

To further illustrate the model: a hypothetical cell is located in the posterior blastoderm (asterisk in either Fig. 2.3C or 2.4, “Blastoderm”). Due to the concentration of the “speed regulator” molecule, the segmentation clock genes in this cell oscillate. The segmentation clock in cells more posterior oscillates faster while it oscillates slower in cells more anterior (if at all). Through time, this will lead to “progressive” waves of clock gene expression from posterior to anterior (Fig. 2.3C or 2.4, “Blastoderm”). The marked cell will express each of the clock genes multiple times as each wave passes from anterior to posterior. The phases of the clock (i.e. the currently expressed pPRG) will arrest, probably due to loss of speed regulator expression during/after gastrulation and the final positional information of the cell is provided. After germband formation, another hypothetical cell (again marked by an asterisk in either Fig. 2.3C or 2.4, “Germband”) “starts” in the posterior SAZ, expressing the segmentation clock due to activation by the “speed regulator”. This cell will leave this posterior domain through axial elongation of the germband that shifts the “speed regulator” expression domain more posterior in relation to the rest of the embryo. The cell will then transiently become part of the anterior SAZ, where the clock phase is arrested by the wavefront. The exact molecular nature of the wavefront is debated, but it is situated at the boundary of the posterior and anterior SAZ. The cell will subsequently end up in the segmented germband. Depending on the time at which a cell will leave the posterior SAZ, it will arrest in a different state, i.e. a different pPRG expression or stripe. For any given cell in the SAZ, this process is repeated until patterning and axial elongation stop. The cells then have received their positional input and the germband is fully segmented.

While the “speed regulator” model is based on and was tested with the aperiodic *Tribolium* gap gene cascade, according to its authors it is also applicable to the segmentation clock (i.e. oscillating gene expression).

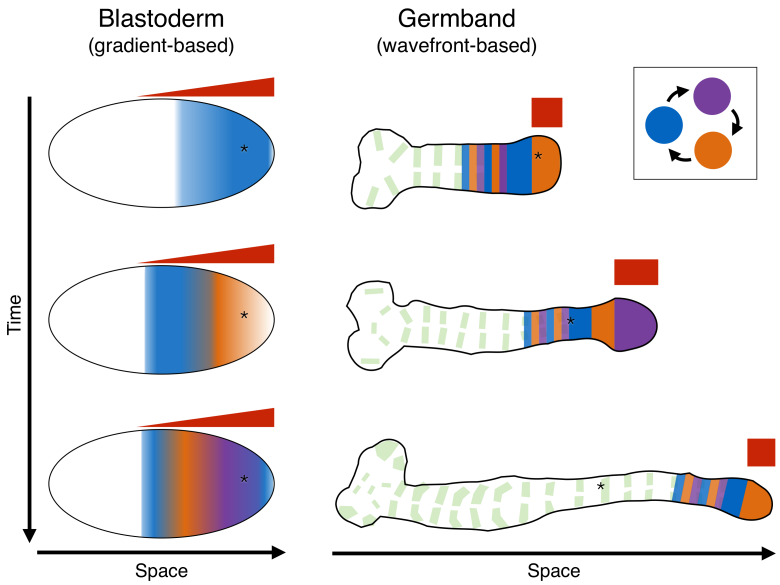

Figure 2.4 – The "speed regulator" model II

This figure also represents the speed regulator model as in Fig. 2.3, but directly applied to the topology of a *Tribolium* embryo and the expression of the pPRGs during both blastoderm and germband stages. The speed regulator molecule forms a posterior-to-anterior gradient in the blastoderm and a posterior expression domain (in the SAZ) during the germband stages. The asterisk marks a hypothetical cell during both blastoderm and germband patterning, see text more for details. Note: as in Fig. 2.3, the arrows in the small top-right panel do not represent regulation, but the ability to progress for one stage to the next (oscillate). (based on Zhu et al., 2017)

2. Timing Factor model

The second model (Clark et al., 2019), that I called “segmentation by timing factors” is based on recent work from Clark (2017) and Clark and Peel (Clark and Peel, 2018). In it they argue that the important steps of segmentation and their regulation are largely conserved, but are shifted in time or place (Fig. 2.5 C) between *Drosophila* and *Tribolium*. These stages are defined as (1) the early (or “upper”) pair-rule gene network (pPRGs), (2) the late (or “lower”) pair-rule gene network (sPRGs), and (3) the segment polarity network. While these stages in *Drosophila* are sequential, more or less occurring one after the other and in line with its hierarchical segmentation cascade, the same stages need to occur all at once in different regions along the AP axis of *Tribolium* (see Fig. 2.5C). These stages are regulated by a conserved set of “timing factors” (Fig. 2.5A) and represent the aforementioned wavefront. The expression of each timing factor ((*Tc*-)*cad*, (*Tc*-)Dichaete and (*Tc*-)*odd-paired* ((*Tc*-)*opa*)) correlates with each stage either temporally (*Drosophila*) or spatially (*Tribolium*) (see Fig. 2.5C). The early PRG network represents the segmentation clock in the posterior of the *Tribolium* SAZ (and comparable to the function of the zebra elements in *Drosophila*). This stage is controlled by (*Tc*-)*cad* (and (*Tc*-)*Dicheate*) and

provides the phases of the different PRGs to be expressed along the AP axis (comparable to what the speed regulator is proposed to do). The second stage, the late PRG network, is the pattern resolution stage of the pPRGs in *Tribolium*, as they emerge from the posterior SAZ. During this stage, the pPRG stripes are splitting and secondary pair-rule genes are being expressed. This stage is controlled by (*Tc*-)*Dichaete* alone (and is comparable to the 7-to-14 stripe transition in *Drosophila*). The third and last stage, the segment polarity stage, occurs anterior to the SAZ in *Tribolium* and corresponds to the segmented and now also extended *Drosophila* germband. This stage is controlled by (*Tc*-)odd-paired.

Due to the overall evidence of the necessity of posterior Wnt signaling for segmentation, I further included a "posterior signaling center" (Fig. 2.5A) controlling the spatiotemporal regulation (or at the very least *Tc-cad*, for which there is ample evidence (Ansari et al., 2018; Beermann et al., 2011; Oberhofer et al., 2014))

Again, to illustrate the model: A hypothetical cell (asterisk in Fig. 2.5) in the posterior SAZ starts under the influence of *Tc-cad* (and *Tc-Dichaete*) and the segmentation clock is active in this cell. Upon leaving the posterior SAZ, the cell is now only under the influence of *Tc-Dichaete* in the anterior SAZ and the segmentation clock phase freezes (i.e. one PRG remains expressed) and sPRGs are expressed based on the cell's pPRG expression. Entering the non-SAZ *Tc-opa* domain, the segment polarity genes become expressed. The positional information previously obtained is now translated into a segmental position. Repeating this process with every cell in the SAZ will result in a segmentally patterned germband.

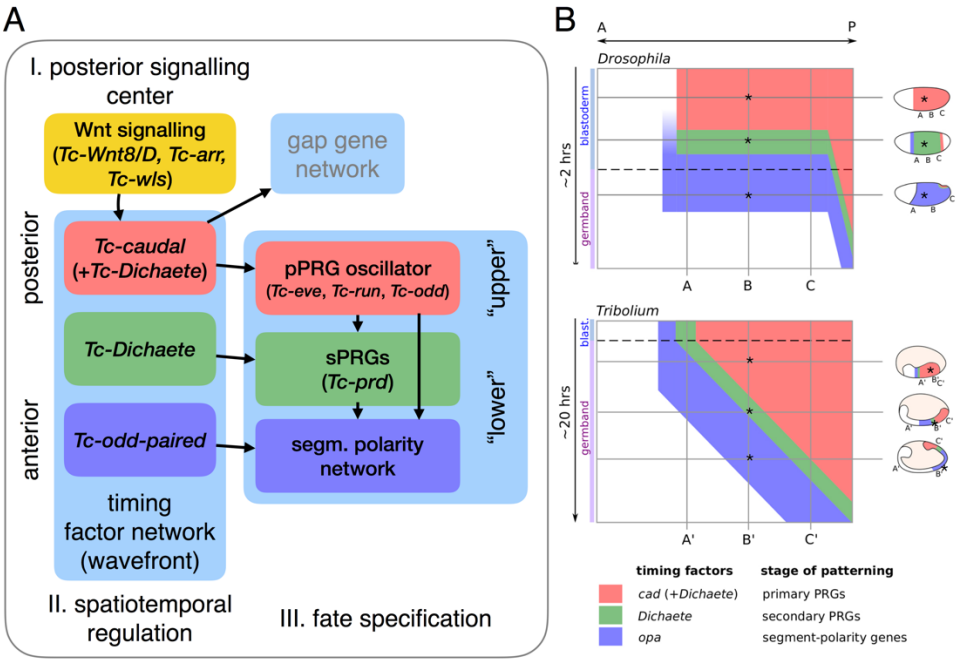

Figure 2.5 – The "timing factor" model

(A) The three stages of *Tribolium* segmentation, as defined by and modified from Clark, Peel and Akam (2019). **I.** The "posterior signaling center" is located in the posterior and in mainly made up of Wnt signaling components. It activity is required for *Tc-caudal* expression. **II.** The "spatiotemporal regulation" are the timing factors (*Tc-caudal*, *Tc-Dichaete* and *Tc-odd-paired*) that are active in difference regions of the germband and responsible for the regulation of different phases of the fate specification process. III. The "fate specification" is performed by the primary and secondary PRGs and the segment polarity network. Simplified, the oscillation of the pPRGs is controlled by *Tc-caudal*, sPRGs are controlled by *Tc-Dichaete* and the segment polarity network is controlled by *Tc-odd-paired*. The PRGs further control the expression of the segment polarity genes. The three stages are occurring in different regions of the germband, with the pPRG oscillation ("upper" fate specification) in the posterior while sPRGs and segment polarity gene patterning ("lower" fate specification) is occurring in the anterior (relative to each other). **(B)** Differences in timing between the stages of segmentation in *Drosophila* (simultaneous segmentation) and *Tribolium* (sequential segmentation). In *Drosophila* (upper panel), the effectors of each stage are affecting all segments, but are expressed at different times. In *Tribolium* (lower panel), all three stages and their effectors are expressed at once, but in different regions of the germband. In both cases, each cell will receive all three signals to determine its positional information. Note: Arrows in A do not imply activating regulation, but rather only shows regulation or influence (be it activating or repressing). Gene mentioned in A are only exemplary for any given process and not representing the whole repertoire of genes involved. Modified from Clark et al. (2019).

Despite all these explanations regarding the involvement of similar genes and gene regulatory networks as well as the evolvability of short- into long-germ modes of segmentation, the main difference in body axis patterning between *Drosophila* and *Tribolium* remains. That is the use of a SAZ to progressively pattern the AP axis during germband elongation. The outcome, however, is the same in both: a germband, subdivided into segments by the segment polarity genes that demark (para-)segment borders.

2.1.7 Evolution and conservation of segmentation in (eu-)arthropods

As mentioned, sequential segmentation or short-germ embryogenesis is thought to represent the ancestral mode of arthropod segmentation (Sander, 1976). Even within the insects long-germ embryogenesis is only found within the holometabola (Davis and Patel, 2002). A plethora of studies have not only shown sequential segmentation in other arthropod species, but also identified key genes commonly involved in the process.

For example, in the centipede *Strigamia maritima*, similar genes are involved in segmentation. The expression pattern of *Sm-eve1*, *Sm-runt*, *Sm-hairy2* and *Sm-odd-related1* (*Sm-odr1*) start with a two-segment periodicity as soon as they emerge in the posterior disk (the SAZ). They later resolve into segmental stripes (or fade as Sm-*odr1* does) upon entering a transition zone. *Sm-sloppy-paired* and *Sm-pax3/7-2* appear later and are regarded sPRGs (Green and Akam, 2013). Interestingly, *Sm-cad* is expressed in segmental rings emanating from the posterior disk and has a few segments overlay with *Sm-odr-1* before fading away (Chipman et al., 2004).

In the spider *Cupiennius salei*, both *Cs-Delta* and *Cs-Notch* are involved in posterior segmentation (Stollewerk et al., 2003) as are *Cs-hairy*, *Cs-even-skipped*, and *Cs-runt* (Damen et al., 2000). Delta-Notch signaling is, as mentioned above, necessary in the patterning of vertebrate somites (Jouve et al., 2000). More detailed studies in the common house spider *Parasteatoda tepidariorum* also revealed that both Delta-Notch and Wnt signaling via *Pt-Wnt8* are required for segmentation (McGregor et al., 2008; Schönauer et al., 2016). *Pt-Wnt8* is necessary for the formation of the SAZ and opisthosomal segments (McGregor et al., 2008) while Delta-Notch signaling is required for the expression of *Pt-Wnt8*. Both signaling pathways are further required for the expression of pair-rule genes in the SAZ, and that at least in part, occurs via *cad* (Schönauer et al., 2016). Recently, in *Parasteatoda* a Sox gene (*Pt-Sox21b-1*) was identified to play a major role in posterior segmentation (Paese et al., 2018). This gene is closely related to *Dicheate*, whose role as a timer gene in both *Drosophila* and *Tribolium* segmentation is explained above (Clark and Peel, 2018). This is interesting in so far that Sox genes also play a role in vertebrate segmentation. *Tribolium* and the common house spider therefore not only control PRGs similarly (El-Sherif et al., 2015), but also share more genes involved in segmentation. This could very well present a conserved part of embryonic segmentation in arthropods. There is, however, no pair-rule expression of the (oddly-named) pair-rule genes in spiders. Also

the involvement of Delta-Notch signaling in *Tribolium* segmentation could not be shown so far or might indeed have been lost (Clark, Peel and Akam (2019) suggest Toll genes, with limitations, as a possible alternative for that case).

Even in the annelid *Platynereis dumerilii*, a member of the Lophotrochozoa, which are considered the third main branch of the bilaterians (besides the Deuterostomes and Ecdysozoa), orthologs of *Pd-caudal* and *Pd-even-skipped* are expressed in a posterior growth region and are involved in posterior growth and segmentation (de Rosa et al., 2005). Both *Pd-engrailed* and *Pd-wingless* are segmentally expressed (Prud'homme et al., 2003) and hedgehog-signaling was shown to regulate segment formation (Dray et al., 2010).

There is a strong level of conservation regarding the genetic key players orchestrating segmentation in all these animals. Yet interesting, there are also differences in the details of the mechanisms. This exemplifies the importance of understanding segmentation in greater detail in not only one or two model systems. This further includes the long-standing question if segmentation has evolved *de novo* several times convergently (and apparently using quite similar mechanisms) from using evolutionary "old" genes or if there is a common origin to segmentation. These examples show that comparative studies in a great number of different species are needed to shed light on the conserved genetic basis of segmentation. For such detailed studies novel tools are required to increase the functional toolkits of model species besides *Drosophila*.

2.2 RNAi as a tool in developmental biology

To reveal details of complex developmental processes, like e.g. segmentation, it is necessary to develop and test novel and advanced techniques to study gene function in a broad range of model organisms. In this thesis, I tested such a novel approach to reveal greater details of *Tribolium* segmentation by optimizing temporal inhibition of RNAi gene knockdown. This novel approach is based on Viral suppressors of RNAi (VSRs) explained in more detail in the following chapter 2.3.

The "discovery" of RNAi (Fire et al., 1998) and its subsequent use as a tool in the life sciences enabled the investigation of cellular and developmental processes in species where genetic modifications are either not possible or not practical. Large genetic screens for any given biological process are limited to a very small number of highly developed

model species like *Drosophila melanogaster*. While multiple unbiased (forward) genetic screens in other model insect species have been performed (like *Tribolium castaneum* (Maderspacher et al., 1998; Sulston and Anderson, 1996; Trauner et al., 2009) and *Nasonia vitripennis* (Pultz et al., 2000)), neither was saturated, mainly due to technical reasons. And even with more and more sequenced (high-quality) genomes, many developmental studies and screens are still relying on the *Drosophila* candidate gene approach. This is ultimately a limitation for research of arthropod development since *Drosophila* shows a rather diverged embryonic development.

However, reverse genetic screens, utilizing RNAi, have emerged as a strong alternative to conduct unbiased genetic screens and were already performed successfully in *Caenorhabditis elegans*, *Drosophila*, cell culture, and most recently *Tribolium* (Schmitt-Engel et al., 2015).

Another advantage of RNAi is that it can be applied at different developmental stages. In *Tribolium*, for example, dsRNA can be injected at the embryonic, larval (Tomoyasu and Denell, 2004), pupal (Posnien et al., 2009a), or adult stage. The latter two also offer the application of parental RNAi (pRNAi, Bucher et al., 2002), another huge advantage of certain insect or arthropod species over others. In pRNAi, either injected dsRNA or already processed siRNA is spread throughout the body of the injected individual (dsRNA via the hemolymph, siRNA often via systemic RNAi mechanisms), and is transported into the developing oocytes. This later enables the collection of embryos in which both maternal and zygotic gene functions are knocked down. This is accompanied by the technical advantage that injecting only a limited number of individuals results in several hundred offspring, often showing a phenotypic range of the gene of interest.

The joined knockdown of both maternal and zygotic gene functions, however, can also be a disadvantage. A maternal or early zygotic phenotype might mask a possible later function of the gene of interest. Nevertheless, pRNAi in *Tribolium* is so efficient that a genome-wide screen was performed (Schmitt-Engel et al., 2015) and identified novel genes and gene functions in variety of different (developmental) processes, like head patterning, axis formation and even pest control (Ansari et al., 2018; Kitzmann et al., 2017; Schultheis et al., 2019; Siemanowski et al., 2015; Ulrich et al., 2015). The high “efficacy” of *Tribolium* (p)RNAi led to the question if the RNAi response could be further modified. Especially how it could be modulated to either enable early gene function while blocking later functions

or vice versa. Also, the use of tissue-specific RNAi as established in *Drosophila* would be of great interest for other species as well, especially since (p)RNAi by injection of dsRNA always targets all tissues of the animal.

2.3 Modulating RNAi by viral suppressors of RNAi

VSRs have evolved out of the necessity of viruses to overcome antiviral defenses of their (prospective) hosts. Especially plants and insects heavily rely on RNA interference (RNAi)-based strategies to defend themselves against viral infections (Csorba et al., 2009; van Mierlo et al., 2011) since they do not possess an adaptive immune system comparable to that of (higher) vertebrates. Conversely, plant and insect viruses have evolved strategies to counteract and overcome these innate defenses. One common strategy is to inhibit the RNAi pathways via Viral Suppressors of RNAi (VSRs) (further reviewed in Csorba et al., 2009; van Mierlo et al., 2011). A plethora of viral proteins capable of suppressing RNAi silencing were identified[4]. Just as diverse as the viral proteins are the mechanisms of action by which they inhibit RNAi: from binding dsRNA and inhibiting its processing, inhibiting dsRNA or siRNA processing proteins, to inhibiting Argonaut or RISC itself. The resulting evolutionary arms race further led to multiple examples of co-evolution of virus suppressor and host RNAi proteins (Csorba et al., 2009).

Using VSRs as a possibility to modulate the RNAi response in *Tribolium* was previously tested in our group (Ulrich, 2015). Several VSRs were tested for their ability to block RNAi using knockdowns of certain body colour enzymes or transgenic GFP. Among them, only the VSR from the Cricket paralysis virus (CrPV), *CrPV-1A*, showed reliable RNAi inhibition (Ulrich, 2015). CrPV-1A was previously been shown to modulate the antiviral response in *Drosophila* by antagonizing an effector protein of the RNAi pathways, the endonuclease Argonaute 2 by either directly binding (Nayak et al., 2010) or E3 ligase-mediated degradation of it (Nayak et al., 2018). While at first, no interference of CrPV-1A with the endogenous miRNA pathways that is mediated by Argonaute 1 (Ago1) was reported (Nayak et al., 2010), later analysis showed that a fraction of the endogenous miRNA can be loaded onto Ago2. Their function is therefore also impaired by CrPV-1A (Besnard-Guérin et al.,

[4] The Swiss Institute of Bioinformatics (SIB) has a useful overview of suppressors of RNAi including virus name and order, protein sequence, mechanism of action, and references, accessible at https://viralzone.expasy.org/891 (Suppressor of RNA silencing, 2020)

2015). Nevertheless, Ulrich (2015) did observe no adverse effects of CrPV-1A on development or reproduction. Multiple transgenic lines, including lines where CrPV-1A is ubiquitously expressed by an *α-Tubulin 1* promoter were kept for several generations without any observation of developmental abnormalities, reduced fecundity or reduced life span (Gregor Bucher, personal communication). Ulrich (2015) also created a transgenic line where *CrPV-1A* was put under the control of the endogenous *Tribolium* heat-shock promoter (Schinko et al., 2012), enabling temporal control over the inhibition of RNAi. In initial tests the functionality of this transgenic heat-shock CrPV line ("hsCrPV") was confirmed to rescue cuticle phenotypes using previously defined heat-shock treatment parameters (in the following text, the transgenic line will simply be called "hsVSR" for "heat shock VSR line") (Material and Methods section; Oberhofer, 2014).

2.4 Aims

The subdivision of the body or body structures into segmental units is present in at least three large animal phyla (arthropods, annelids, and chordates). For many species it was shown that the development of this segmentation is realized using oscillatory gene expression within a clock-and-wavefront patterning system. In the main arthropod model organism *Drosophila melanogaster*, segmentation was studied in great detail, but *Drosophila* employs the derived mode of simultaneous segmentation. So far, functional studies of the more ancestral arthropod segmentation clock-mechanism were mainly performed in the red flour beetle *Tribolium castaneum*, but were limited to permanent RNAi knockdowns. Using parental RNAi, target genes are downregulated from the very beginning of embryogenesis. In *Tribolium*, RNAi-mediated knockdown of segmentation genes leads to breakdown of segmentation. This early breakdown makes it difficult to infer complex gene functions and interactions during the segmentation process.

Our lab has created a temporally controlled RNAi inhibition system, hsVSR, utilizing heat shock-induced expression of a Viral Suppressors of RNAi (VSR). This system enables the inhibition of RNAi at almost any time during development.

The aim of my thesis was to gain a better understanding of sequential segmentation in arthropods by optimizing the hsVSR system in *Tribolium* for studying these later gene functions. Specifically, I asked what happens to posterior segmentation if RNAi-induced segmentation breakdown is inhibited during later stages of germband development.

Would segmentation re-initiate or would the breakdown be irreversible? Further, I wanted to know at what level of segmentation a rescue might be possible and characterize the molecular and genetic consequences.

3 Material and Methods

3.1 Strains and husbandry

Tribolium castaneum beetles were reared using standard conditions and methods (Bucher, 2009). If not stated otherwise, specimens for experiments (e.g. injected pupae/beetles, egg collections) were kept at 32°C and 40% relative humidity (RH), while general stock keeping was done at 28°C and 40% RH.

The transgenic RNAi inhibitor line (in the original thesis called “hsCrPV”) containing the construct pBac[3xP3-DsRedaf;Tc'hsp5'-CrPV1A-3'UTR] (Ulrich, 2015) was used for the RNAi rescue experiments and allowed the expression of a VSR upon heat shock treatment. In the following text the RNAi inhibitor line will simply be called “hsVSR” (for “heat shock VSR”). The “hsVSR” line is based on the *vermilion white* (v^w) strain (Lorenzen et al., 2002). In the following text, “v^w” is often referred to as the “wild type control” since v^w and hsVSR are genetically identical except for the aforementioned transgenic element. “RNAi wild type control” will refer to dsRNA injected v^w beetles or offspring embryos. The transgenic heat shock *hunchback* line (hs-hb) (Distler, 2012) contains a heat shock inducible *hunchback* construct allowing ectopic expression of the gap gene hunchback upon heat shock treatment (Boos et al., 2018).

3.2 RNA interference

Functional gene analysis was performed via parental RNAi according to established methods (Bucher et al., 2002; Posnien et al., 2009a). For rescue experiments in the hsVSR line, female pupae were injected with double stranded RNA (dsRNA) against target gene. For the gap gene timer reset experiment, female pupae for the hshb line were injected with dsRNA against *Tc-eve* and crossed with hsVSR males. Injections were performed using a “FemtoJet express” device (Eppendorf) and glass capillaries (borosilicate) pulled with a P-2000 needle puller (Shutter Instruments).

Injected dsRNA was *in-vitro* transcribed using the MEGAscript™ T7 Transcription Kit (Life Technologies). Templates were amplified using T7 promoter sequence overhang containing primers (either binding T7 promoter directly, or binding to other promoter sequences in the plasmid [T3, SP6], or being either plasmid or gene specific (Table 3.1). Concentrations

necessary to obtain both high penetrance and severe cuticular phenotypes were determined beforehand and are indicated in table 3.1.

Table 3.1 – Clones for dsRNA/riboprobe synthesis

Gene/clone	Concentration for pRNAi	Clone/dsRNA length (approx.)[5]	Clone origin (if known)	Primers (with T7 overhang)
Tc-arrow	100 ng/µl	~1800 bp	N. Posnien; cDNA	T7, SP6
Tc-even-skipped	1000 ng/µl	~1400 bp	Unknown; cDNA	SP6, T7
Tc-odd-skipped	500 ng/µl	~380 bp	Unknown	SP6, T7
Tc-paired	500 ng/µl	~540 bp	W. Damen (?)	T7, SP6
Tc-runt	500 ng/µl	~1500 bp	S.e Brown; cDNA	T7, SP6
Tc-wingless[6]	Not used for RNAi	1100 bp	J. Schinko; cDNA	Not amplified
Tc-Wnt8/D	100 ng/µl	~500 bp	R. Schröder	T7, T3
Tc-wntless	100 ng/µl	~600 bp	this work; cDNA	Gene specific

3.3 Molecular cloning

To generate dsRNA for functional gene analysis via RNAi, the genes of interests first had to be cloned from embryonic cDNA. For most of the genes studied in this thesis coding sequence fragments of the genes were already cloned in appropriate plasmids and available (see table 3.1). The genes which were not already cloned (Tc-wntless) were identified from the current Tribolium gene set (Tcas5.2) on iBeetle-Base (Dönitz et al., 2015; Herndon et al., 2020) using the *Drosophila* ortholog protein sequence and blast search (Altschul et al., 1990). Coding sequence was amplified from embryonic (0-72h) cDNA with gene-specific primers (synthesized by Eurofins) (Table 3.2) using the Phusion DNA polymerase (selfmade). PCR fragments were cloned into appropriate vectors using standard procedures (Sambrook and Russell, 2001). The *Tc-Wnt8/D* clone was provided by R. Schröder (University of Rostock). Sequences for clones used in this work are attached in the supplementary file “clones_phd_FK.docx”.

[5] If the length of the transcribed dsRNA fragment is different (i.e. shorter) than the clone from which is made, the length of the dsRNA is given. If no length is given, the clone was not used to produce dsRNA.
[6] Tc-wingless was used only as a riboprobe

Table 3.2 – Primer list

primer name	sequence	purpose
for dsRNA w/ T7 overhangs		
pJET_Rv_T7	GAATTGTAATACGACTCACTATAGGAAGAACATCGATTTTCCATG	amplify pJet insert with T7 promoter seq.
pJET_Fw_T7	GAATTGTAATACGACTCACTATAGGCGACTCACTATAGGGAGAGC	amplify pJet insert with T7 promoter seq.
T7-SP6	TAATACGACTCACTATAGGATTTAGGTGACACTATAGA	amplify with T7 overhang from SP6 promoter seq. site
T7-T3	TAATACGACTCACTATAGGAATTAACCCTCACTAAAGGG	amplify with T7 overhang from T3 promoter seq. site
T7	GAATTGTAATACGACTCACTATAGG	amplify with T7 overhang from T7 promoter seq. site
FK147_wls_sh_FW-T7	TAATACGACTCACTATAGGACCATGACTACTACCTTCTG	gene specific wls-T7 primers
FK148_wls_sh_RV-T7	TAATACGACTCACTATAGGAGTACATACTAGCGGAAATC	gene specific wls-T7 primers
qPCR primers		
FK_eve7_fwd	TCGCCGCACAACTCAATCTC	even-skipped exon
FK_eve7_rev	TGGCGTTTGTCTTTCATGCG	even-skipped exon
FK_eve_intron_1_fwd	GCGTTTTATTTGAGCGGGCA	even-skipped intron
FK_eve_intron_1_rev	CGCTCGCATCAAGGTGTTTT	even-skipped intron
FK_crpv1a_2_fwd	GGAGCTTGCTGCTCAAGAACT	VSR
FK_crpv1a_2_rev	TAGTTGTGGTTTGGACTGCACA	VSR
FK_odd_1_fwd	AGGGACCACAGGTACATCCA	odd-skipped exon
FK_odd_1_rev	TTGAGATTGGAGCGCTGGTT	odd-skipped exon
FK_run_1_fwd	GGTACTTGGGGTAGTTGTCGG	runt exon
FK_run_1_rev	ACACGCTTTCTCGCACTGTA	runt exon
VT_RPS3.3F1	AGGGTGTGCTGGGAATTAAAG	rps3 for normalization
VT_RPS3.3R1	GGGTAGGCAGGCAAAATCTC	rps3 for normalization
VT_GapDH3fw1	CGTTTCCGTTGTGGATTTGAC	GapDH for normalization
VT_GapDH3rv1	AACGACCTCTTCCTCCGTGTA	GapDH for normalization
VT_alpha-tubulin3fw1	CGCCAATAACTACGCCAGAG	α-Tubulin1 for normalization (not used)
VT_alpha-tubulin3rv1	CGAACGAGTGGAAAATCAAGAA	α-Tubulin1 for normalization (not used)
VT_actin-3fw1	TGGCTACTCGTTCACAACCAC	Actin for normalization (not used)
VT_actin-3rv1	GCCATTTCCTGTTCAAAGTCC	Actin for normalization (not used)
gene specific primers		
wntl_F1	ATGCCGGGAACAATCCTCGA	almost full length wntless (wls/wntl) form cDNA
wntl_R2	CCGGTAGATTATACCTTCGTAG	almost full length wntless (wls/wntl) form cDNA

3.4 Heat shock treatment

To express the VSR and investigate the effect of RNAi inhibition on segmentation, staged egg collections were heat shock-treated (hs-treated) at appropriate time points (see Figs. 4.2, 4.10, 4.12 and 4.21). The main conditions for the heat-shock treatment (2x10 min at 48°C, 2h recovery in between) are based on previous theses from our lab (Oberhofer, 2014; Ulrich, 2015). Since a detailed description of the hs-treatment procedure itself is not available in written from, and personal observations have indicated that variations in the outcome could occur upon minute changes in the procedure, it is detailed below.

Collected embryos of dsRNA injected animals of either the hsVSR or wild type control line (v^w) are kept at 32°C in a small *Drosophila* vial until the appropriate heat-shock time point. A water bath is pre-heated to 48°C. The eggs to be hs-treated are transferred to small (40ml) glass beakers with a **flat bottom.** The beaker is "closed" with a piece of perforated aluminum foil. The foil keeps most of the heat in the beaker, but the perforation prevents it from becoming a small-scale pressure vessel. The glass beakers are kept in the 48°C water bath for 10 min, with the bottom of the beaker submerged in it. Not all eggs can be transferred back into the plastic vials after the hs-treatment at the same time. Therefore, the beakers are kept with their bottom submerged in room-temperature water so that the hs-treatment does not continue due to the remaining heat in the glass beaker itself. After transferring the embryos back into the vials, they are allowed to recover for two hours at 32°C, until they are hs-treated again, for 10 min at 48°C, following the same procedure as mentioned above. These twice hs-treated eggs are kept at 32°C until embryos fixation or cuticle preparations. If variations to the procedure were made, they are indicated in the text. These mainly concern the number of hs-treatments or the recovery time in-between hs-treatments. Both the treatment temperature and duration remained unchanged in all cases.

For all tested genes except *Tc-torso*, at least two independent repetitions of each rescue experiment were performed.

3.5 Fixation

Treated and untreated embryos of desired age were fixed according to standard methods as previously described (Schinko et al., 2009) with one minor change: volume of 37% formaldehyde solution reduced to 200µl. Embryos were stored in methanol at −20°C.

3.6 L1 cuticle preparation

Treated and untreated embryos for cuticle preparation of first instar (L1) larvae were allowed to develop for at least 4 days at 32°C. Larvae (and eggs) were washed twice in 50% bleach, mounted in a 1:1 mixture of Hoyer's solution and lactic acid (Anderson, 1954) and incubated for 24h-48h at 60°C. Cuticles were analyzed using a Zeiss AxioPlan 2 or a Zeiss AxioScope using both DIC optics and autofluorescence of the cuticles. For blastodermal segments, appendages were counted. For paired appendages, the presence of only one was counted as half a segment present. For the number of abdominal segments, paired tracheal openings (in the text referred to as stomata) were counted. Two opposing tracheal openings were assumed to belong to one abdominal segment. Presence of half an abdominal segment (in the case of an uneven number of abdominal segments) were counted as such.

(Note to Figs. S7.4 and S7.8: while structures indicative of stomata were observed, it was unclear if these were indeed tracheal openings (due to previously published results and the overall strong phenotype of the cuticles). As to not overestimate a possible rescue of abdominal segments, in later iteration of the rescue experiments, structures indicative of stomata in untreated cuticles were counted as presence of abdominal segment(s).

3.7 Alkaline phosphatase and HCR *in-situ* stainings

To analyze the gene expression pattern after RNAi and/or hs-treatment, the RNA expression was visualized using two different methods. Single *in-situ* hybridization was performed as previously described (Schinko et al., 2009) using digoxigenin (DIG)-labeled riboprobes targeting *Tc-wg* (DIG RNA Labeling Kit, Roche), detected by anti-DIG-AP antibodies (Roche) and visualization by NBT/BCIP. The only modification was the omission of the Proteinase K treatment of the embryos.

Hybridization chain reaction (HCR) *in-situ* staining (Molecular Instruments) was performed according to manufacturer's instructions following the "HCR v3.0 protocol for whole-mount fruit fly embryos" protocol with the following modifications (provided by Eric Clark and Olivia Tidswell): 5% Dextrane sulphate (instead of 10%) in both the "30% probe hybridization buffer" and "Amplification buffer". Stained embryos were rehydrated in decreasing methanol series (75%, 50%, 25% in PBT). HCR probe sets for each target gene

(except *Tc-even-skipped*) with specific amplifier sequences were synthesized according to provided accession number by Molecular Instruments (see table 3.2). HCR Probes for *Tc-even-skipped* with specific amplifier sequences were ordered from Molecular Technologies (see table 3.2). Binding sequences are known but not published because they are the intellectual property of Molecular Instruments and Molecular Technologies, respectively.

Table 3.3 – HCR targets, NCBI accession number, attached amplifier (incl. Alexa fluorophore used for imaging) and lot number.

Target	**NCBI accession number**	**Amplifier/Alexa fluorophore**	**Lot number**
Tc-caudal	NM_001039409.1	B1 / Alexa-488	PRA974
Tc-even-skipped	NM_001039449	B1 / Alexa-488	3483/D413
Tc-runt	XM_964184.3	B2 / Alexa-594	PRA978
Tc-odd-skipped	XM_008198532.2	B3 / Alexa-546	PRA971
Tc-wingless	NM_001114350	B4 / Alexa-647	PRA975

3.8 Mounting, Imaging and image processing

Fluorescent HCR stainings of germbands were mounted in 90% glycerol or VectaShield (Vectorlabs) and documented using a Leica SP8 confocal laser scanning microscope (cLSM) (20x objectives with 100% glycerol as immersion medium) and the Leica LAS-X software (v 3.5.2). Cuticles of L1 larvae were documented using either a Leica SP5 inverted cLSM (10x air objective) with Leica LAS-X software or a Zeiss AxioPlan 2 (10x air objective) with ImagePro 6 utilizing the cuticle's autofluorescent properties. Corrections of brightness and contrast were performed with FIJI (Schindelin et al., 2012).

For both pPRG stripe counting and HCR classes, see Fig. S7.12 and table S7.1 for raw data (high resolution images of HCR class germbands attached, see supplementary file “hcr classes all embryos_high.pdf” (PDF, ~130MB). For *Tc-wg* head stage analysis, the Fig. S7.11 for overview of all *Tc-wg* head stages and table S7.1 for corresponding excel file for raw data.

.

3.9 qPCR

To characterize gene expression after *Tc-eve* RNAi and subsequent RNAi inhibition by hs-treatment, total RNA from embryos was isolated using the Quick-RNA Tissue/Insect Kit (Zymo Research) with DNase on-column digest (DNaseI Set, Zymo Research). cDNA was synthesized using the MAXIMA First Strand cDNA Synthesis Kit for RT-qPCR (Thermo Fisher Scientific) according to manufacturer's instructions.

qPCRs were performed using the CFX96 Real-Time PCR System (Bio-Rad Laboratories) with 5x HOT FIREPol® EvaGreen® qPCR Mix Plus (ROX) Master mix (Solis Biodyne). Used qPCR primers are indicated in table 3.2 (synthesized by IDT). Reference genes (GAPDH and RPS3) were identified using RefFinder (Xie et al., 2012). qPCR data analysis was done in the CFX Manager 3.1 (Bio-Rad Laboratories) and pyQPCR[7] with the delta-delta-Ct method (Livak and Schmittgen, 2001; Schmittgen and Livak, 2008).

3.10 Statistical analysis

Comparisons of abdominal segment numbers in cuticles and comparisons of number of expression stripes in germbands were done, if not stated otherwise, using unpaired, two-sided Mann–Whitney U tests for independent samples. All measured data points (see supplementary files) were included in the calculations and were not checked for being outliers beforehand (except by the plotting R packages (ggplot2), considering data above 1.5 *IQR of the 75th percentile or below 1.5 *IQR of the 25th percentile as outliers, indicated in in the respective plots in red). Comparisons of stripe proportions in germbands were done using the Pearson's Chi-squared Test for Count Data with simulated p-values by Monte Carlo simulations (B=1000). All graphs (if not stated otherwise) and statistical calculations were performed using R (v3.5.2; R Core Team, 2018) and RStudio (v1.1.x; RStudio Team, 2015) with the following packages: dplyr (Wickham et al., 2020), ggplot2 (Wickham, 2016), ggpubr (Kassambara, 2020), ggsignif (Ahlmann-Eltze, 2019), patchwork (Pedersen, 2019), readxl (Wickham and Bryan, 2019), reshape2 (Wickham, 2007).

[7] available at http://pyqpcr.sourceforge.net/

4 Results

4.1 Segmentation rescue by RNAi inhibition during germ-band elongation

Segmentation in *Tribolium* has at its core a segmentation clock that is active in both the blastoderm and the germband. So far, analyses of the dynamics of posterior segmentation were mainly based on observations of the expression of segmentation genes and the resulting phenotypes after gene knockdown. Such a permanent loss of function, however, cannot reveal more complex regulatory processes in the segmentation clock or during segmentation in general. In *Tribolium*, tools to rescue the expression of (segmentation) genes at any given time were not present (see Introduction for details). However, previous work showed that expression of a Viral Suppressor of RNAi (VSR) (CrPV-1A) can inhibit RNAi gene knockdown (Ulrich, 2015), and, subsequently, often rescues phenotypes in *Tribolium* pupae and adults. I applied heat shock-inducible VSR expression and subsequent inhibition of RNAi to answer the question what happens when a gene necessary for posterior segmentation is rescued after initial knockdown (Fig. 4.1A).

Preliminary experiments indicated that the combination of RNAi and heat shock can lead to further loss of segmentation (Ulrich, 2015). A rescue of abdominal segments by the hsVSR system could therefore be obscured by heat shock-induced loss of segments. The expression of the VSR is necessarily linked to hs-treatment, resulting in a confounding variable. This makes it difficult to distinguish between the possibly “negative effect” of the hs-treatment and the “positive effect” of the VSR expression (see Fig. 4.1B). To control for this possible downside of the system, I included a RNAi wild type control (vermilion white, vw; see Lorenzen et al., 2002), missing the heat-shock inducible VSR construct. This way, I could compare between VSR treatment (hs-treatment and VSR expression) and only hs-treatment in the context of RNAi knockdown.

Three time points for the expression of the VSR were chosen, with slight modifications, based on an earlier experimental design ((Ulrich, 2015) and schematically shown in Fig. 4.1A). The first time point (10-13h AEL) covers the transition from differentiated blastoderm to early germband and the beginning of posterior segmentation by the SAZ. The second time point (13-16h) coincides with the earlier stages of germ band elongation and further segmentation of abdominal segments. The last time point (16-19h) covers late germ band stages of elongation and posterior segmentation (see schematic embryos in Fig. 4.1A, lower right).

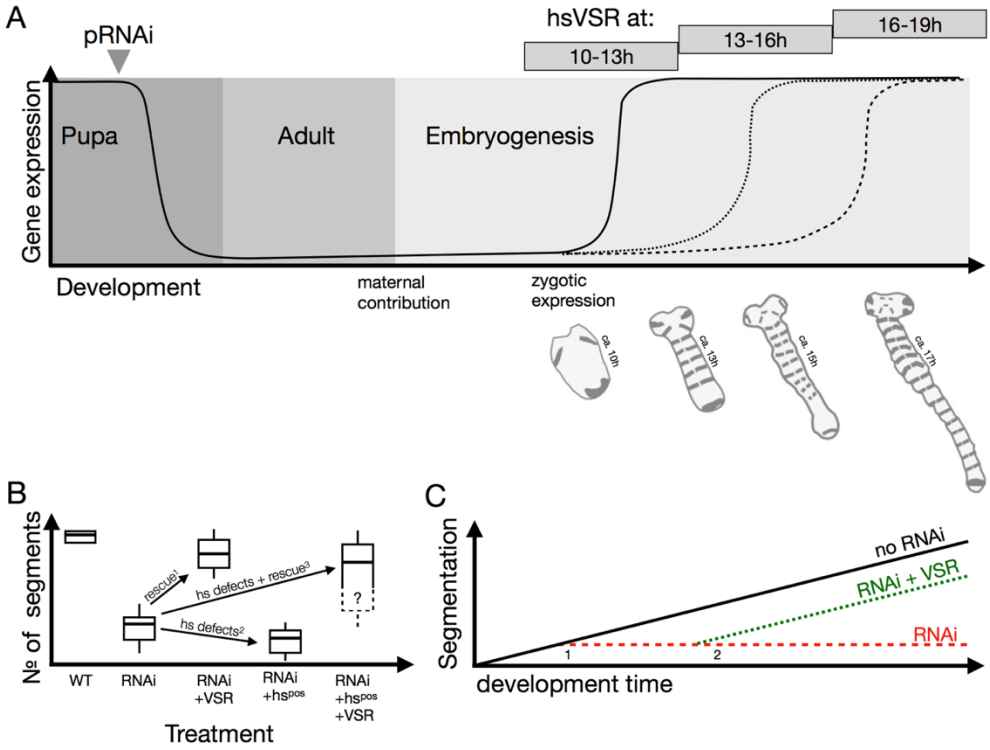

Figure 4.1 – The hsVSR system

(A) Schematic representation of hsVSR treatment. pRNAi causes gene expression to drop in injected animals (solid line). RNAi effect is transmitted to eggs, causing depletion of both maternal and/or zygotic transcripts during embryogenesis. hsVSR treatment inhibits RNAi at different time points during germband elongation (time window indicated above and exemplary germband shown below) and results in increase of gene expression of previously knocked down gene (solid and dashed lines on the right). **(B)** Hypothetical considerations about the possible influence of hsVSR treatment in embryos. RNAi will cause loss of segments compared to WT. RNAi combined with VSR ([1]), irrespective for VSR delievery would cause rescue of segments. RNAi and hs-treatment ([2]), on the other hand, could further decrease segment number (hs defects). Combination of all three ([3]) results in a possible mixture of segment number due to both rescue byVSR and hs defect due to hs-treatment. **(C)** Without RNAi, there is a "constant" increase in segment number (albeit not linear as schematically depicted here) until the germband is fully segmented. RNAi leads to breakdown of segmentation (1), the time point of break down depends on the gene in question. VSR expression (2) will results in rescue of segmentation, but with the possibility that wild type segment number cannot be achieved anymore. Panel A modified from Ulrich (2015).

(Note: in the following text and figures, the system to express the heat shock-inducible VSR and the transgenic line carrying the respective transgene are referred to as "hsVSR" and "hsVSR line", respectively. Further, "hs-treatment" will refer to heat shock treatment, regardless of whether this treatment will lead to expression of the VSR or not. "RNAi wild type controls" or "vw" indicate embryos from a wild type line (vermilion white, v^w) that underwent RNAi, and if mentioned, hs-treatment, but cannot express the VSR. Further, segments patterned during the blastoderm (head and thorax, see introduction) are

referred to as “blastoderm segments”. Segments patterned from the posterior SAZ (see introduction) are referred to as “abdominal segments”. Further, “rescue” or “ability to rescue” is, if not stated otherwise, always a rescue of the observed phenotype. I assumed that if a phenotype was rescued, this rescue was based on the inhibition of the RNAi machinery by the VSR expression)

4.1.1 hsVSR proof-of-concept and controls: *Tc-paired* and *Tc-torso*

I chose the secondary pair-rule gene *Tc-paired* (*Tc-prd*) for a proof-of-concept experiment to test if the hsVSR system has the ability to rescue posterior segmentation by inhibition of an ongoing RNAi response. *Tc-paired* is required to activate *Tc-engrailed* (*Tc-en*) expression in odd-numbered segments in the elongating germband throughout the segmentation process and is itself a target of the segmentation clock (Choe et al., 2006). Knockdown of *Tc-prd* transcripts via parental RNAi leads to a classic pair-rule gene phenotype with cuticles missing every other segment (Choe and Brown, 2007). *Tc-prd*’s position downstream of the segmentation clock makes it a good candidate to test the hsVSR system in the context of segmentation and to function as a positive control.

To ensure that the rescue effect is temporally correlating with ongoing expression of the candidate gene, a second gene, *Tc-torso*, was chosen to function as a negative control. Torso signaling is necessary for abdominal segmentation in *Tribolium* (Schoppmeier and Schröder, 2005), but contrary to *Tc-prd*, it is maternally contributed and thus active exclusively before the first hs-treatment time point. Hence, the hs-treatment should not be able to influence this early function (see Figs. 4.1A and 4.2 for schematic overview of hsVSR system and hs-treatment time points). Thus *Tc-paired* RNAi was suggested to be rescuable by the hsVSR system while *Tc-torso* RNAi should not.

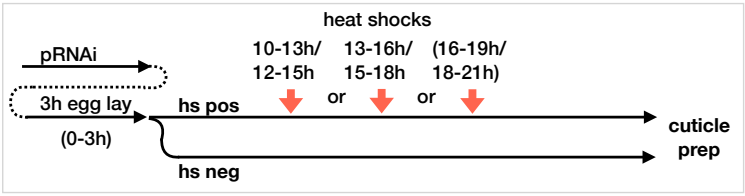

Figure 4.2 – hsVSR rescue after pRNAi in cuticles, experimental procedure

Parental RNAi (pRNAi) is performed in hsVSR (and wild type (vw)) animals. RNAi embryos are collected for 3h (0-3h) and either heat shock treated at 10-13h, 13-16h or 16-19h (second hs-treatment time also indicated). After approx. 3-4 days, cuticles of L1 larvae (if any) had developed and were prepared for cuticle analysis according to material and methods.

***Tc-paired* RNAi**

In accordance with previous findings (Choe and Brown, 2007) *Tc-prd* parental RNAi without hs-treatment resulted in cuticles missing mandibles (Md), labium (Lab), the second thoracic segment (T2), and a median number of four remaining abdominal segments (Fig 4.3A^{i} and A^{ii} for exemplary cuticle and 4.3B and C for segment numbers). This specific knockdown phenotype was observed in both the hsVSR line and RNAi wild type controls (see Fig 4.3 B and C).

Early hs-treatment resulting in expression of the VSR at 10-13h increased the median to 7.5 abdominal segments (Fig 4.3A^{iii} and plot in Fig 4.3C) in the hsVSR line. Further rescue of more anterior segments was observed for Md (25%, “a” in Fig. 4.3A^{iv}), Lab (30%) and the second thoracic segment (80%) (Fig. 4.3A^{iii}/A^{iv} and B). The wildtype RNAi control cuticles showed an unchanged median number of four abdominal segments and no additional blastodermal segments (see “vw, 10-13h” in Fig 4.3B and C).

Likewise, later VSR expression at the second hs-treatment time point (13-16h) increased the median number of abdominal segments to six segments, but also only in the hsVSR line. I also observed cuticles showing less than four abdominal segments. This might indicate the aforementioned possible downside of our system (Fig. 4.1B) where the hs-treatment by itself leads to further loss of segments (see “hsVSR, 13-16h” in Fig. 4.3C). In the RNAi wild type control, no rescue was observed, but also no significant decrease below a median of four abdominal segments.

Only VSR expression at the last time point (16-19h) failed to rescue abdominal segments. While the median remained at four segments, the percentage of cuticles showing less than four segments increased for both the hsVSR and the vw wild type line. In the latter, the number of cuticles with less than four abdominal segments was even larger. This could

indicate that this time window might be more susceptible to heat shock damages than the earlier ones.

It should be noted at this point that experimental outcomes showed a certain degree of variability. As a consequence, the results of repetitions sometimes diverged in both the ability to rescue and its efficiency to do so – probably due to comparably small differences in the hs-treatment itself. For example, in a previous iteration of the *Tc-prd* rescue experiment (see Fig. S7.1 for data), the early timepoint led to cuticles with both in- and decrease from the median number of segments. Only the second treatment time point showed a clear and statistically significant increase in median segments number.

Hence, due to the apparent sensitivity of the system, I relied on experimental outcomes that were reproduced in at least two independent experiments (with only a few exceptions, which I will specifically mention). This also highlights the importance to include RNAi wild type controls to control for the confounding variable of hs-treatment and VSR expression.

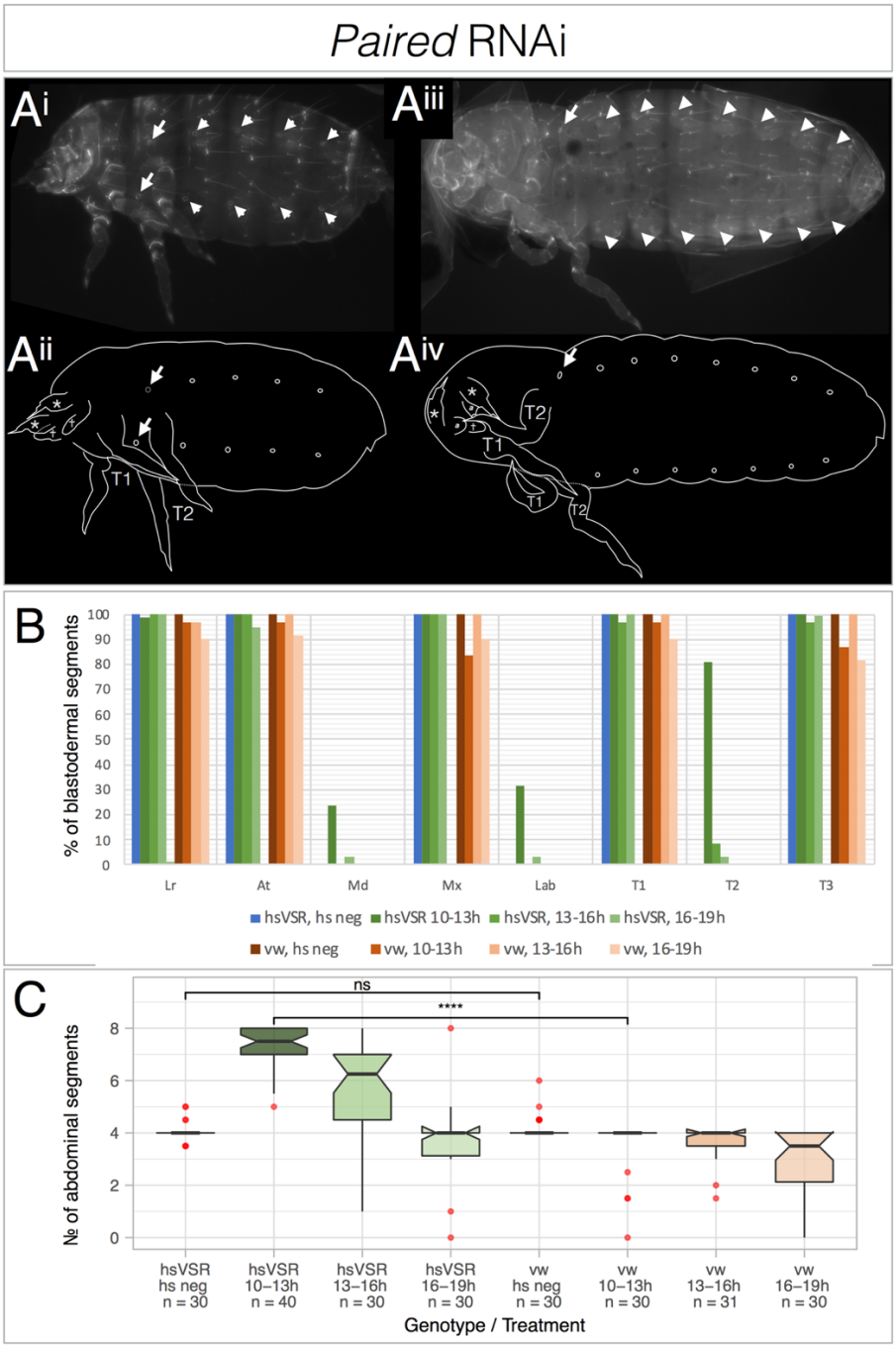

Figure 4.3 – Proof-of-concept: Tc-paired RNAi

pRNAi against the secondary pair-rule gene *Tc-paired* (*Tc-prd*) results in a classic pair-rule gene phenotype with every other segment missing. VSR expression rescued segmental phenotype and posterior segmentation. **(A)** Exemplary non-heat shocked (A^{i}) and heat shocked (A^{iii}) cuticles (line drawings of respective cuticles in A^{ii} and A^{iv}) after Tc-prd RNAi in the hsVSR line. The number of abdominal segments without hs-treatment is four, while with hs-treatment, the number of abdominal segments increased to seven. **(B)** Bar chart detailing the presence of blastodermal segments after *Tc-prd* RNAi and different hs-treatment conditions in hsVSR and wild type (wv) line. While no heat shock treatment resulted in the classic pair-rule gene phenotype, hs-treatment rescued blastodermal segments. No rescue was observed in the RNAi wild type controls (vw). **(C)** Boxplot showing the number of abdominal segments for the cuticles of the corresponding conditions in B. Significant increase in abdominal segment number was observed after hs-treatment in the hsVSR line, but no recue was observed in the RNAi wild type controls (wv). Possible outliers (see material and methods) are marked in red..

***Tc-torso* RNAi**

Similar to previously published results (Schoppmeier and Schröder, 2005), parental *Tc-torso* RNAi resulted in loss of most abdominal segments (median of 1.5 segments, Fig. 4.4B) while the blastodermal segments were present (Fig. 4.4A). As expected, due to its maternal contribution and early function, no rescue of abdominal segments by hs-induced VSR expression was observed for neither time point. Contrary, the median number of abdominal segments decreased after hs-treatment compared to non-heat shocked cuticles, again showing the presence of hs-defects as mentioned earlier and in figure 4.1 B. The earliest VSR timepoint even led to a reduction of the third thoracic segment to roughly 65%, while all other blastodermal segments at all other timepoints were unaffected.

Considering these results, I was able to show that the hsVSR system can be used to investigate whether or not (posterior) segmentation can be re-initiated after breakdown by re-introduction (i.e. RNAi inhibition) of a previously knocked down component during germ band elongation. I showed this by rescuing the secondary pair-rule gene *Tc-paired*. I also showed, using *Tc-torso* RNAi, that the rescue is time-specific and correlates with the expression and activity window of the gene in question.

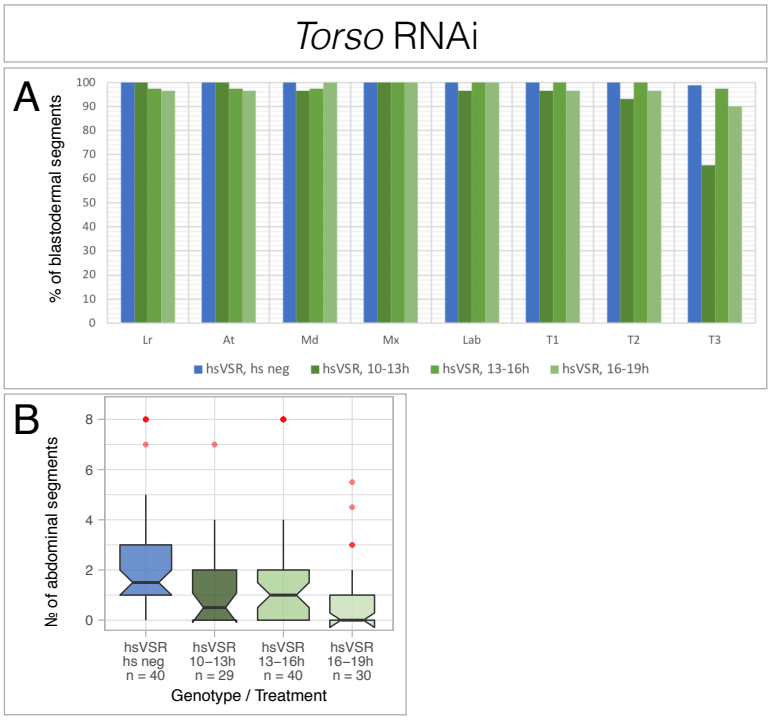

Figure 4.4 – Proof-of-concept: Tc-torso

pRNAi against the maternal effect gene *Tc-torso* (Tc-tor) results in loss of most abdominal segments. VSR expression did not rescue any abdominal segments **(A)** Bar chart detailing the presence of blastodermal segment after *Tc-tor* RNAi and different heat shock treatment conditions in hsVSR line. pRNAi did not result in loss of blastodermal segments, while early hs-treatment ("10-13h") led to small decrease of the third thoracic segments **(B)** Boxplot showing the number of abdominal segments for the cuticles of the corresponding time points in A. RNAi led to loss of abdominal segments. Hs-treatment did not result in any increase (no rescue), but rather loss of remaining segments. Possible outliers (see material and methods) are marked in red.

4.1.2 The segmentation breakdown after Wnt pathway component knock-down is irreversible

The Wnt ligand co-receptor *Tc-arrow* (*Tc-arr*) is expressed ubiquitously during embryogenesis (Bolognesi et al., 2009). The Wnt ligand Tc-Wnt8/D is specifically expressed in the SAZ during embryogenesis (Bolognesi et al., 2008a). *Tc-wntless*, required for the secretion of Wnt ligands, is expressed ubiquitously as well (Bolognesi et al., 2008b). *Tc-Wnt8/D* mediated signaling as part of the "posterior signaling center" is assumed to be important specifically for initiation or maintenance of parts of the SAZ and abdominal segmentation. Both *Tc-arr* and *Tc-wls* are cofactors necessary for Wnt signaling in general (Bänziger et al., 2006; He et al., 2004). Fittingly, RNAi of *Tc-arr* or double RNAi of *Tc-Wnt8/D* and *Tc-wls* lead to loss of abdominal segmentation in germbands. Their cuticle phenotype, however, is even more drastic, most often resulting in completely unsegmented cuticle remnants or "cuticle balls" (Bolognesi et al., 2008b; Bolognesi et al., 2009). With the knowledge that the hsVSR system can be used to address the question if re-initiation of posterior segmentation after breakdown is possible, I asked whether the inhibition of RNAi of Wnt pathway component would lead to the re-initiation of segmentation and a rescue of the cuticle phenotype. A rescue of abdominal segments would mean that the "posterior signaling center" can re-initiate after RNAi-mediated breakdown.

Tc-arrow

Parental *Tc-arr* RNAi had two predominant phenotypes: "Empty eggs" and unsegmented cuticles. The "Empty eggs" phenotype literally describes an empty egg, because the embryos did not develop far enough to secrete a cuticle. "Empty eggs" do occur regularly in wild type and RNAi egg collections up to a portion of 20-30% (Posnien et al., 2009a; Schinko et al., 2008). For *Tc-arr* RNAi I observed close to 45% empty eggs (of all eggs collected, see Fig. 4.5a). This is less than what was previously reported (Bolognesi et al., 2009).

The second observed phenotype, unsegmented cuticles, describes cuticles remnants that show no sign of external segmentation, but are clearly cuticles, often still inside there egg shells. The percentage of unsegmented cuticles was very high (close to 95% of developed cuticles scored, see Fig. 4.5a) Their occurrence after *Tc-arr* RNAi was previously reported as well (Bolognesi et al., 2009).

RNAi inhibition by VSR expression at 10-13h had multiple effects. It did lower the percentage of empty eggs from close to 45% to less than 30%. More dramatically was the rescue of unsegmented cuticles. While without VSR expression, close to 95% showed no segmentation, VSR expression at 10-13h lowered this number to less than 10%. Consequently, the percentage of cuticles with identifiable segments increased (see “hsVSR, 10-13h” in Fig. 4.5A). The pre-gnathal segments did show a higher percentage of rescue than gnathal or thoracic segments (See “Lr” and “Ant” for “hsVSR, 10-13h” in Fig. 4.5A).
A slightly different result could be observed after VSR expression at the second time point (13-16h). While pre-gnathal appendages were rescued to a lower extend, rescue of gnathal and thoracic segments increased (see “hsVSR, 13-16h” in Fig. 4.5A) when compared to the earlier time point.

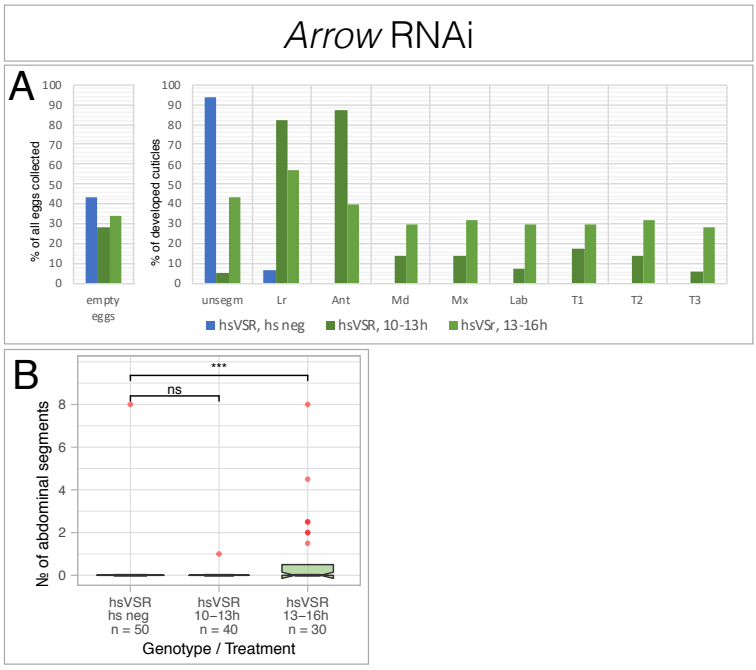

Figure 4.5 – RNAi of the “posterior signaling center”: Tc-arrow

pRNAi against the Wnt pathway component *Tc-arrow* (*Tc-arr*) results in unsegmented cuticles. VSR expression rescues blastodermal segemnts, while no conclusive rescue of abdominal segmentation was observed. **(A)** Bar chart detailing the presence of blastodermal segment after *Tc-arr* RNAi and different hs- treatment conditions in hsVSR line. No heat shock treatment resulted in close to 50% empty eggs (no cuticle). In those eggs with cuticles, mainly no segmentation could be observed. Hs-treatment rescued blastodermal segments. **(B)** Boxplot showing the number of abdominal segments for the cuticles of the corresponding conditions in A. No abdominal segments were observed non-heat shocked cuticles. Hs-treatment did not result in rescue of abdominal segments (significant comparison for “13-16h” is discussed in the text). Possible outliers (see material and methods) are marked in red.

Abdominal rescue of hs-treated cuticles was not observed for the early time point (when compared to non-heat shocked cuticles), but there was a significant increase at the later rescue time point in one of the repetitions (compare “13-16h” in Fig. 4.5B to Fig. S7.2B). While the median of the number of abdominal segments remained at zero, more individual cuticles showed an increase in abdominal segment number ("hsVSR, 13-16h" in Fig. 4.5B).

If this represents a bona fide rescue of abdominal segmentation or rather just a rescue of the later segment polarity function of Wnt signaling is unclear, especially since no significant abdominal rescue was observed for any earlier time points. Also, the calculation of significance does include all data points, including possible outliers (as defined in the material and methods and shown in red in all abdominal segment box plots). While removal of all considered outliers still resulted in an significant increase at 13-16h, the two remaining data points with abdominal segments also showed rescued blastodermal segments. The rescue of segment polarity function would therefore explain the increase of both blastodermal and abdominal segments described above.

In an earlier iteration of this experiment, the overall phenotype of the *Tc-arr* RNAi was weaker, aside from the higher percentage of empty eggs (see Fig. S7.2 A and B), with even non-heat shocked cuticles showing a high percentage of segmental appendages and abdominal segments. Yet, the same pattern of rescue of empty eggs and unsegmented cuticles was observed, as was the more pronounced rescue of anterior-most structures (Fig. S7.2A, “Lr” and “Ant”). No significant increase in the number of abdominal segments was observed and the increase in the third and fourth quartile (see Fig. 7.2B) for the latter two time points might again not represent a bona fide rescue of segmentation, but rather a stabilization of previously established segmental borders, which require Wnt signaling.

Tc-Wnt8/D, Tc-wls

Tc-Wnt8/D knockdown mainly causes the “Empty eggs” phenotype as well as complete loss of segmentation that results in small and spherical “cuticle balls”, comparable to *Tc-arr* RNAi (Bolognesi et al., 2009). Its RNAi germ band phenotype, on the other hand is described as rather mild (Bolognesi et al., 2008b). A double knockdown together with *Tc-wntless* (*Tc-wls*), on the other hand, results in a much higher percentage of severe phenotypes like unsegmented cuticles and truncated germbands missing abdominal segments (Bolognesi et al., 2008b).

Performing *Tc-Wnt8/D*;*Tc-wls* double RNAi, I observed complete penetrance of the severe, unsegmented cuticle phenotype. 100% of scored eggs containing cuticles were unsegmented. The "Empty eggs” phenotype, however, was less severe with only close to 40% of all collected eggs (see Fig.4.6B)

Early VSR expression at 10-13h reduced the percentage of empty eggs (25%) and, more dramatically, of unsegmented cuticles (5%) while increasing the percentage of cuticles with labrum (Lr) and antennae (Ant) both above 80%. Other gnathal or thoracic segment appendages were rescued only negligibly (Fig. 4.6B, “hsVSR, 10-13h”)

Later VSR expression at 13-16h showed a similar, yet weaker rescue of empty eggs (30%) while unsegmented cuticles were again rescued with high efficiency (less than 5%) and subsequently resulted in an increase of both labrum and antennae, 80% and 60%, respectively. Abdominal rescue was not observed for any hs-treatment time points (Fig. 4.6 C).

Similar as observed for *Tc-arr* RNAi, an earlier iteration of the Tc-Wnt8/D; *Tc-wls* RNAi rescue experiment showed a similar rescue pattern. The percentage of empty eggs was higher (Fig. 7.3A). The earliest hs-treatment time point rescued the unsegmented phenotype, again resulting in more cuticles with pre-gnathal appendages (Fig.S7.3A, “hsVSR 10-13h”). The second time point, at 13-16h, was less effective in rescue of blastodermal segments when compared to the results above (compare “hsVSR 13-16h” in Fig. 4.6B to Fig. S7.3A). Abdominal rescue was not observed for any time point.

In summary all these VSR treatments did not lead to any rescue of abdominal segments for *Tc-Wnt8/D*; *Tc-wls* or only a minor rescue for *Tc-arr*. The segmentation machinery did not appear to re-initiate in both cases because then (more) abdominal segments would have been expected. Hence, the breakdown of the SAZ after loss of Wnt signaling (Beermann et al., 2011) appears to be irreversible, even if the knocked-down components are brought back to the system.

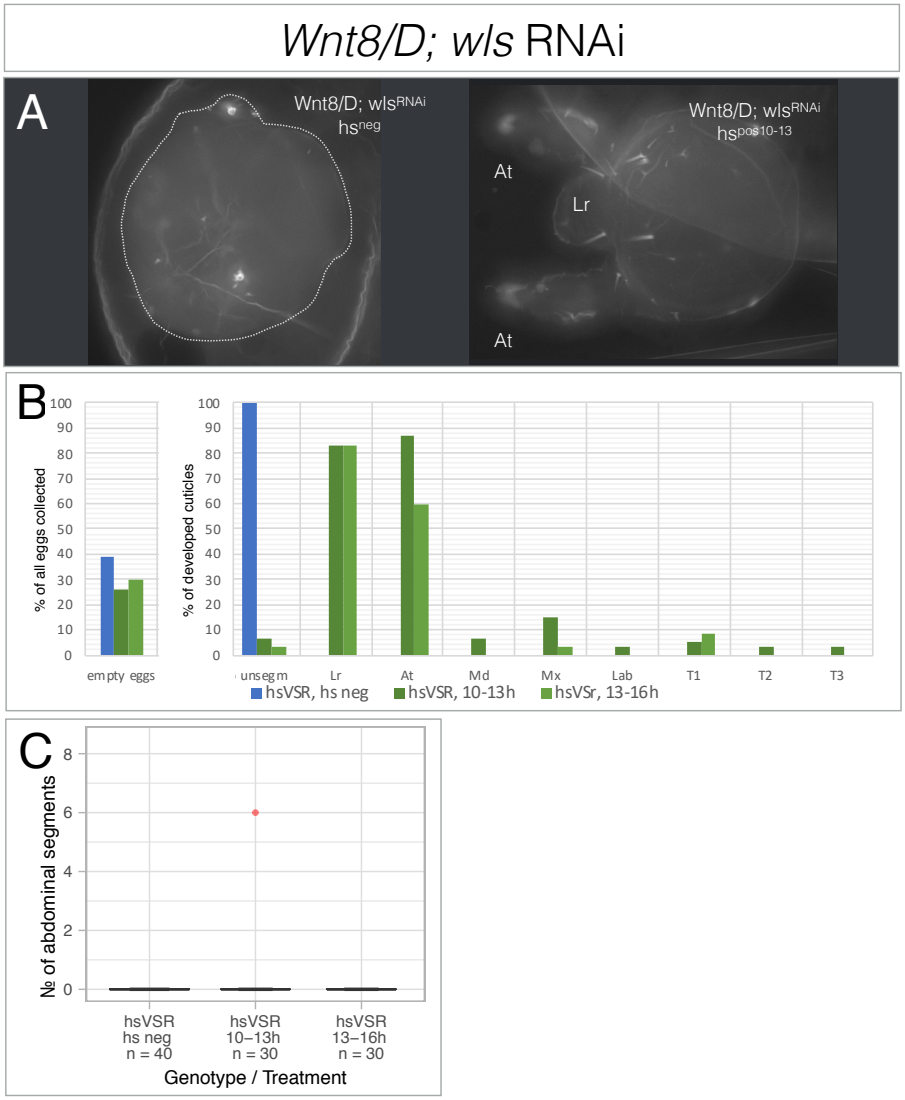

Figure 4.6 – RNAi of the "posterior signaling center": Tc-Wnt/D; Tc-wls

Double pRNAi against the Wnt pathway components Tc-Wnt8/D and *Tc-wntless* (*Tc-wls*) results in unsegmented cuticles. VSR expression rescues blastodermal segemnts, while no conclusive rescue of abdominal segmentation was observed. **(A)** Exemplary non-heat shocked (left) and heat shocked (right) cuticles. **(B)** Bar chart detailing the presence of blastodermal segment after *Tc-Wnt8/D*;*Tc-wls* double RNAi and different hs-treatment time points in hsVSR line. No heat shock treatment resulted in 40% empty eggs (no cuticle). In those eggs with cuticles, no segmentation could be observed. Hs-treatment rescued blastodermal segments with prevalence of anterior over posterior ones. **(C)** Boxplot showing the number of abdominal segments for the cuticles of the corresponding conditions in B. No abdominal segments were observed in non-heat shocked cuticles. Hs-treatment did not result in rescue of abdominal segments. Possible outliers (see material and methods) are marked in red.

4.1.3 Early rescue of primary pair-rule gene phenotype in cuticles indicates reversibility of posterior segmentation breakdown

The next class of segmentation genes to be investigated were the primary pair-rule genes (pPRG) *Tc-even-skipped* (*Tc-eve*), *Tc-runt* (*Tc-run*), and *Tc-odd-skipped* (*Tc-odd*). As mentioned in the introduction, the current model states that these pPRGs are oscillating in the SAZ to form the segmentation clock (El-Sherif et al., 2012; Sarrazin et al., 2012) Furthermore, *Tc-eve* probably is the first of these three genes in the loop to be activated, because its RNAi knockdown leads to the lowest number of pre-gnathal segments (0 for *Tc-eve*, 1 for *Tc-run*, and 2 for *Tc-odd*, see Choe et al., 2006).

4.1.3.1 Tc-even-skipped

As previously reported, *Tc-eve* RNAi leads to complete breakdown of segments, resulting in cuticles with no gnathal, thoracic or abdominal segments (Choe et al., 2006). Performing parental RNAi of *Tc-eve* transcripts resulted in cuticles with labrum (Lr) and antennae (Ant) remaining in both the hsVSR line and the RNAi wild type controls (vw; see “hs neg” in Fig. 4.7A^{i}/^{ii} and 4.7B). Interestingly, and in contrast to previously published results (Choe et al., 2006), a pair of stomata posterior of the remaining labrum was almost always present (90%, see Fig. 4.7C, “hs neg”).

Expression of the VSR at the earliest time point (10-13h) did rescue both blastodermal and abdominal segments (Fig. 4.7A^{iii}/^{iv}). A strong rescue was observed for the mandibles (Md) and one thoracic segment (75% and 85%, respectively). This thoracic segment could be of T1 identity based on absence of tracheal openings and the apparent anterior-to-posterior rescue gradient. Also, close to 30% of maxillae (Mx) were rescued (Fig. 4.7B). The median number of abdominal segments increased to four segments (with individual cuticles showing as many as 6-7 abdominal segments) (see “hsVSR, 10-13h” darkgreen in Fig. 4.7C). The hs-treated RNAi wild type control did not show any increase in abdominal segments number nor of blastodermal segments ("vw, hs 10-13h” in Fig. 4.7B and C).

VSR expression at the second time point (13-16h), in contrast, did not significantly rescue the number of abdominal segments. Few cuticles were observed with more than the average one abdominal segment (see “hsVSR, 13-16h” in Fig. 4.8B). This, in contrast, was counterbalanced by cuticles with additional loss of segments. Hence, it is possible that the negative effect of the hs-treatment hides a minor rescue effect. The rescue of blastodermal

segments was also strongly reduced in the late treatment (see Md, Mx, and T1 in Fig. 4.7B). No change in segment number was observed for the RNAi wild type control ("vw" in Fig. 4.7B and C).

Out of three repetitions of this experiment, one experiment not only failed to show significant rescue of abdominal segments, but showed a significant decrease in segment number (Fig. 7.5B). This particular experiment still showed rescue of blastodermal structures like mandibles (25%) and one thoracic segment (45%) (see Fig. S7.5A), but it appears that the hs-treatment induced loss of segments outweighed any rescue. The other two experiments (see Figs. S7.4 and 4.8), however, clearly showed the rescue of both abdominal and blastodermal segments upon VSR expression at the transition from differentiated blastoderm to germband stage (10-13h).

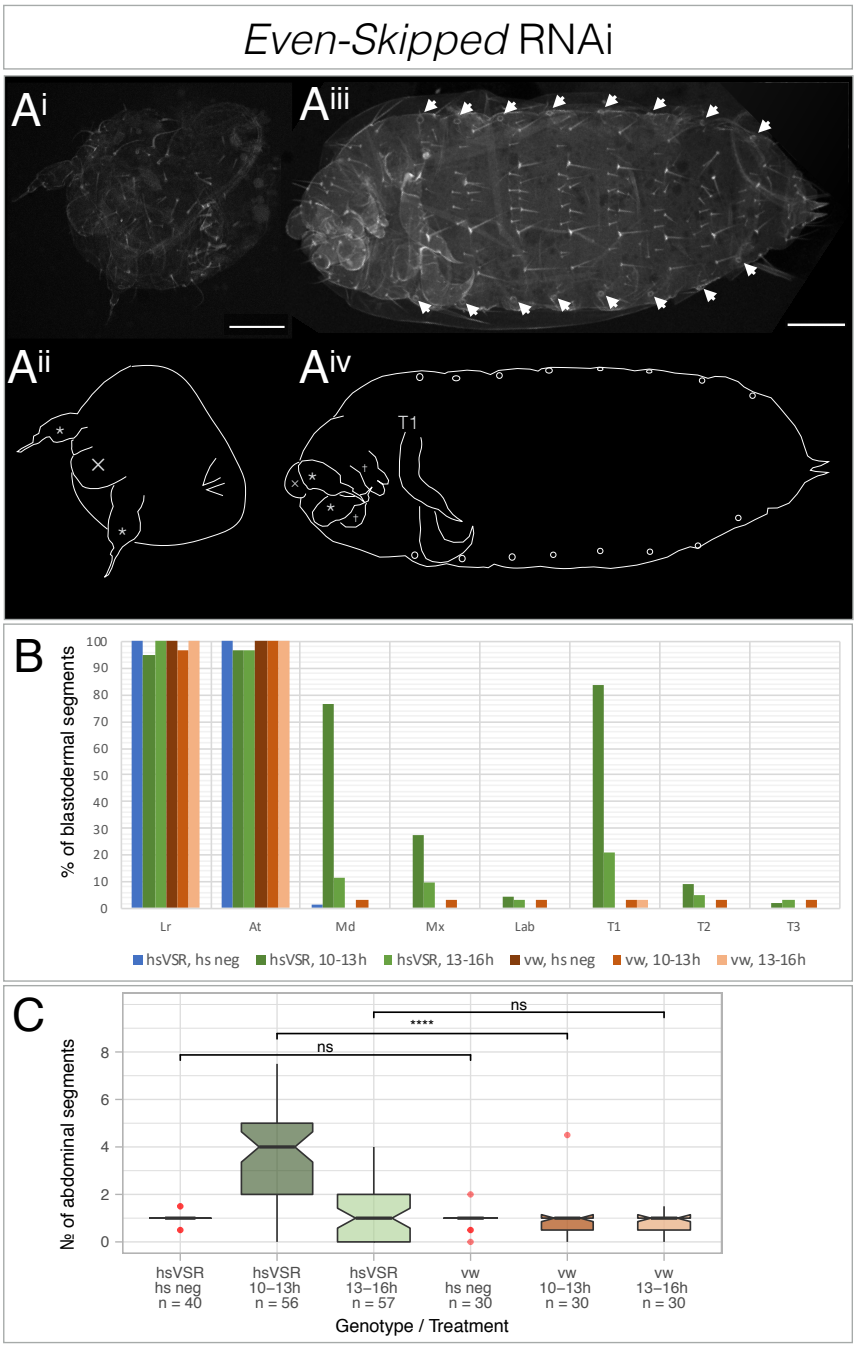

Figure 4.7 – RNAi of the segmentation clock: Tc-even-skipped

pRNAi against the pPRG *Tc-eve* results in loss of all gnathal, thoracic and abdominal segments. Hs-treatment in the hsVSR line rescues segmentation. **(A)** Exemplary non-heat shocked (A^{i}) and heat shocked (A^{iii}) cuticles (line drawings of respective cuticles in A^{ii} and A^{iv}) after *Tc-eve* RNAi in the hsVSR line. No gnathal, thoracic or abdominal segments are present (A^{i}, A^{ii}). Hs-treatment resulted in rescue of segmentation and cuticles with gnathal, thoracic and abdominal segments ($A^{iii,}$ A^{iv}). Stomata indicative of abdominal segments marked by short arrows in A^{iii} **(B)** Bar chart detailing the presence of blastodermal segment after *Tc-eve* RNAi and different hs-treatment conditions in hsVSR and wild type (wv) line. While no heat shock treatment resulted in the classic PRG phenotype, hs-treatment rescued blastodermal segments. No rescue was observed in the RNAi wild type controls (vw). **(C)** Boxplot showing the number of abdominal segments for the cuticles of the corresponding conditions in B. Significant increase in abdominal segment number was observed after hs-treatment in the hsVSR line, but no recue was observed in the RNAi wild type controls (wv). Possible outliers (see material and methods) are marked in red.

4.1.3.2 Tc-runt

Parental *Tc-run* RNAi resulted in cuticles with only one remaining gnathal segment, the mandibles (see "ª" in Fig. 4.8A^{ii} and "Md" in Fig. 4.8B). This result is in line with previously published results (Choe et al., 2006). The observed median number of abdominal segments after *Tc-run* RNAi in the hsVSR line without hs-treatment was 0.25, while the RNAi wild type control median was zero. A few cuticles did show stomata openings (like the cuticle shown in Fig. 4.8A^{i}/^{ii}, white arrows), indicating the possible presence of an abdominal segment (see material and methods for comments on counting abdominal segments based on stomata openings). Less than 15% of non-heat shocked cuticles showed other blastodermal segments, mainly a thoracic segment in less than 20% of cuticles (see "vw hs neg" in Fig. 4.8B).

Early VSR expression (10-13h) rescued the number of both blastodermal and abdominal segments (Fig. 4.8A^{iii}/^{iv}). The latter were rescued to a median number of three abdominal segments, with some cuticles showing five or more rescued abdominal segments (see "hsVSR, 10-13h" in Fig. 4.8C). Blastodermal rescue of the Mx (55%, marked † in Fig. 4.8A^{iv}) and the first and second thoracic segment (65% and 45%, respectively; T1 marked in Fig. 4.8A^{iv}) was observed as well (Fig. 4.8B). A few blastodermal structures decreased in number, like the Lr (to 60%), antennae (At, to 80%) and Md (to 75%). As indicated above, this is most likely due to the hs-treatment itself, since a similar decrease can also be observed in the RNAi wild type control ("vw hs 10-13h" in Fig. 4.8B).

Inhibiting RNAi at 13-16h still showed significant, albeit weaker rescue of abdominal segments, with a median number of one abdominal segment. Also, one thoracic segment was rescued in 40% of cuticles (see "hsVSR, 13-16h" in Fig 4.8AB). Only the late VSR expression time point at 16-19h failed to rescue abdominal segments when compared to the RNAi wild type control.

The *Tc-run* RNAi rescue experiment has been repeated three times. Only the third iteration (presented above) did rescue abdominal segments, while the earlier two iterations failed to rescue segmentation (Figs. S7.6B and S7.7B). Blastodermal segment rescue in the earlier two experiments was also weak with one thoracic segment being rescued, but barely above 30% (see "T1" in Figs. S7.6A and 7.7A). I attribute the observed variation to the dual consequences of the heat-shock treatment: rescuing segmentation by RNAi inhibition on the one hand and hs-defects in cuticles on the other hand. Given this complex system,

minor experimental differences (as briefly mentioned in the Material and Methods) could lead to diverging outcomes. Another repetition is clearly needed to increase confidence with that data.

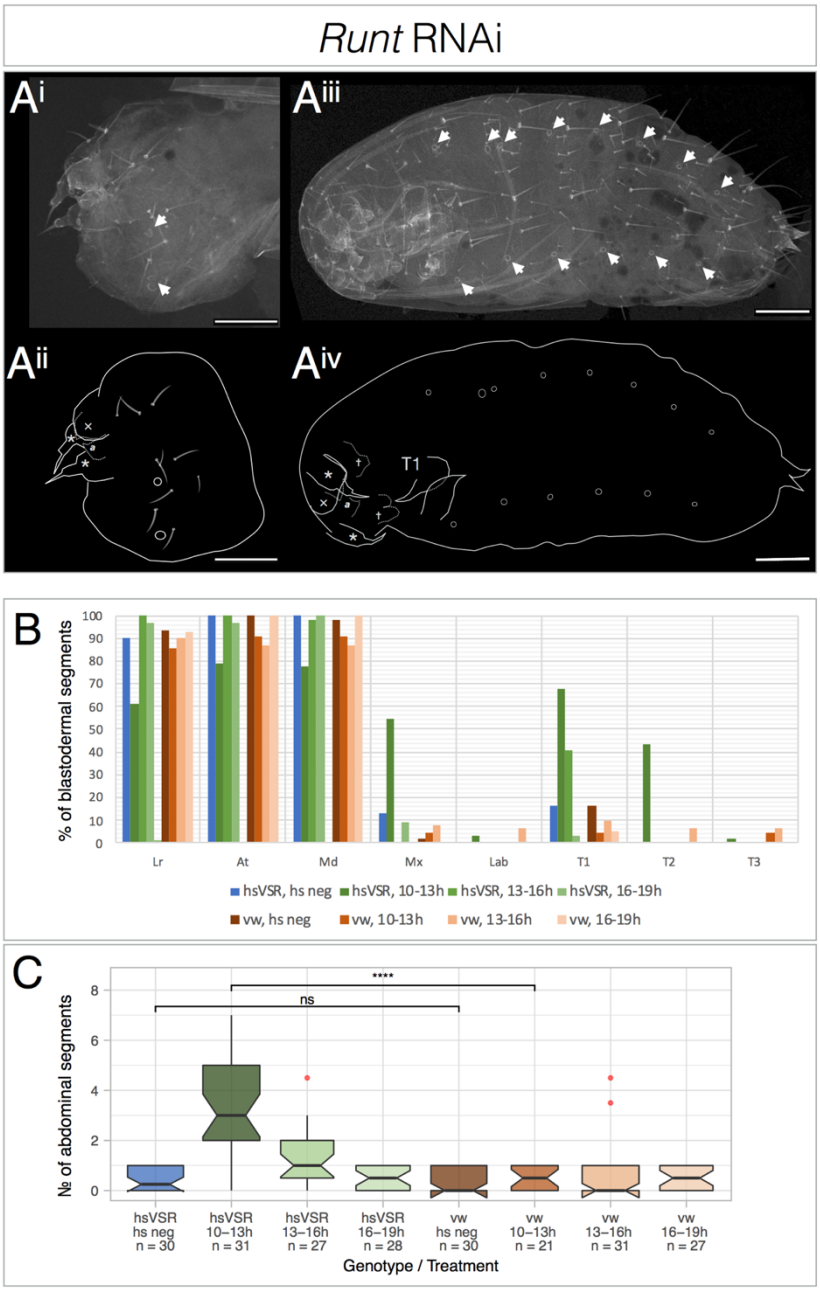

Figure 4.8 – RNAi of the segmentation clock: Tc-runt

pRNAi against the pPRG (*Tc-run*) results in loss of almost all gnathal, thoracic and abdominal segments, except for the mandibles (Md). Hs-treatment in the hsVSR line rescues segmentation. **(A)** Exemplary non-heat shocked (A^{i}) and heat shocked (A^{iii}) cuticles (line drawings of respective cuticles in A^{ii} and A^{iv}) after *Tc-run* RNAi in the hsVSR line. Except for the mandibles, no other gnathal, thoracic or abdominal segments are present, except for an occasional pair of stomata (see material and methods) (white arrows in A^{i}, A^{ii}). Hs-treatment lead to rescue of segmentation and resulted in cuticles with gnathal, thoracic and abdominal segments (A^{iii}, A^{iv}). Stomata indicative of abdominal segments marked by short white arrows in A^{iii} **(B)** Bar chart detailing the presence of blastodermal segment after *Tc-run* RNAi and different hs-treatment conditions in hsVSR and wild type (wv) line. While no heat shock treatment resulted in cuticles with only the mandibles remaining, hs-treatment further rescued maxillae and one thoracic segment. No rescue was observed in the RNAi wild type controls (vw). **(C)** Boxplot showing the number of abdominal segments for the cuticles of the corresponding conditions in B. Significant increase in abdominal segment number was observed after hs-treatment in the hsVSR line, but no recue was observed in the RNAi wild type controls (wv). Possible outliers (see material and methods) are marked in red.

4.1.3.3 Tc-odd-skipped

Tc-odd RNAi knockdown resulted in cuticles missing all segments posterior to the maxillae (Mx) (" † " in Fig. 4.9A[ii] and B), as previously published (see Choe et al., 2006). The median number of abdominal segments after *Tc-odd* RNAi was between 1 to 1.5 segments in both the non-heat shocked hsVSR and RNAi wild type control line (see "hs neg" in Fig. 4.9C). This phenotype is slightly weaker than the complete loss of abdominal segmentation described in Choe et al. (2006).

VSR expression at 10-13h is the only time point after *Tc-odd* RNAi at which a significant rescue of abdominal segments was observed in the hsVSR line when compared to the RNAi wild type control line. The median abdominal segment number increased to 3 with a small number of cuticles showing up to 8 rescued segments (Fig. 4.9C). One thoracic segment was the only blastodermal segment that was rescued (to 30%) (see "hs 10-13h" in Fig. 4.9B and C). There was no rescue of either blastodermal or abdominal segments in neither hsVSR nor RNAi wild type control line for the later hs-treatment time point ("hs 13-16h" in Fig. 4.9B and C)

Tc-odd, like the other two pPRG RNAi rescue experiments, has been repeated three times. While the first rescue experiment iteration failed to rescue any segments (Fig S7.8 A and B), in the second repetition were a few cuticles with an increased number of abdominal segments. In the statistical analysis, these cuticles were counterbalanced by others that had lost segments ("hs 10-13h" in Fig. S7.9B), again most likely due to heat shock damage. While a trend was indicated, statistical analyses revealed no significant increase for the early treatment time point (see Fig. S7.7B). Only the last repetition (the one presented above) showed significant rescue of abdominal segments when compared to both non-heat shocked hsVSR cuticles and hs-treated cuticles of the RNAi wild type control line.

In summary I found that a re-initiation of segmentation after breakdown is possible. I was able to show for each of the three pPRGs, at least once, that segmentation can be rescued with the hsVSR system. Rescue, however, does only appear possible when RNAi is inhibited at the transition from blastoderm to germband and the early stages of posterior segmentation (i.e. 10-13h). The median number of rescued abdominal segments was lower than the total number of abdominal segments in wild type L1 larvae and I never observed a "full rescue" to eight abdominal segments. Either the time needed to restore the

machinery necessary for segmentation (i.e. the segmentation clock) and the downstream effectors is too long to restore segmentation or there might be a “timing system” in place that tracts the overall time of development. This would also explain the decreasing efficacy of abdominal rescue with later hs-treatment time points.

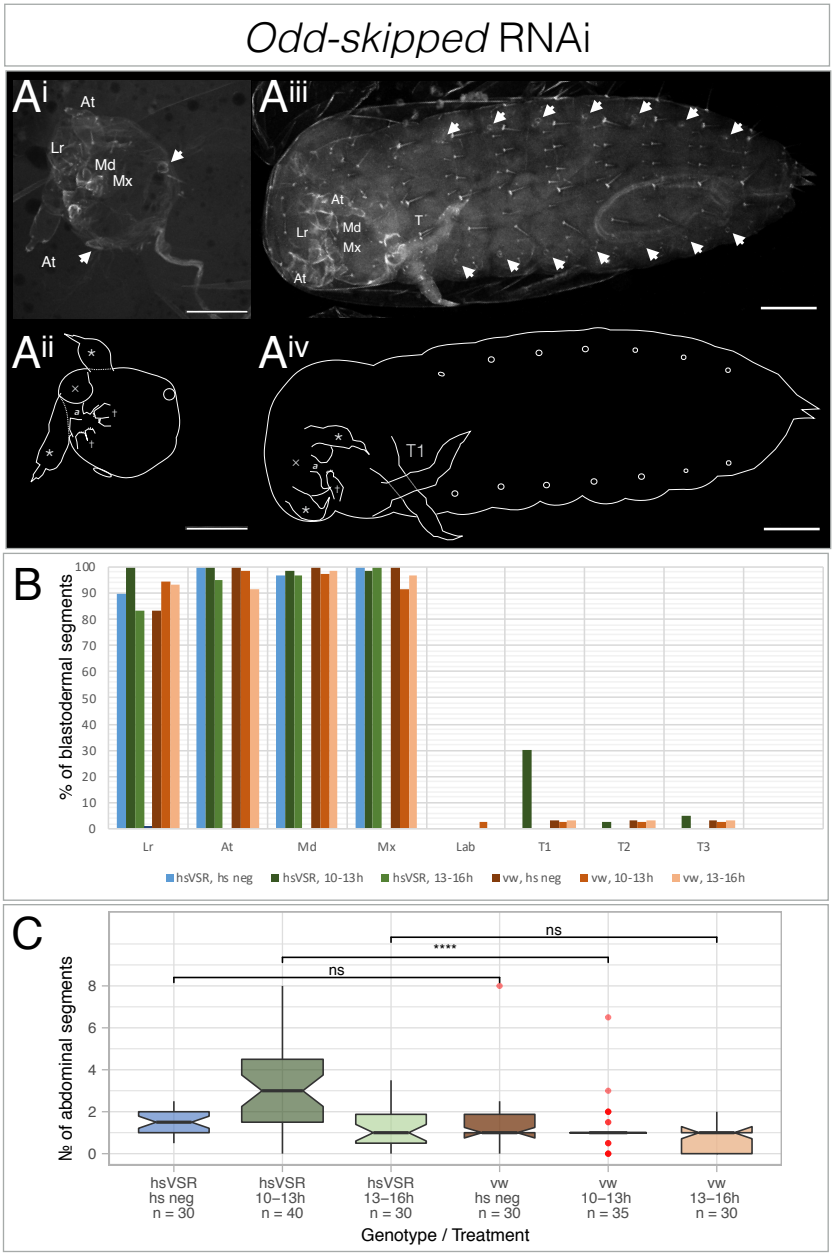

Figure 4.9 – RNAi of the segmentation clock: Tc-odd-skipped

pRNAi against the pPRG *Tc-odd* results in loss of gnathal, thoracic and abdominal segments posterior of the maxillae (Mx). Hs-treatment in the hsVSR line rescues segmentation. **(A)** Exemplary non-heat shocked (A^{i}) and heat shocked (A^{iii}) cuticles (line drawings of respective cuticles in A^{ii} and A^{iv}) after *Tc-odd* RNAi in the hsVSR line. Except for the Md (^{a}) and Mx (†), no other gnathal, thoracic or abdominal segments are present, except for one pair of stomata (see also material and methods) (white arrows in A^{i}, A^{ii}). Hs-treatment resulted in rescue of segmentation and cuticles one thoracic and abdominal segments (A^{iii}, A^{iv}). Stomata indicative of abdominal segments marked by short white arrows in A^{iii} **(B)** Bar chart detailing the presence of blastodermal segment after *Tc-odd* RNAi and different hs-treatment conditions in the hsVSR and wild type (wv) line. Non-heat shocked cuticles showed Md and Mx, but no other posterior segments. Hs-treatment in hsVSR rescued one thoracic segment. No rescue was observed in the RNAi wild type controls (vw). **(C)** Boxplot showing the number of abdominal segments for the cuticles of the corresponding conditions in B. Significant increase in abdominal segment number was observed after hs-treatment in the hsVSR line, but no recue was observed in the RNAi wild type controls (wv). Possible outliers (see material and methods) are marked in red.

4.2 *Tc-eve* RNAi rescue by hsVSR restores pPRG expression

To check whether the segmentation clock did indeed properly re-initiate after VSR rescue, I wanted to take a closer look at the expression of the segmentation clock genes before and after the expression of the VSR in pPRG RNAi germbands. Cuticle is secreted at the end of embryonic development and a lot of developmental processes (including potentially compensatory mechanisms) occur in-between VSR expression and cuticle secretion three days later. Hence, it was important to directly score for the re-establishment of the segmentation clock shortly after the hs-treatment.

For this purpose, I repeated the *Tc-eve* pRNAi, hs-treated embryos at the most efficient time point at 10-13h , fixed germbands shortly thereafter and visualized the gene expression of the primary pair-rule genes by Hybridization Chain Reaction (HCR, see Choi et al., 2018). *Tc-eve* RNAi was chosen because it showed the most robust response in the cuticle rescue experiments and because of its proposed position as the “first” pPRG to be activated within the segmentation clock.

4.2.1 Heat shock induced developmental delay

First, I needed to determine the appropriate time point for germ band fixation. Heat shocks applied to developing embryos are known to cause a developmental delay (Boos et al., 2018; Schinko et al., 2012). To be able to compare fixed non-heat shocked to hs-treated germbands, I needed to estimate that delay. This delay could be ignored when performing cuticle analysis because the end point of embryonic development is comparable even if different time was needed to reach it (L1 larvae in the case of cuticle analysis).

To that end, I performed *in-situ* hybridization for the segment polarity gene *Tc-wingless* (*Tc-wg*) and counted *Tc-wg* stripes in non-heat shocked and hs-treated embryos to compare their developmental age. While RNAi could further increase the developmental delay, I did not consider it in this analysis.

Three-hour egg lays of the hsVSR line (0-3h) were split into four groups (“hs neg 17-20h” representing a late segmentation stage, “hs pos 17-20h”, “hs pos 22-25h”, “hs pos 27-30h”). The “hs pos” groups were heat shocked as in the hsVSR treatments (at 10-13h 2h later) and all four were fixed at the given time points (see Fig. 4.10 for schematic overview).

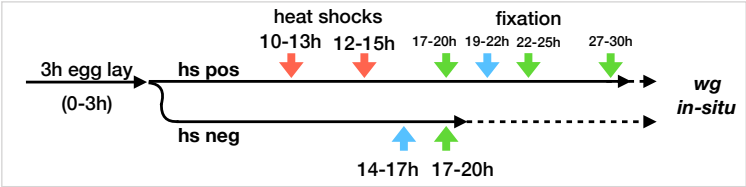

Figure 4.10 – Developmental delay after heat shock treatment, experimental procedure

Embryos were collected for 3h (0-3h) and either not hs-treated (hs neg) or hs-treated (hs pos) at 10-13h (the second hs-treatment at 12-15h is also indicated). "Hs neg" and "hs pos" embryos were fixed at time points indicated (14-17h, 17-20h, 19-22h, 22-25h, 27-30h) and *Tc-wingless* (*Tc-wg*) *in-situ* hybridization was performed.

In non-heat shocked germbands I observed a median number of 14 *Tc-wg* stripes (excluding the ocular and antennal stripes). The number of *Tc-wg* stripes in hs-treated embryos fixed at the same time was 0 (zero) and the germbands were barely elongated (not shown). This drastically demonstrated the introduced developmental delay by the hs-treatment at 10-13h. Heat shocked embryos fixed at 22-25h showed a median number of 6.5 *Tc-wg* stripes while embryos fixed at 27-30h showed a median number of 9 *Tc-wg* stripes with few germbands showing more than 10-12 or more stripes (see Fig.4.11A).

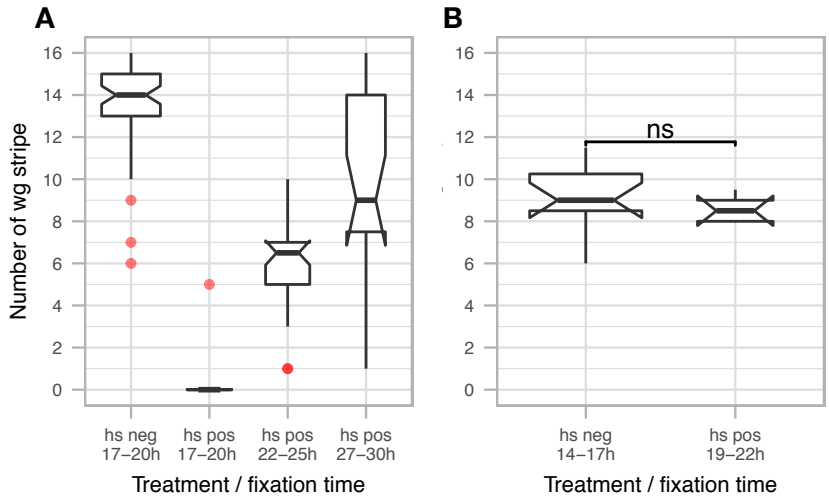

Figure 4.11 – Developmental delay after heat shock treatment

(A) Boxplot showing the number of *Tc-wg* stripes in germbands either non-heat shocked or heat shocked at 10-13h and fixed at different times after hs-treatment as indicated (see Fig. 4.10). Non-heat shocked germbands (fixed at 17-20h) showed a median of 14 *Tc-wg* stripes, while hs-treated germbands fixed at the same time show no *Tc-wg* stripes (counting started at the mandibular *Tc-wg* stripe). Hs-treated embryos fixed at 22-25h showed a median of 6.5 *Tc-wg* stripes and embryos fixed at 27-30h showed a median of 9 *Tc-wg* stripes. **(B)** Boxplot showing the number of *Tc-wg* stripes without heat shock treatment (hs neg) fixed at 14-17h and with heat shock treatment (hs pos) fixed at 19-22h. There is no significant difference between the number of *Tc-wg* stripes between these two time points. *Tc-wg* stripes were visualized by hybridization chain reaction. Possible outliers (see material and methods) are marked in red.

Non-heat shocked germbands were already close to being fully segmented (Nagy and Carroll, 1994). Therefore, I chose an earlier fixation time point (14-17h) to obtain germbands for the following HCR stainings that still undergo segmentation. Further tests revealed that non-heat shocked germbands fixed at 14-17h showed no significant difference in *Tc-wg* stripe numbers compared to hs-treated germbands fixed at 19-22h. see Fig. 4.11B.

In summary, I showed that the applied hs-treatment as shown in Fig. 4.12 resulted in a developmental delay of roughly 5h-6h compared to non-heat shocked embryos. Similar developmental delays after (a single) hs-treatment have been reported before (Boos et al., 2018). Knowing the introduced developmental delay and appropriate fixation time points, I could continue to investigate the rescue of segmentation observed in cuticles in more detail.

4.2.2 hsVSR treatment rescues pPRG expression in *Tc-eve* RNAi germ bands

One aim of my thesis was to reveal whether the rescue of segmentation observed in cuticles depends on the re-initiation of segmentation clock gene expression. I therefore performed parental *Tc-eve* RNAi in the hsVSR and RNAi wild type control line. The resulting embryos from both hs-treated and non-heat shocked samples were fixed according to the scheme in Fig. 4.12.

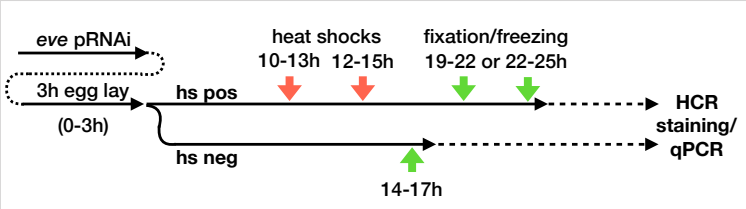

Figure 4.12 – Tc-eve RNAi for HCR/qPCR sample collection, experimental procedure

Tc-eve pRNAi was performed in hsVSR animals. Eggs were collected for 3h (0-3h). Non-heat shocked embryos (hs neg) were either fixed and flash frozen in liquid nitrogen at 14-17h. Heat shock treated embryos (hs pos) were either fixed or frozen in liquid nitrogen at time points indicated. Embryos for HCR stainings were stored in MeOH at -20°C. Samples for qPCR analysis were stored at-80°C until further processing.

In fixed germband embryos I analyzed the expression of the primary pair-rule genes *Tc-eve*, *Tc-run*, and *Tc-odd* as well as the segment polarity gene *Tc-wg* as a segmental marker. The expressions of the genes were detected by HCR. HCR utilizes a chain reaction amplification of signal by fluorescently labelled DNA amplifiers which can bind to amplifier-specific

labelled DNA probes that bind specifically to the target transcripts (Choi et al., 2018). I used the unaffected and dynamic *Tc-wg* expression in the head in order to stage germ bands (see Fig. S7.11 for *Tc-wg* staging overview). A comparison of this staging between the *Tc-eve* RNAi samples showed that the germbands, both hs-treated and non-heat shocked for both lines (hsVSR and v^w), were in a similar developmental stage (Fig. 4.13A). In a second head stage analysis, I compared the *Tc-wg* head stage between both hs-treated and non-heat shocked non-RNAi wild type v^w to eliminate the possible influence of the RNAi in the first analysis. This second analysis revealed that there might have been a slight age difference between the two chosen time points based on *Tc-wg* head stages (Fig. 4.12B). This difference, however, was not statistically significant. The non-RNAi germbands were also in a slightly later *Tc-wg* head stage than the *Tc-eve* RNAi germbands (despite the same fixation time), probably due to the RNAi itself (compare Fig. 4.13 A to B). These two head stage analyses confirmed that my fixation time points were chosen in a way that enabled me to compare non-heat shocked and heat shocked embryos.

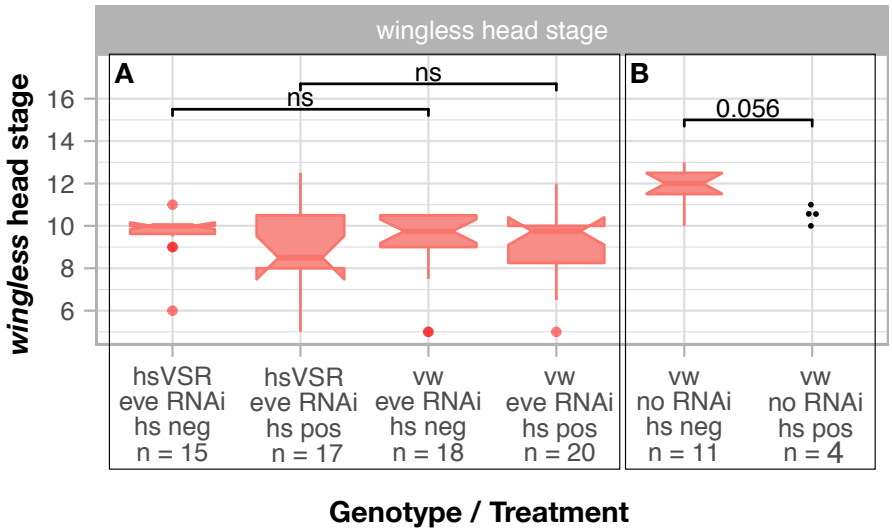

Figure 4.13 – Tc-wg head stage analysis in non-heat shocked and heat shocked germband

Boxplots showing the *Tc-wg* head stage compared between germbands without (hs neg) and with hs-treatment (hs pos) used for HCR stainings and pPRG stripe analysis. **(A)** Comparisons between germbands from the hsVSR and RNAi wild type control (vw) lines. After *Tc-eve* RNAi and fixed at different time points to compensate for the developmental delay due to hs-treatment, they showed no significant differences in *Tc-wg* head stages. **(B)** Comparison between non-heat shocked and heat shocked vw germbands without RNAi. Comparison between *Tc-wg* head stages showed a non-significant difference between the samples. For *Tc-wg* head stage overview, see Fig. S7.12. Possible outliers (see material and methods) are marked in red.

In non-heat shocked *Tc-eve* RNAi hsVSR germbands, both the ocular and antennal *Tc-wg* stripes as well as the posterior *Tc-wg* domain patterned normally (see Fig.4.14 A^{vii}). The same was true for non-heat shocked *Tc-eve* RNAi vw wildtype control germ bands (Fig. 4.15A^{vii}). In the trunk of both non-heat shocked hsVSR and vw germbands, I found a broad (i.e. not segmental) but weak *Tc-wg* expression domain.

Interestingly, *Tc-eve* RNAi did not lead to a complete loss of *Tc-eve*, *Tc-run*, and *Tc-odd* expression, as was previously reported (Choe et al., 2006). Rather, *Tc-eve* expression was still present in the posterior of the germband, but most often failed to resolve into proper stripes (Figs. 4.14A^{i} and Fig. 4.15A^{i}). Also, both the anterior unsegmental *Tc-wg* and the posterior unsegmental *Tc-eve* expression were always non-overlapping, forming a boundary in the germband (see Figs. 4.14A^{vi} and 4.15 A^{vi}). Also noticeable was the fact that *Tc-eve* RNAi germbands did not elongate properly and sometimes developed a "bulge" or thickening along the AP axis (often within the broad *Tc-wg* domain, not shown).

In *Tc-eve* RNAi germband without hs-treatment, both *Tc-run* and *Tc-odd* were expressed in stripes but only to some degree (arrowheads in Figs. 4.14A^{iii}/A^{v} and 4.15A^{iii}/A^{v}). These expressional stripe of *Tc-run* and *Tc-odd*, were, compared to wild type (Choe et al., 2006), irregular and poorly resolved. However, if present, the relative positions of the expression stripes were more or less retained. There were no obvious differences in the expression of the pPRGs and *Tc-wg* when comparing non-heat shocked hsVSR germbands with the non-heat shocked RNAi wild type control (vw) germbands, indicating that the *Tc-eve* RNAi had a very similar effect in both lines.

Upon hs-treatment and VSR expression, the expression of *Tc-wg* in *Tc-eve* RNAi germbands did change dramatically. Instead of the unresolved expression domain, segmental *Tc-wg* stripes were formed along the AP axis (arrowheads Fig. 4.14B^{vii}). In addition, also all three pPRG show expression in stripes largely resembling the wildtype pattern (Choe et al., 2006) (arrowheads in Fig. 4.14B^{i}, B^{ii}, and B^{v}). Furthermore, germbands after hs-treatment were elongating, at least in the more posterior region (Fig. 4.14B and not shown). In contrast, in the RNAi wild type control line, hs-treatment did not cause any change in the expression of *Tc-wg* (Fig. 4.15B^{vii}) nor any apparent change in the expression of the pPRGs (Fig. 4.15 B^{i}, B^{iii} and B^{v}).

The presence of remaining *Tc-eve* transcript in non-heat shocked *Tc-eve* RNAi germbands was surprising and contradicted published results (Choe et al., 2006). One explanation

might be the optimization of the dsRNA concentration to a comparably low level. With this optimization, the RNAi still produced a highly penetrant and strong cuticle phenotype (around 1 µg/µl), but did not aim for complete removal of transcripts. Higher concentrations might have led to a stronger reduction of residual mRNA. A second explanation could be that in RNAi only cytoplasmic mRNA is destroyed while nuclear pre-mRNA remains intact. The observed *Tc-eve* signal in *Tc-eve* RNAi germ bands might thus well be nuclear (pre-)mRNA.

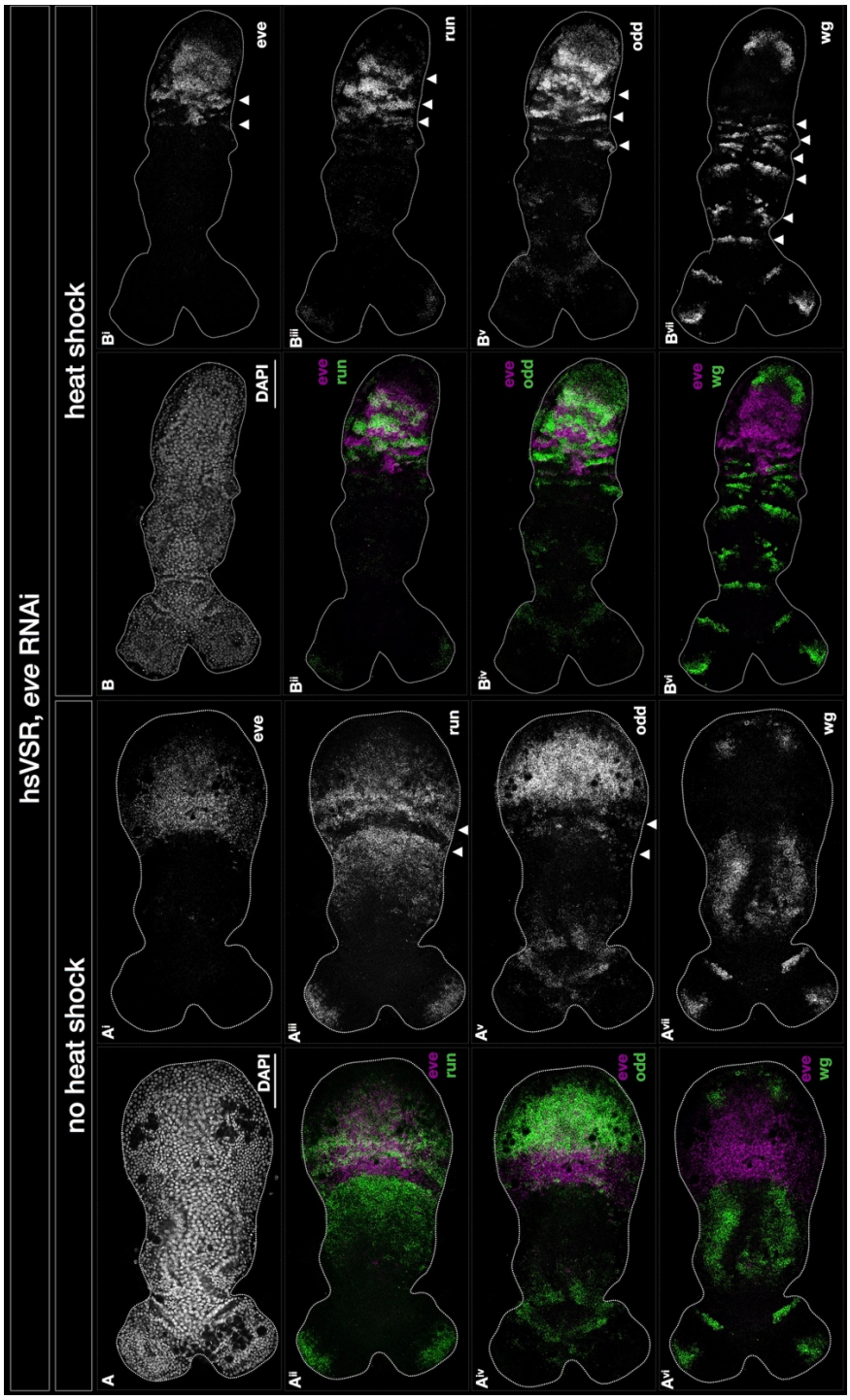

Figure 4.14 –pPRGs and Tc-wg expression after Tc-eve in hsVSR germbands

Anterior to the left. Morphology of germbands visualized by DAPI staining (A, B). Non-heat-shocked (A-A^{vii}) and heat shocked (B-B^{vii}) germbands of the hsVSR line after parental *Tc-eve* RNAi. HCR staining was performed for the three pPRGs *Tc-eve* (*eve*; A^{i} and B^{i}), *Tc-run* (*run*; A^{iii} and B^{iii}) and *Tc-odd* (*odd*; A^{v} and B^{v}) and the segmental marker *Tc-wg* (*wg*; A^{vii} and B^{vii}). Without hs-treatment, both the pair-rule stripes of *Tc-eve* (A^{i}) and the segmental stripes of *Tc-wg* (A^{vii}) are lost, indicating the breakdown of segmentation, while expression of *run* and *odd* (A^{v}) still appear somewhat striped (arrowheads in A^{iii} and A^{v}). Expression of *Tc-eve* and *Tc-wg* portion the embryo into an anterior and posterior half and never overlap (A^{vi}). Upon hs-treatment, pPRG stripes of *Tc-eve*, *Tc-run* and *Tc-odd* returned (arrowheads in B^{i}, B^{iii}, B^{v}), as did the segmental stripes of *wg* (arrowheads in B^{vii}), indicating the proper re-initiation upon VSR expression. See text for further details. Scale is 100µm.

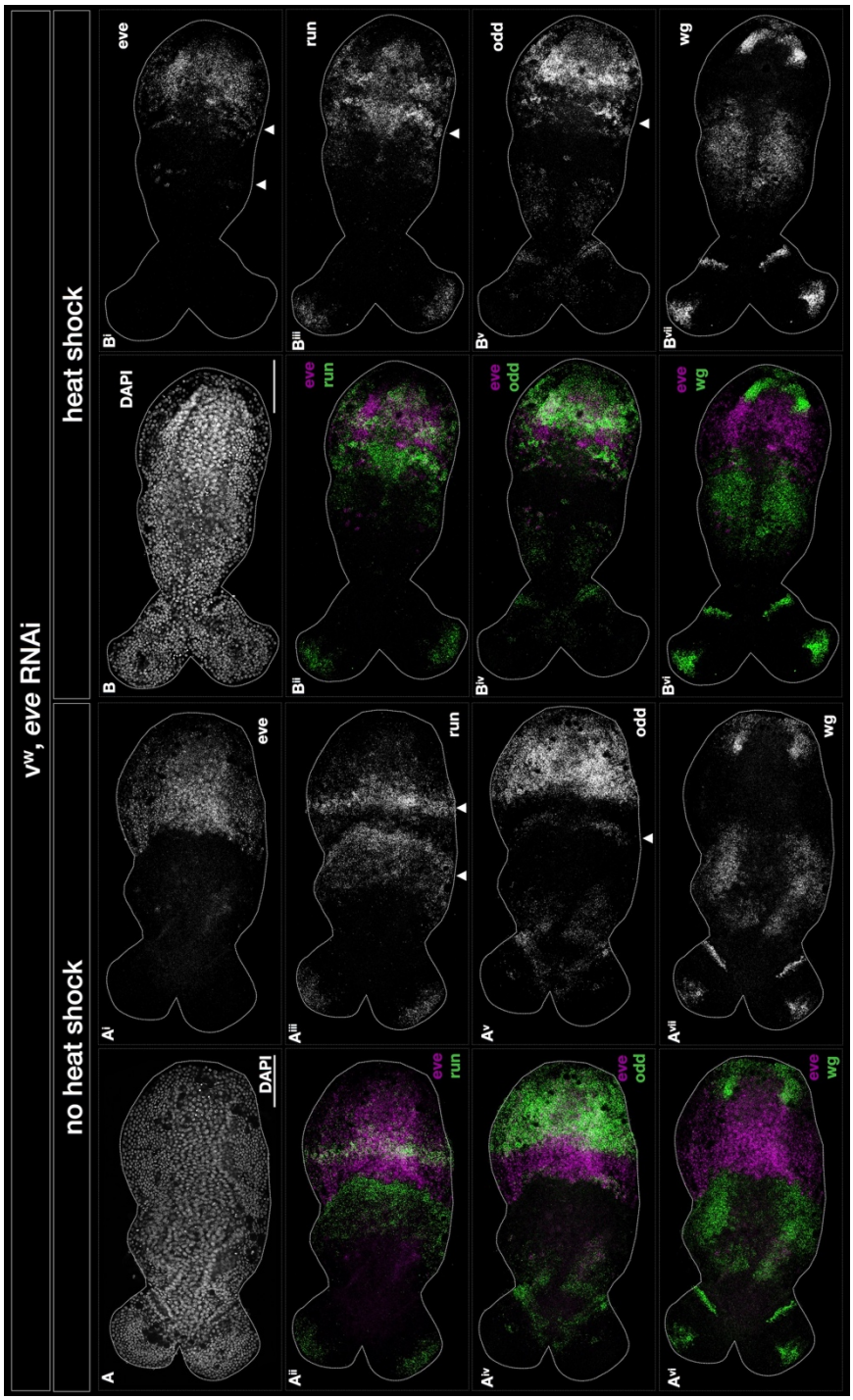

Figure 4.15 – pPRGs and Tc-wg expression after Tc-eve RNAi in vw germbands

Anterior to the left. Morphology of germbands visualized by DAPI staining (A, B). Non-heat-shocked (A-A^{vii}) and heat shocked (B-B^{vii}) germbands of the vw line after parental *Tc-eve* RNAi. HCR staining was performed for the three pPRGs *Tc-eve* (*eve*; A^{i} and B^{i}), *Tc-run* (*run*; A^{iii} and B^{iii}) and *Tc-odd* (*odd*; A^{v} and B^{v}) and the segmental marker *Tc-wg* (*wg*; A^{vii} and B^{vii}). Without hs-treatment, expression patterns are comparable to the non-heat shocked germbands *Tc-eve* RNAi germbands in Fig. 4.14. Both the pair-rule stripes of *Tc-eve* (A^{i}) and the segmental stripes of *Tc-wg* (A^{vii}) are lost, indicating the breakdown of segmentation. Upon hs-treatment, the expression of pair-rule stripes of all three pPRGs and of the segmental marker was unchanged. See text for further details. Scale is 100µm.

4.2.3 Significant increase in *Tc-wg* stripe number reflects rescue of segmentation

To quantify the rescue of segmentation by VSR expression, I counted the number of *Tc-wg* stripes for all conditions and treatments in all documented embryos (see Fig. S7.12). Comparing the number of *Tc-wg* stripes by Mann-Whitney U tests revealed a significant increase in *Tc-wg* stripes expressed in hs-treated *Tc-eve* RNAi hsVSR germbands ("hs pos" in Fig. 4.16D) compared to *Tc-eve* RNAi wild type control germbands. Comparison of non-heat shocked germ bands of both lines did not show any significant differences ("hs neg" in Fig. 4.16D). The significant increase in segmental *Tc-wg* stripes is an early reflection of the increase in segments in hs-treated *Tc-eve* RNAi cuticles of the hsVSR line (see Fig.4.7C).

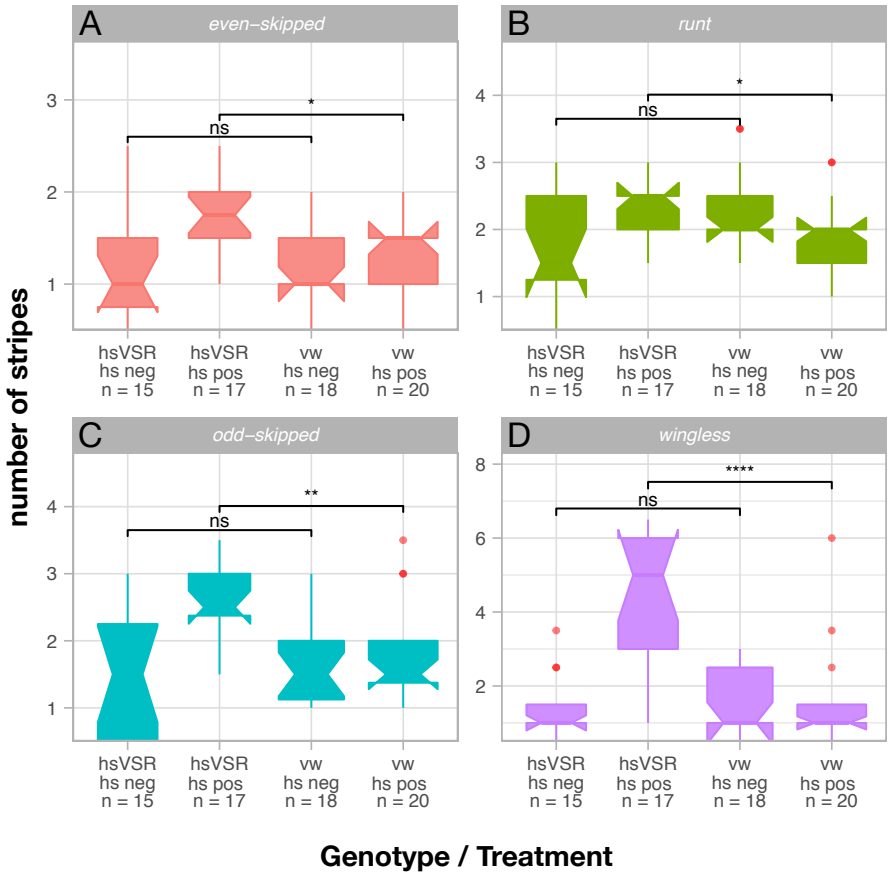

Figure 4.16 – Quantification of pPRG stripes after Tc-eve RNAi in germbands

Boxplots showing the number of pair-rule **(A-C)** and segmental *Tc-wg* **(D)** stripes. Comparisons of stripes between heat shocked hsVSR and RNAi wild type control germbands showed a significant increase in the number of both pair-rule and segmental stripes, further supporting the re-initiation of segmentation after VSR expression. No significant changes between hsVSR and RNAi wild type control (vw) germbands without heat shock treatment were seen. Possible outliers (see material and methods) are marked in red.

4.2.4 Re-initiation of segmentation is further supported by pPRG stripe numbers and rescue classes

I also performed quantification of pPRG stripes in non-heat shocked and hs-treated germbands of both the hsVSR and RNAi wild type control lines. Quantification and comparisons by Mann-Whitney U tests revealed a significant increase of their number in hsVSR germbands after hs-treatment when compared to hs-treated RNAi wild type controls (Figs. 4.16A, B and C). This further explains both the increase in *Tc-wg* stripes (Fig 4.16D) as well as the subsequent rescue of segmentation in cuticles (Fig. 4.7C).

Because quantifying the low number of pPRG stripes might obscure the signal, I complemented the analysis with a second method to compare pPRG expression of non-heat shocked to hs-treated germbands. I sorted all well documented germbands into three different classes: “Close to WT” (WT), “intermediate” (+/-) and “all stripes lost” (-) for each of the three pPRGs (see Figs. S7.12 for all documented germ bands in their respective classes). Germ bands in the “WT” class were those that showed pPRG expression that appeared close to normal (hence “wild type”) (e.g. *Tc-eve* pattern in embryo “1a” in Fig. S7.12A). The “intermediate” class contained all germ bands whose pPRG expression was clearly not wild type, but they still showed some sort of striped pattern (e.g. *Tc-eve* pattern in embryo “4b” in Fig. S7.12A). The “all stripes lost” class contained all those germ bands in which the pPRGs had lost their striped expression pattern altogether (e.g. *Tc-eve* pattern in embryo “3a” in Fig. S7.12A). This classification was done for each of the pPRGs individually. Comparisons of the proportions of the three classes for each treatment and gene by Chi-Square tests (with Monte Carlo simulations, see material and methods) were performed. They revealed a significant difference for the *Tc-eve* stripe classes between heat shocked hsVSR germbands and heat shocked vw germ bands. The “intermediate” class increased in proportion, mainly at the expense of the “all stripes lost” class (see Fig. 4.17A). For the other two pPRGs, *Tc-run* and *Tc-odd*, a respective trend appears to be present. I observed a decrease in the proportions of the “all stripes lost” class upon hs-treatment in the hsVSR line, but the p-values (0.08 for *Tc-run* and 0.1 for *Tc-odd*) did not reach significance levels (Fig. 4.17B and C). The result for the *Tc-eve* stripes, however, further supports the result that segmentation is rescued after RNAi breakdown due to proper re-initiation of pPRG and subsequent segmental *Tc-wg* expression

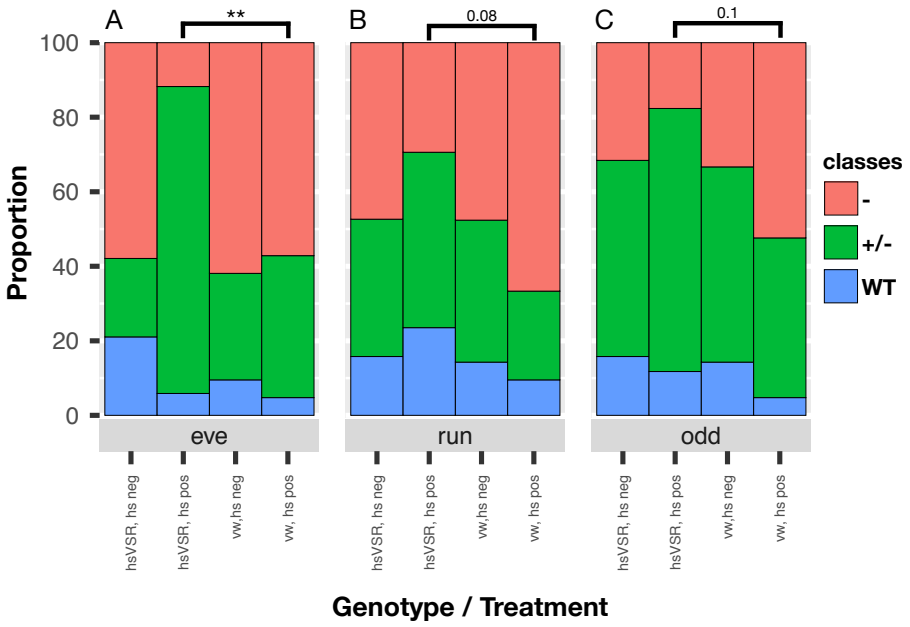

Figure 4.17 – pPRG rescue classes after Tc-eve RNAi in germbands

Stacked car charts showing the proportions of each rescue class (Close to WT ("WT"), intermediate ("+/-") and all stripes lost ("-") within each treatment condition for the three pPRGs after *Tc-eve* RNAi. Rescue classes are colour-coded and indicated to the right. Treatment conditions are indicated below each bar. Germbands used for rescue classification were the same germbands used for the analysis in Fig. 4.16. Significant differences were observed in the proportion of the rescue classes for *Tc-eve* stripes after hs-treatment in the hsVSR line when compare to the RNAi wild type control (A). All other comparisons were non-significant, but a general trend was observable. Increase of the "intermediate" often at the expense of the "all stripes lost" class can be observed for hs-treated hsVSR germbands (B and C). See Fig. S7.12 for all imaged and classified germbands.

4.2.5 *Tc-eve* RNAi does not cause breakdown of the SAZ

The re-initiation of segmentation indicated that the SAZ itself might be unaffected by pPRG RNAi-mediated breakdown of segmentation. I asked whether *Tc-eve* RNAi caused loss of segmentation "only" due to loss of regular pPRG expression (i.e. breakdown of the segmentation clock) or if *Tc-eve* RNAi also had a reciprocal influence on the SAZ itself. Therefore, I detected the expression of the SAZ marker genes *Tc-cad* and *Tc-wg* in *Tc-eve* RNAi embryos using HCR to visualize the SAZ and score SAZ independent gnathal and thorax and SAZ dependent abdominal segmentation.

Tc-wg expression was not segmental in any of the screened *Tc-eve* RNAi germbands but expressed in a broad domain anterior of the SAZ. The non-segmental posterior *Tc-wg* expression was present (Fig. 4.18). The expression of *Tc-cad* was still present in the posterior of screened germbands and similar to the expression in wild type germbands (Copf et al., 2004). (Fig. 4.18). Thus, the SAZ itself, judged by the expression of *Tc-cad* and

Tc-wg, appeared intact and restricted to the posterior region of the elongating embryo. Therefore, *Tc-eve* RNAi did not lead to breakdown of the SAZ. This is in line with a model where *Tc-eve* (and the segmentation clock) acts downstream of the SAZ genes *Tc-cad* and *Tc-wg* / "posterior signaling center" (Fig. 2.5A).

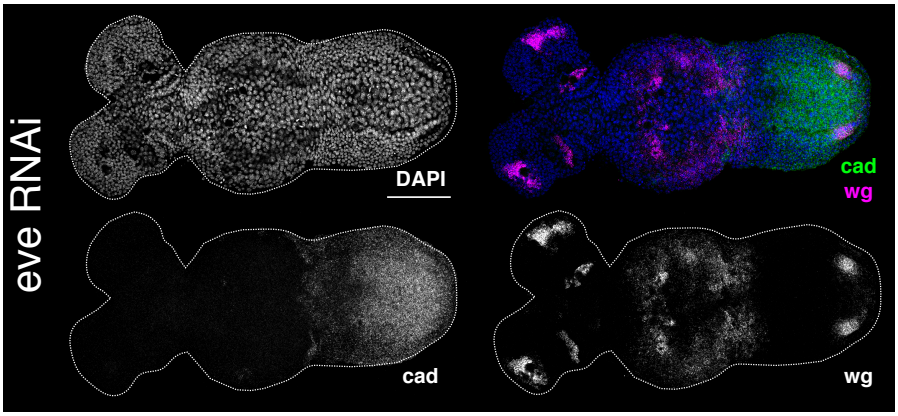

Figure 4.18 – Tc-cad and Tc-wg expression after Tc-eve RNAi

Anterior to the left. HCR staining for *Tc-cad* and *Tc-wg* in a non-heat shocked germband after *Tc-eve* RNAi. *Tc-cad* is still expressed in the posterior in the SAZ. Counterstaining with *Tc-wg* shows loss of segmental stripes and breakdown of segmentation. *Tc-wg* expression in the head and the SAZ was unaffected. Scale is 100µm

4.3 qPCR reveals possible autoregulation of *Tc-eve*

While *Tc-eve* RNAi was effective enough to cause a severe and highly penetrant phenotype in both cuticles and in the germband (Figs. 4.7, 4.14 and 4.15), I still wanted to quantify both the RNAi knockdown and VSR rescue efficiencies in greater detail. To that end, I performed q PCR for the three pPRGs *Tc-eve*, *Tc-run* and *Tc-odd*, the VSR open reading frame, and intronic *Tc-eve* transcripts. The latter was included because of the HCR results that suggested that I might have uncovered autoregulation of *Tc-eve*, causing upregulation of *Tc-eve* transcripts (including pre-mRNA still containing intronic sequences) upon its RNAi. I used the same time points as in in the HCR experiment (see schematic in Fig. 4.12) for the sample collection of both non-heat shocked and hs-treated hsVSR and vw wildtype RNAi control embryos. Unfortunately, due to the nature of the hsVSR experiments I was only able to secure one biological replicate for the most important and interesting time points: non-heat shocked and treated *Tc-eve* RNAi in hsVSR.

As expected, the VSR expression was increased in the hs-treated but not in the non-heat shocked samples of the hsVSR line. Also, no VSR signal was detected in the wild type

controls upon hs-treatment since they did not contain the heat shock reactive transgene (not shown). Heat shock treatment alone (no RNAi) reduced the amount of transcript for all three pPRGs (see “xxx, pos” in Fig. 4.19 or Tbl. 4.1) in both the hsVSR and wild type control.

Surprisingly, *Tc-eve* RNAi did reduce the amount of *Tc-eve* transcript only slightly more efficiently than the hs treatment alone (without RNAi) (compare “xxx, neg” to “*eve*, neg” in Fig. 4.19 or Tbl. 4.1). *Tc-eve* RNAi did also, however, reduce the amount of transcript of the other two pPRGs, *Tc-odd* and *Tc-run*. Given the strong phenotype and the clear rescue upon hs-VSR treatment, it was surprising that *Tc-eve* itself was neither strongly downregulated nor rescued by hs-VSR treatment. However, gene regulation acts in the nucleus while RNAi acts in the cytoplasm. If the gene is upregulated in the nucleus by an autoregulatory loop it could happen that *Tc-eve* mRNA in the cytoplasm is reduced (inducing the phenotype) while its transcript abundance in the nucleus is enhanced (obscuring the cytoplasmic reduction). In order to test this, we included an intronic probe for *Tc-eve*, which would report nuclear pre-mRNA but not cytoplasmic mRNA. Indeed, I observed that the amount of intronic *Tc-eve* transcript upon *Tc-eve* RNAi was strongly increased. This increase was detected in all *Tc-eve* RNAi samples except for where the RNAi effect had been inhibited by hsVSR treatment (“hsVSR, *eve*, pos” in “*eve* intron” in Fig.4.19 and Tbl.4.1). These results are in line with a scenario where *Tc-eve* RNAi first caused a decrease in *Tc-eve* mRNA, eventually resulting in upregulation (or de-repression) of *Tc-eve* transcription, resulting in more pre-mRNA. Since mature transcripts were degraded upon nuclear export, only premature transcripts remained. This is further supported by the fact that RNAi rescue by VSR expression in the hsVSR line returned the intronic expression signal to normal. That is because a rescue of *Tc-eve* expression would cause a return to a more normal *Tc-eve* regulatory situation. It would also explain the *Tc-eve* HCR signal observed in *Tc-eve* RNAi germbands (see Fig. 4.14 and 4.15).

In summary, the qPCR results hints to an unexpected (and as of yet unpublished) autoregulation of *Tc-eve* transcription, which compensates for the cytoplasmic RNAi mediated *Tc-eve* decay.

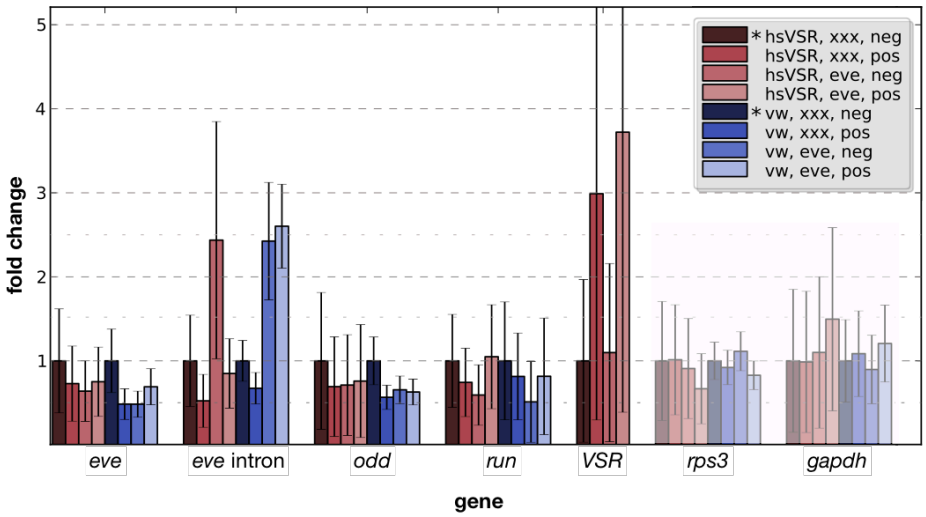

Figure 4.19 – qPCR gene expression fold changes after Tc-eve RNAi and hsVSR rescue

qPCR analysis of *Tc-eve* RNAi (eve) and non-RNAi (xxx) embryos showing fold changes in gene expression with and without hs-treatment in the hsVSR and wild type (vw) line. Samples conditions are indicated in the upper right corner. qPCR analysis was performed for coding regions of the three pPRGs *Tc-eve* (*eve*), *Tc-run* (*run*), and *Tc-odd* (*odd*), the expressed VSR (*VSR*), and intronic *Tc-eve* (*eve* intron). Normalization was performed using two house-keeping genes (*rps3* and *gapdh*). See text for details.

Table 4.1 – qPCR gene expression fold changes after Tc-eve RNAi and hsVSR rescue

line	RNAi	treatment	***eve***	***odd***	***run***	***eve* intron**	**VSR**
hsVSR	xxx	neg	1	1	1	1	1
hsVSR	xxx	pos	0.73	0.69	0.74	0.52	2.99
hsVSR	*eve*	neg	0.64	0.71	0.59	2.44	1.1
hsVSR	*eve*	pos	0.75	0.76	1.05	0.85	3.72
vw	xxx	neg	1	1	1	1	x
vw	xxx	pos	0.49	0.57	0.81	0.67	x
vw	*eve*	neg	0.48	0.66	0.51	2.43	x
vw	*eve*	pos	0.69	0.63	0.82	2.6	x

(values indicated are corresponding to bar charts in Fig. 4.19)

4.4 Gap genes are unlikely a timing factor for the segmentation clock

Another observation of the cuticle rescue in section 4.1.3 was that the time point of the VSR expression (i.e. hs-treatment) after *Tc*-eve RNAi appeared to have a strong influence on the number of rescued abdominal segments. Since the blastodermal structures are pattered early i.e. during the blastoderm stages, the rescue of blastodermal structures is logically linked to the early expression of the VSR. It was, however, unclear if the

breakdown of segmentation by *Tc-eve* RNAi and subsequent rescue would restart abdominal segmentation from the "beginning" or if after the rescue segmentation resumes from a place in time defined by an unknown timing mechanism that is not the segmentation clock itself. Since segmentation has to stop at some point, a mechanism is necessary that detects this point in time during development. I already shortly discussed that the time needed to restore the genetic machinery necessary for segmentation might take too long to restore abdominal segments after a late hs-treatment. Another, possibly complementary explanation could be the presence of an overall timing mechanism to track development and/or patterning time, and to provide a "stop signal" for said processes.

I showed that the SAZ itself does not seem to be impacted by *Tc-eve* RNAi (Fig. 4.18), meaning that other processes requiring the SAZ could still function. This assumption is based on the continued expression of *Tc-cad*, the putative "speed regulator" molecule (see introduction). It is known that the gap gene cascade, the sequential expression and posterior-to-anterior propagation of the gap genes from the SAZ, is controlled by *Tc-cad* (Boos et al., 2018). The gap gene network is also considered a candidate to convey the information necessary for segmentation timing and termination (Andrew Peel, personal comm.; Clark et al., 2019).

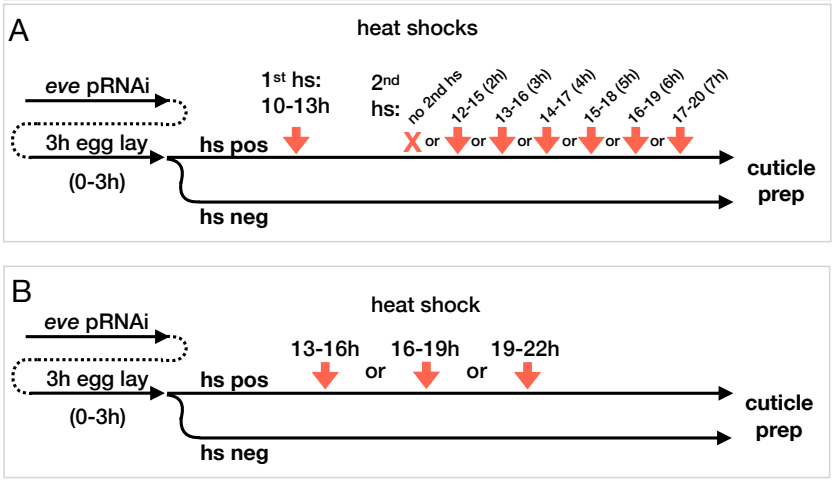

Figure 4.20 – Reset of the putative patterning timing factor, experimental procedures

For both experiments, *Tc-eve* pRNAi was performed in the hshb line and crossed to the hsVSR line. Embryos were collected for 3h (0-3h) and either heat shock treated (hs pos) or not (hs neg). **(A)** Influence of early rescue and putative timer reset at later time point. All embryos (except hs neg) received the first hs-treatment at 10-13h. The second hs-treatment was given as indicated in the A (no 2nd hs-treatment to 7h after first hs-treatment). **(B)** Influence of later rescue and putative timer reset. All embryos (except hs neg) received hs-treatment once as indicated in B.

Recently, it was shown that the ectopic expression of the *Tribolium* gap gene *Tc-hunchback* (*Tc-hb*) (hs-hb, see Distler, 2012) is resetting (or restarting) the gap gene cascade in *Tribolium* (Boos et al., 2018). Utilizing this restart of the gap gene cascade, I wanted to test the hypothesis that the gap gene network might be the aforementioned timing mechanism that acts independently of the segmentation clock.

I made use of the fact that both the VSR expression and the ectopic expression of *Tc-hb* necessary for the gap gene cascade restart require heat shock treatment. The idea was to perform *Tc-eve* RNAi (i.e. disrupting segmentation) in a cross of the both lines (hsVSR × hshb) and, by hs-treatment, both rescue the *Tc-eve* RNAi while simultaneously restart the gap gene cascade at different time points during germ band extension.

In the first experiment (Fig. 4.20A), embryos in total received two heat-shocks. A first early heat shock at 10-13h and then a second heat shock after different intervals (from 2h to ca.7.5h after the first one). The idea behind this was that the first heat shock at 10-13h rescues the *Tc-eve* RNAi (as previously shown, see section 4.1.3) and also restarts the gap gene cascade (Boos et al., 2018). A second heat shock would, for a second time, inhibit *Tc-eve* RNAi and restart the gap gene cascade, this time during rescued segmentation. This second hs-treatment would reset the putative segmentation timer and results in cuticles with more abdominal segments compared to cuticles from “normal” hsVSR rescue experiments (section 4.1.3).

In the second experiment (Fig. 4.20B), only a single heat shock treatment was applied at three different time points (13-16h, 16-19h, or 19-22h) to rescue both *Tc-eve* RNAi and reset the gap gene cascade (i.e. the timing mechanism) at the same time. These three time points are later than the time point for which efficient rescue of *Tc-eve* RNAi by the hsVSR system was shown (section 4.1.3). If the gap gene cascade does act as a timer for segmentation, one would expect rescue of segmentation after *Tc-eve* RNAi at later time points than previously shown.

Unexpectedly, *Tc-eve* RNAi in the cross hsVSR × hshb was much less efficient than in homozygous hsVSR (compare “hs neg“ in Fig. 4.21 to Fig. 4.7C). Non-heat shocked cuticles showed an average of 4.5 and 3.75 abdominal segments, in the first and second experiment, respectively (see “hs neg” Fig 4.21A and B). A less efficient RNAi was also observed for the blastodermal segments (compare “hs neg” in Figs. S7.10A and B to Fig. 4.7B).

In the first experiment (Fig. 4.21A), the single heat shock treatment at 10-13h significantly increased the median number from 4.5 to 6 abdominal segments (Fig. 4.21A, “hs pos (once)”). In cuticles with two hs-treatments, 2h apart, the efficacy of the rescue further and significantly increased (this hs-treatment conditions are comparable to the hs-treatment in the previous pPRG rescue experiment, section 4.1.3). However, these rescued cuticles already showed eight abdominal segments (which is the wild type number of abdominal segments of L1 larvae). A comparison between this rescue experiment and the one in Fig. 4.7 (*Tc-eve* RNAi in the homozygous hsVSR line) showed a similar number of rescued abdominal segments (3-3.5 segments, median to median). Whether this was due to a similar rescue efficacy or because the maximum number of abdominal segments is eight and therefore the rescue in this experiment couldn’t get more efficient remains unclear. Interestingly, the rescue efficacy for samples with an increased time between hs-treatments did not immediately decline, but remained stable for hs-treatment intervals up to 5h (Fig. 4.21A). Only if the interval between hs-treatment was more than 5h the median efficacy of abdominal segment rescue declined. But it never dropped below the median of the sample that received only a single heat shock treatment. Importantly, only few cuticles showed supernumerical numbers of abdominal segments (~3% (n=30) in “6h apart”,~6% (n=30) in “4h apart” and “6h apart”, ~8% (n=26) in “7.5h apart” and ~13% (n=30) in “3h apart”, see Fig. 4.21A). For homozygous hshb cuticles additional trunk segments were reported in 30-40% of the analyzed cuticles after hs-treatment at 10-13h AEL, (Distler, 2012). I observed even less additional segments. Therefore, I did not consider those few to be an example of resetting the segmentation clock and timer. Given the weak *Tc-eve* phenotype these experiments, however, remain preliminary and need to be repeated.

In the second experiment (Fig. 4.21B), where samples were given only a single heat-shock, the median number of abdominal segments in non-heat shocked cuticles, as mentioned above, was 3.75 segments (and therefore again higher than the number of abdominal segments in homozygous hsVSR cuticles after *Tc-eve* RNAi, see Fig. 4.7C). Neither rescue nor supernumerary abdominal segments could be observed for any of the hs-treatment time points (Fig. 4.21B). I already knew from the *Tc-eve* RNAi rescue experiments in homozygous hsVSR embryos (section 4.1.3) that hs-treatment later than 10-13h AEL was unlikely to rescue abdominal segmentation (Figs .4.7C, S7.4B). The fact that the reset of the

gap gene cascade in combination with the *Tc-eve* RNAi rescue did also not result in an increase of abdominal segments, compared to non-heat shocked embryos, can mean two things: either the gap gene cascade is not involved in a "patterning timing system" or that a reset of the gap gene cascade later that 10-13 AEL might not be possible. This would also explain the absence of any effect in the first gap gene reset experiment (Fig. 4.21A) and that a second, at a later interval applied reset might actually not work.

The number of blastodermal segments after *Tc-eve* RNAi without heat shock treatment in the cross hsVSR × hshb was also higher than after *Tc-eve* RNAi in homozygous hsVSR animals (compare "no treatment" in Fig. S7.10A and B to "hs neg" in Fig. 4.7B). Again, one thoracic segment, probably T1, was more likely to remain than the other two thoracic segments after *Tc-eve* RNAi. Heat shock treatment increased the percentages of blastodermal segments. Interestingly it appears that a second hs-treatment applied later (>5h) can results in a stronger rescue of blastodermal segments than an earlier applied, second hs-treatment. However, this observation does not hold true for all segments nor all second hs-treatment time points (Fig. S7.10A).

Taken together, these two pilot experiments could not confirm that the gap gene cascade is or is part of the elusive "patterning timing system", providing temporal information to the segmentation clock. Further studies including what effect the gap gene cascade reset has on *Tc-eve* RNAi without the VSR background would be helpful. Further, some more controls to validate the negative nature of these results are needed.

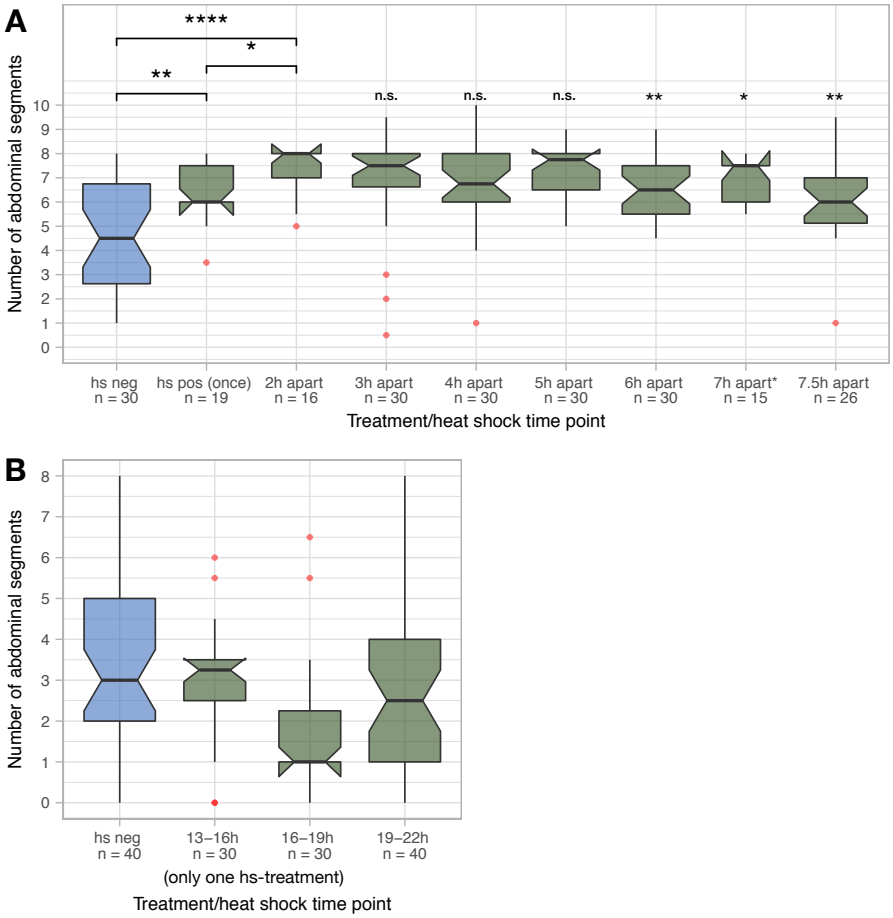

Figure 4.21 – Abdominal segments after Tc-eve RNAi and heat shock treatment in hsVSR × hshb

Boxplot showing the number of abdominal segments after *Tc-eve* RNAi in the cross hsVSR × hshb for the indicated hs-treatment conditions. For experimental procedure, see figure 4.20 and text. **(A)** *Tc-eve* RNAi without hs-treatment resulted in a median of 4.5 abdominal segments. Heat shock treatment at 10-13h (applied to all conditions except "hs neg") did increase (i.e. rescue) abdominal segmentation and two hs-treatment ("2h apart") were more effective then only one hs-treatment ("hs pos (once)"). For hs-treatment 3h to 5h apart, the efficacy of rescue did not decrease. Only if 5h or more lay between the first and second hs-treatment did the efficacy decrease. Only few cuticles with supernumerical segments were observed (see text). Rescue of *Tc-eve* RNAi and later reset of the putative timing system did not result in further increase in rescue.. Brackets indicate statistical significances between samples. If no bracket is present, comparison was done with the "2h apart" sample and significance is indicated above the sample. **(B)** A combination of late (≧13-16h) VSR expression (i.e. rescue of *Tc-eve*) and reset of the putative timing system did not result in any rescue of abdominal segmentation. A late reset of the timer, if possible, does not influence the rescue of abdominal segmentation. Possible outliers (see material and methods) are marked in red.

5 Discussion

In this thesis, I could demonstrate that the rescue of segmentation after RNAi-induced breakdown by RNAi inhibition via the hsVSR system is possible. In a proof-of-concept experiment I showed that rescue of gene function from RNAi knock-down is possible in a time-specific way. A re-initiation of the segmentation clock in both the blastoderm and SAZ after knock-down of the pair rule oscillator (i.e. “early or “upper” fate specification) is possible, while restoring abdominal segmentation on the level of the posterior organizer (i.e. Wnt signaling) seems not possible. In the following sections, I will first give some general remarks about the tool and my proof-of-concept experiments. I will then discuss the results of my rescue experiments and put them into the context of already published results. Lastly, since I was able to show that VSRs have the ability to work in a complex genetic network, I will point out the great potential of VSRs to overcome longstanding challenges of *Tribolium* research.

5.1 hsVSR: RNAi can be inhibited in a time dependent manner

The use of RNAi as a functional tool in developmental biology has increased the scope of species in which reverse genetics can be performed. In the second-best established insect model organism for functional genetics, *Tribolium castaneum*, parental RNAi (pRNAi) is so efficient that a genome-wide RNAi screen was successfully initiated (iBeetle screen) and is being finished (G. Bucher, personal comm.). So far, this screen has led to the discovery of new gene functions in many aspects of *Tribolium* development (e.g. Ansari et al., 2018; Kitzmann et al., 2017; Schmitt-Engel et al., 2015; Schultheis et al., 2019; Siemanowski et al., 2015; Ulrich et al., 2015). Using a more traditional *Drosophila* candidate gene approach, these genes and their functions would probably not have been identified. Parental RNAi, however, results in knockdown of gene function in all tissues of both the mother and the embryo. More answer specific questions of gene function in complex genetic networks or the reveal the function of genes with temporally different or pleiotropic roles were difficult. Only recently, Viral suppressors of RNAi (VSR) have emerged as a functional tool in the life sciences. VSR inhibit specific steps in the RNAi machinery and therefore enable a modulation of the RNAi response. Using VSRs, a more nuanced application of RNAi in *Tribolium* became possible (Ulrich, 2015). Our newly established “heat shock VSR” system (hsVSR) is a novel and unpublished system to control the expression of the VSR of the

Cricket Paralysis Virus (*CrPV-1A*) in *Tribolium castaneum* at a specific time by heat-shock treatment. It can thus inhibiting RNAi at any developmental stage, except for very early blastodermal stages, where heat-shock mediated expression does not work (Schinko et al., 2012).

In a previous thesis from our lab (Ulrich, 2015), multiple viral suppressors of RNAi (incl. CrPV-1A) were tested as transgenic constructs for their ability to inhibit RNAi and rescue RNAi phenotypes. In these initial tests, body colour markers (i.e. enzymes) or transgenic GFP were used to access rescue ability of the VSRs. As mentioned earlier, "rescue" or "ability to rescue" is, if not stated otherwise, always a **rescue of the observed phenotype**. I assumed that if a phenotype was rescued, this rescue was based on the inhibition of the RNAi machinery by the VSR expression. Both body colour enzymes and GFP are "downstream" factors in the respective developmental or regulatory network (i.e. they do provably not feed back to the network but just function) Therefore, a "downstream" gene function is more likely to be rescuable than more "upstream" gene function. This is based on the assumption that if a more downstream factor is knocked down via RNAi and, subsequently, the RNAi is inhibited via VSR, there will be a more direct link from re-initiated expression to function. In the case of knockdown and subsequent RNAi inhibition of a more upstream situated factor, the regulatory network as a whole needs to be re-initiated to fulfil its ultimate function. The expectation would be: the more "downstream" a factor is (or the lower the level), the more likely is a successful rescue of the phenotype, while the more "upstream" a factor is, the phenotypic rescue becomes less likely. The "timing factor" model proposed by Clark, Peel and Akam (2019) does define some useful "levels" within the segmentation process. Also, segmentation in *Tribolium* is not only scientifically interesting but also represents a complex developmental process with various levels. So, it is well suited to test the expectation from above and reveal the functionality of the hsVSR system to study complex developmental processes.

5.1.1 Proof of concept using segmentation

The process of segmentation has the purpose to establish the (para-)segment boundaries and thereby define and delimit the segments themselves.

The overall aim of my thesis was to answer the question whether the breakdown of segmentation after RNAi of the segmentation clock or upstream factors is irreversible or if

a re-initiation of segmentation is possible. But before I could start to test my candidate genes, I needed to ensure whether rescue of RNAi segmentation phenotypes using the hsVSR system is in principle possible. I also needed to ensure that a possible rescue of gene function by hs-treatment correlates with the expression time of the gene in question, i.e. I needed to ensure that the rescue is time-specific.

For that purpose, I chose the genes *paired* (*Tc-prd*) and *torso* as a proof-of-concept and negative control, respectively (see section 4.1.1). During segmentation, *Tc-prd* acts as a secondary pair-rule gene that is expressed in cells shortly after they left the SAZ. Its function is necessary to express segment polarity genes in odd-numbered (para-)segments (Choe and Brown, 2007) and importantly, it is a zygotically expressed gene. Its rescue should test whether segmentation in general is rescuable by the hsVSR system. Torso signaling, on the other hand, is provided maternally (therefore much earlier than the first rescue time point) and is, necessary for the initiation of the SAZ (Schoppmeier and Schröder, 2005). Its function in establishing the SAZ has ceased before the blastoderm became sensitive to heat-shock mediated expression. Hence, rescue of its function was not expected and was meant to act as the negative control to confirm that the time point of RNAi inhibition needed to correlate with the time window of expression and function of the gene of interest. Both criteria to use the hsVSR system were successfully met. My results could clearly show that there was a rescue of the number of abdominal segments after *Tc-prd* RNAi (Fig. 4.3C), but no rescue after *Tc-tor* RNAi (Fig. 4.4B).

During *Tribolium* segmentation, *Tc-prd* expression can be seen as a mere transient (downstream) read-out of the initial (and also transient, but more upstream) pPRG pattern (see Fig. 2.2D). It therefore makes sense that the extent of observed segmental rescue by hsVSR in *Tc-prd* RNAi cuticles is time-dependent (compare timepoints in Fig. 4.3 C). After *Tc-prd* RNAi, the segmentation clock continues to oscillate in the SAZ and patterns the elongating germ-band in a two-segment periodicity (Maderspacher et al., 1998). Since *Tc-prd* is missing, only every other segmental border can be established (those not dependent on *Tc-prd* expression). Early RNAi inhibition (10-13h) leads to early rescue of the transient *Tc-prd* expression and function, and therefore more anterior segmental borders can be rescued. Later RNAi inhibition (13-16h) only rescues those more posterior segmental borders (or segments) where the transient *Tc-prd* expression can still perform its function. The more anterior borders, which were patterned before the RNAi inhibition, are lost

because *Tc-prd* function was missing in the respective time window. In summary, rescue of RNAi is possible in a time dependent manner with the hsVSR system.

The *Tc-tor* RNAi further confirmed that the time window of gene function to be rescued has to temporally correlating with the VSR expression. While the role of *Tc-tor* function in segmentation becomes apparent during germband elongation, its actual function in Torso signaling is active much earlier during the early blastoderm (Schoppmeier and Schröder, 2005).

Another important observation was the loss of segments due to the heat shock treatment itself (see Figs. 4.3 C and 4.4 C, compare “hs neg” to hs-treatment timepoints; schematically shown in Fig. 4.1B). This means that in this work and in future applications of this system, it is essential to separate the heat-shock effect from the RNAi-inhibition effect. Thus, it is necessary to include an RNAi wild type control that is heat-shocked as well, to better distinguish hs-defects from non-rescue and to control the resulting confounding variables.

In summary, the proof-of-concept and the negative control experiments confirmed the two necessities for successful application of the hsVSR system to investigate segmentation and probably also other complex developmental processes: rescue of gene function during segmentation and time-specificity of the rescue.

5.2 Re-initiation of the segmentation clock is possible

The initial question I wanted to answer using the hsVSR system was whether the breakdown of segmentation after RNAi is irreversible or if re-initiation (i.e. rescue) of segmentation is possible.

In *Tribolium,* all stages (or levels) of segmentation, in stark contrast to *Drosophila*, are occurring at once, but spatially separated in the developing germband (see Fig. 2.2C-E and Fig. 2.5). The rescue of segmentation on the level of the sPRGs (Fig. 4.3 and section 5.1) showed that rescue of segmentation by hsVSR is in general possible. This led me to ask the following questions regarding the rescue of segmentation:

(1) Does re-initiation of segmentation depend on the level in the segmentation process?
(2) Is the extent of re-initiation of segmentation and the rescue of specific structures (e.g. head/thorax vs. abdomen) time-dependent
(3) What do these results contribute to the segmentation models currently proposed for *Tribolium*?

5.2.1 Is a rescue of segmentation possible at any level above the secondary PRGs?

The upstream-most components in the segmentation process provide the conditions required for establishment and maintenance of the posterior SAZ. These can be further divided into the actual „initiation factors" (e.g. *Tc-tor*) (Schoppmeier and Schröder, 2005) and other factors functioning as the "posterior signaling center", both in the blastoderm and germband (mainly Wnt signaling components like *Tc-wg*, *Tc-Wnt8/D* and co-factors like *Tc-arrow* and *Tc-wntless*) (Beermann et al., 2011; Bolognesi et al., 2008b; Bolognesi et al., 2009; Oberhofer et al., 2014) (Fig. 2.5A). Some of the Wnt signaling components (mainly the ligands) play a role in both blastoderm and germband (mutual regulation of Wnt and *Tc-cad* (Ansari et al., 2018; Beermann et al., 2011; Oberhofer et al., 2014)). The function of the co-factors in segmentation appears to be limited to the germband/SAZ (Bolognesi et al., 2009). Downstream, the "spatiotemporal regulation" and the "fate specification" occurs (according to the model proposed by Clark et al., 2019). The spatiotemporal regulation is represented by the timing factor network (Clark and Peel, 2018) and includes *Tc-cad*, the proposed speed regulator (Zhu et al., 2017). The spatiotemporal regulation

provides input for the fate specification, represented by the pPRGs, (early or „upper“ fate specification [*Tc-eve*, *Tc-run* and *Tc-odd*]) (Choe et al., 2006; El-Sherif et al., 2012; Sarrazin et al., 2012), the sPRGs (later or “lower” fate specification like *Tc-prd*) (Choe and Brown, 2007) and the segment polarity genes (Choe and Brown, 2009) (see Fig. 2.5A).

The expectation, as stated above would be: the more “downstream” a factor (or its level) is, the more likely is a successful rescue of the phenotype, while the more “upstream” a factor (or level) is, the phenotypic rescue becomes less likely[8].

5.2.1.1 The rescue of the pPRGs consolidates their role in the segmentation clock

Rescue of the “downstream” *Tc-prd* phenotype (lower fate specification) was expected and I could also experimentally proof this expectation. It was, however, unclear in how far the system built by the oscillating primary pair rule genes (upper fate specification) could re-initiate and whether this would also be possible for the genes constantly expressed in the SAZ (partially “spatiotemporal regulation” and “posterior signaling center”).

The next level above the sPRGs are the pPRGs, namely *Tc-eve*, *Tc-run* and *Tc-odd*. These genes most likely make up a segmentation clock that patterns the AP axis during both the blastoderm and germband stages (Choe et al., 2006; Clark et al., 2019; El-Sherif et al., 2012; Sarrazin et al., 2012). I was able to show that a rescue of segmentation after RNAi of the segmentation clock genes *Tc-eve*, *Tc-run*, or *Tc-odd* is possible. A statistically significant increase in abdominal segments in cuticles was observed in comparing hsVSR rescues to RNAi wild type controls (Figs. 4.7C, 4.8C, 4.9C). To test if a proper re-initiation of segmentation via a restored segmentation clock had occurred, I further analyzed the germband expression of the segment polarity gene *Tc-wg* and all three pPRGs in hs-treated *Tc-eve* RNAi germbands. These results show that in *Tc-eve* RNAi germbands after RNAi inhibition, the pPRGs and the segment polarity gene *Tc-wg* are expressed in stripes again (Figs. 4.14, 4.16 and 4.17). Thus, I could confirm that proper re-initiation of segmentation by the segmentation clock had occurred. In non-heat shocked *Tc-eve* RNAi or RNAi wild type control germbands, in contrast, the striped pattern of the pPRGs and especially the

[8] This simplification ignores genes that are involved in multiple different processes at different times, like e.g. *Tc-wg*. As a segment polarity gene, it is situated downstream in the segmentation process (lower “fate specification). Its expression in the posterior during both blastoderm and germband stages, however, also makes it part of the “posterior signaling center”. This, of course, complicates things and narrows down the possible selection of genes testable by RNAi inhibition with hsVSR.

segmental stripes of *wg* remained (mostly) lost (Figs. 4.15, 4.16), reflecting the breakdown of segmentation on the genetic and cuticular level.

The oscillation of both *Tc-eve* and *Tc-odd* had been individually demonstrated in germbands before (El-Sherif et al., 2012; Sarrazin et al., 2012). If and how their oscillations are depending on each other, however, was not fully known. I could clearly show that a re-initiation of segmentation after RNAi-induced breakdown for all three pPRGs is possible. This analysis further confirms that these three genes belong to one functional group: RNAi of any of them leads to complete breakdown of segmentation while for all of them, hsVSR mediated RNAi inhibition restores segmentation. Hence, they are distinct from *Tc-prd* (which does not lead to breakdown) and Wnt signaling (which appears to lead to an irreversible breakdown).

5.2.1.2 Rescue of the putative posterior organizer is unlikely

On the next higher levels of the segmentation process, genes are active that are either required for the spatiotemporal regulation ("timing factors") or the maintenance of segmentation ("posterior signaling center") (Bolognesi et al., 2008b; Bolognesi et al., 2009; Clark et al., 2019; Copf et al., 2004; Oberhofer et al., 2014). *Tc-cad* was considered a candidate gene for the "spatiotemporal regulation" level. The "posterior signaling center" is represented by *Tc-Wnt8/D* in combination with *Tc-wls* and *Tc-arr*.

Unfortunately, *Tc-cad* itself, a gene highly interesting due to its prominent role in the SAZ and as a putative timing factor in the segmentation process could not be tested with the hsVSR system for technical reasons. Parental RNAi (both pupal and adult) of *Tc-cad* in *Tribolium* leads to severe sterility of the injected individuals (Gregor Bucher & Michalis Averof, pers. communication). I performed small-scale tests to optimize the pRNAi procedure for *Tc-cad* knockdown. Specifically, I tried to reduce the concentration of dsRNA to prevent sterility after pRNAi, but still produce phenotypes – this was unsuccessful (data not shown). Since a large number of embryos is required for the rescue experiment and its subsequent analysis (limited time window per egg collection), I also decided against embryonic RNAi (which has previously successfully been used to investigate *Tc-cad* function during embryogenesis, see Benton et al., 2013). Also, embryonic RNAi is much more labor-intense and affected by technical variation due to injection compared to pRNAi

and was not established in combination with the hsVSR system. However, the expression of *Tc-cad* is closely linked to posterior Wnt signaling (Ansari et al., 2018; Beermann et al., 2011; Oberhofer et al., 2014). Similar feedback between *cad* and Wnt signaling (*Wnt8* in particular) is also known from spiders (McGregor et al., 2008; Schönauer et al., 2016).

For the tested Wnt pathway components at the level of the "posterior signaling center" (*Tc-arr* and *Tc*-Wnt8/D with *Tc-wls)*, no clear rescue of posterior segmentation could be observed. Rescue of (anterior) blastodermal segments (Fig. 4.5 A and Fig. 4.6), however, acted as an "internal control" and showed that RNAi inhibition had taken place (Figs. 4.5B, 4.6B, S7.2A and S7.3A). This indicates that once the segmentation/patterning signaling center in the posterior is lost due to RNAi, it cannot be re-initiated or restored to continue patterning the AP axis. It was previously shown that there is autoregulatory feedback of Wnt signaling (Beermann et al., 2011; Oberhofer et al., 2014) as well as feedback between *Tc-cad* and Wnt signaling (Ansari et al., 2018). Breakdown of these feedback loop via Wnt pathway component RNAi appears irreversible and once they are lost, they cannot re-initiate. On the other hand, if the signaling center was restored, it is situated so far "upstream" in the segmentation process that the "downstream" components necessary to facilitate its function might not be activated quickly enough.

The observed rescue of anterior segments (Fig. 4.5B and Fig. 4.6B) after Wnt pathway RNAi is most likely not a rescue of early segmentation. I rather reflects independent effects of later Wnt signaling on the segment polarity level. This assumption is based on data from *Tc-arr* and *Tc-Wnt8/D*;*Tc-wls* RNAi germbands (Bolognesi et al., 2009). The cuticle phenotype after RNAi appears rather severe and most often shows no visible segmentation. However, in early germbands anterior primary pair-rule and segment polarity gene expression can still be found, but quickly fade during further development. This fading is especially pronounced in *Tc-wls* RNAi germbands, that show no loss of (abdominal) segments (Bolognesi et al., 2008b; Bolognesi et al., 2009). These Wnt pathway component RNAi therefore not only disrupt the "posterior signaling center" necessary for (posterior) segmentation (via *Tc-cad)*, but also disrupt the conserved feedback loop of the segment polarity genes that involves Wnt signaling and is necessary for segmental boundary maintenance (Brown et al., 1994; Choe and Brown, 2009; Farzana and Brown, 2008; Heemskerk et al., 1991; Ingham et al., 1991; Mohler and Vani, 1992). RNAi inhibition,

especially in Tc-arr RNAi animals (Fig. 4.5A), could rescue this later function, resulting in rescued anterior segments, while the earlier function (posterior signaling center) involved in abdominal patterning cannot re-initiate.

To confirm the segment boundary stabilization hypothesis, stainings of segment polarity genes *Tc-arr* or *Tc*-Wnt8/D; *Tc-wls* RNAi germbands would be necessary.

It was repeatedly shown that the knockdown of Wnt signaling leads to breakdown of segmentation in arthropods, probably due to autoregulation of Wnt signaling and its positive feedback loop with *cad* (e.g. Beermann et al., 2011; Bolognesi et al., 2008b; Bolognesi et al., 2009; McGregor et al., 2008; Schönauer et al., 2016; reviewed in McGregor et al., 2009). For the first time, my experiments asked the question whether this network and its function ("spatiotemporal regulation" in posterior segmentation) can re-initiate after RNAi inhibition. My data suggests that it cannot re-initiate, meaning that autoregulation of Wnt signaling and feedback to and from (*Tc*-)*cad* are necessary for its maintenance.

5.2.1.3 Other examples for rescue of oscillatory systems

So far, oscillations of a segmentation clock during segmentation in arthropods were only shown in *Tribolium* (El-Sherif et al., 2012; Sarrazin et al., 2012). Similar mechanisms, however, are assumed to be a common feature in arthropod segmentation (Clark et al., 2019; Peel and Akam, 2003; Peel et al., 2005). The concept of a segmentation clock, however, was first formulated and experimentally shown during vertebrate somitogenesis (Palmeirim et al., 1997b). In a publication from Riedel-Kraus and colleagues (2007), a rescue experiment similar to the ones presented in this work was performed in the zebrafish *Danio rerio*. In the publication, the authors show that Delta-Notch signaling is necessary to synchronize the oscillation between cells in the PSM during somitogenesis. Chemical treatment with a known Delta-Notch antagonist perturbated somite formation by unlinking the oscillation between cells and resulted in perturbated somitogenesis. After removal of the antagonist the linked oscillation was rescued and normal somitogenesis in the same individual continued (Riedel-Kruse et al., 2007). While this study demonstrated that desynchronized oscillation in zebrafish perturbates segmentation, which can be rescued to properly segment the zebrafish AP axis, this study did not stop the oscillation itself and restarted it. Also, as mentioned earlier, while Delta-Notch signaling has been proposed to

be involved in *Tribolium* segmentation (Clark et al., 2019), no functional data proving this hypothesis has been published so far (Aranda, 2006; Aranda et al., 2008). Nevertheless, in other arthropods the involvement of Delta-Notch signaling (often together with Wnt signaling) has been shown (Chipman and Akam, 2008; Schönauer et al., 2016; Stollewerk et al., 2003). Hence, to the best of our knowledge, this work is the first experiment where posterior segmentation was rescued after a breakdown.

5.2.1.4 Rescue of the segmentation clock by a permissive upstream factor?

The segmentation clock is a dynamic process and its breakdown via RNAi of the pPRG stops the clock from oscillating properly. Since RNAi inhibition after pPRGs RNAi in *Tribolium* rescues the clocks oscillation (this work), the question remains how exactly the upstream factors re-initiate the clock. In *Tc-eve* RNAi germbands, the posterior expression of the upstream factor *Tc-cad* is unaffected (Fig. 4.18). The return to oscillation in the presence of a permissive upstream factor is, for example, observed in *in-vitro* differentiated induced presomitic mosoderm-like (iPSM) cells that are cultured with GSK3β antagonists (i.e. Wnt signaling activated, which is the permissive factor for PSM oscillation) (Matsumiya et al., 2018).

iPMS cells self-organized into a presomitic mesoderm-like tissue and, under the right culture conditions, oscillatory expression waves were observable along a self-organized axis using a transgenic *Hes7* reporter (*hes*/*hes* genes are orthologues of *hairy*). Even signs of forming segments along this axis were present (Matsumiya et al., 2018). This shows that tissue capable of oscillatory gene expression tends to (re-)start oscillating if a permissive upstream factor is present.

In *Tribolium*, *Tc-cad* is probably not only a permissive factor regulating the spatiotemporal expression dynamics of *Tc-eve* (and subsequently the whole segmentation clock). It is, at least in the blastoderm, also required for the continued expression of *Tc-eve*, judged by *in-situ* stainings (El-Sherif et al., 2015). It therefore seems likely that the oscillator in pPRG RNAi is actually (re-)started after RNAi inhibition due to an activating signal from *Tc-cad*.

In summary, my results show that a re-initiation of segmentation is indeed possible at the level of the pPRGs during germband elongation of *Tribolium*. This work demonstrates for the first time that the segmentation oscillator can be stopped and re-initiated.

5.2.2 Gap gene network as part of elusive “patterning timing system” could not be confirmed

As described above, I showed that segmentation can be re-initiation via hsVSR at the level of the pPRGs (upstream “fate specification”), the genetic components of the segmentation clock (section 4.1.3). The experimental setup also allowed ask the question whether there is a “patterning timing system” during patterning of the germband and axial elongation. It is still unknown how segmentation (and axial elongation and patterning in general) is terminated. While not impossible, it seems unlikely that these processes just stop because the SAZ “runs out of cells”. Furthermore, there is as of yet no signal known in *Tribolium* that would measure and indicate an emptying pool of cells. Clark and collogues (2019) propose a possible "inhibitory“ influence of the gap gene network on the “spatiotemporal regulation” of germband patterning to convey information about the duration of segmentation or even provide a sort of “stop signal” via a posterior gap gene.

RNAi of the three pPRGs leads to complete breakdown of the segmentation process as indicated by both cuticles and *Tc-wg* stainings in germbands (sections 4.1.3 and 4.2.2). This in turn leads to elongation defects (Choe et al., 2006). If the elusive “patterning timing system” would be linked to either axial elongation or the segmentation clock itself, it should slow down or stop upon breakdown of segmentation. A re-initiation of segmentation by hsVSR should therefore also restart or continue the timer since a rescue of segmentation necessarily also results in further axial elongation. In that scenario, the time point of rescue would not matter – it should always lead to the same degree of abdominal rescue.

As my results from the pPRGs rescue experiments (section 4.1.3) show, the hs-treatment time point has a great influence on the degree of segmental rescue. Most of the re-initiations of segmentation, meaning the significant increase of abdominal segment number, occurred only for the earliest hs-treatment time point (10-13h). For later hs-treatment time points, in contrast, the effect was strongly reduced or absent (compare “10-13h” to “13-16h” (and 16-19h) in Figs 4.7C and S7.4B). The fact that only early hsVSR treatment can rescue could be because of the temporal delay between hs-treatment, VSR translation and VSR function, and the time required until gene function is rescued sufficiently. Maybe, the later treatments are just too late to rescue a significant number of abdominal segments. Or that the “patterning timing system” is independent of

segmentation and continues to run in the background, even without segmentation or the segmentation clock. The proposed influence of the gap gene network (Clark et al., 2019) might be responsible for such a “patterning timing system”.

I provide some preliminary data that would suggest little to no involvement of the gap gene network (or cascade) in this “timing system. The gap cascade in *Tribolium* proceeds simultaneously and independently with the segmentation clock during axis elongation (Fig. 2.2 C and D) (Marques-Souza et al., 2008) and they share the same upstream regulation by the “speed regulator” molecule *Tc-cad* (Zhu et al., 2017). Ectopic misexpression of the gap gene *Tc-hunchback* (*Tc-hb*) by the *Tribolium* heat-shock promoter (*hs-hb*, see Distler, 2012) during germband elongation is able to restart the gap gene cascade (Boos et al., 2018). Accordingly, after *Tc-eve* RNAi in a cross of the hsVSR line with the hs-hb line (hsVSR × hshb), such a reset should result in a restart of the “patterning timing system” and re-initiation the segmentation clock. This should lead to a similar extent of abdominal rescue at any hs-treatment time point. Two hs-treatments might even increase the total number of abdominal segments beyond the wild type number. A first hs-treatment would rescue the *Tc-eve* RNAi (and reset the timer for a first time). A second hs-treatment would, during already rescued segmentation, reset the timer a second time, starting the timing anew, resulting in more than the usual number of segments

However, my preliminary results showed no increase in total abdominal segment number after *Tc-eve* RNAi in the cross hsVSR × hshb after the application of two heat shocks with varying time intervals (Fig. 4.22A). However, two hs-treatments increased the extent of abdominal segment rescue compared to single hs-treatment. Increasing the time interval between the hs-treatments, also did not lead to significant supernumerical segments, which was a prediction of the involvement of the gap gene cascade in a “patterning timing system”. Two hs-treatment means that *Tc-eve* RNAi is inhibited twice and thus two *Tc-eve* “pulses” happen during germband elongation. In the initial pPRG rescue experiments (section 4.1.3), the time interval between the two hs-treatments was uniformly 2h. I have also shown that two hs-treatments are more effective to rescue abdominal segmentation than only one hs-treatment (compare “hs pos (once)” to “2h apart” in Fig. 4.21A). This means that the second hs-treatment and the resulting *Tc-eve* “pulse” have a functional relevance for the extent of rescue of abdominal segmentation.

If this second pulse is delivered too late, it will lose its influence in the rescue, either due to the time passed in the "patterning timing system" or simply because it is too late to rescue abdominal segments. However, if the timer is reset, the second, later (>5h) *Tc-eve* "pulse" should regain influence in the rescue. There is, however, no significant difference between samples that received two heat-shock treatments more than 5h apart to samples with a single hs-treated. This means that while the time interval between *Tc-eve* pulses to have an influence matters, this interval is not increased by the gap gene cascade reset.

Also, if the first (and only) hs-treatment in hsVSR × hshb crosses after *Tc-eve* RNAi is applied later than 10-13h AEL, there is no rescue effect for abdominal segmentation (Fig. 4.22B). This hs-treatment should have not only inhibited the *Tc-eve* RNAi, but also reset the putative "patterning timing system", therefore resulting in segmentation rescue beyond the time window that was seen in homozygous hsVSR embryos (Fig. 4.7C).

Because of the inability to increase either the extent of abdominal rescue or the time window in which abdominal rescue via RNAi inhibition is possible, a role of the gap gene network to function as an overall "patterning timing system" could not be confirmed. However, these experiments where only preliminary and had some technical difficulties. Thus, further studies are necessary to validate these findings and interpretations. Especially the unexpectedly weak phenotype of the *Tc-eve* RNAi in the hsVSR × hshb cross (see "hs neg" Fig. 4.22) needs to be optimized to enable a more meaningful rescue experiment.

5.2.3 Does blastodermal patterning differ from SAZ mediated patterning?

Head and Thorax segments are pre-patterned during late blastoderm stage early in *Tribolium* development. During this blastoderm stage the first three *Tc-eve* stripes emerge from the posterior in a two-segment periodicity and pattering the three gnathal and three thoracic segments (El-Sherif et al., 2012). However, at the same stage only one *Tc-prd* stripe emerges, patterning the anterior gnathal segments, mandibles (Md) and maxillae (Mx). The second *Tc-prd* stripe emerges later when the early germband is formed (Choe and Brown, 2007). The segment polarity gene pattern during the blastoderm stage is only formed by the first segmental *Tc-engrailed* stripe corresponding to the mandibular segment. Later coinciding with the blastoderm-to-germband transition the second *Tc-engrailed* stripe emerges (Brown et al., 1994). Interestingly, the first *Tc-wg* stripe in the blastoderm corresponds to the future ocular/antennal segment, while the corresponding *Tc-engrailed*

stripe emerges later (Nagy and Carroll, 1994; Oberhofer, 2014; Schinko et al., 2008)). During the blastoderm, on the "upper" fate specification level (pPRGs), all six gnathal and thoracic segments are (pre-)patterned. On the "lower" fate specification level, only the anterior-most two (sPRGs) or one gnathal segments (segment polarity genes) are (pre-)patterned.

The earliest hs-treatment time point was at 10-13h AEL coinciding with the transition from blastoderm to germband. RNAi inhibition of the pPRGs (especially *Tc-eve*) should therefore, if at all, only affected the posterior most pPRG patterned segments (T2 or T3). RNAi inhibition of the sPRGs (Tc-prd) at the same time point, however, could still affect the posterior most gnathal (labium) and all three thoracic segments. Reasoned by the temporal delay between hs-treatment and effect on segmentation, the more posterior a (blastodermal) segment is, the more likely is a rescue by hsVSR.

However, RNAi of the pPRGs and subsequent hs-treatment at 10-13h rescued mainly (anterior) head segments and one thoracic segment. The rescued head segment was predominantly, but not exclusively, the posterior-next to the "normally" remaining head segment (after untreated RNAi) (Figs. 4.7B, 4.8B and 4.9B). Interestingly, the posterior-most head segment, the labium, was hardly rescued. The identity of the rescued thoracic segment was difficult to determine (identification was easy if two leg-bearing segments were present, since one of them often carried the characteristic pair of stomata, but as seen in the *Tc-prd* RNAi cuticles, these stomata can potentially shift position). It was insofar a surprise to see that more anterior segments of the head (and thorax) were rescued instead of the predicted more posterior blastodermal structures (like the posterior thoracic segments).

One possible explanation for the observed yet unexpected rescue of anterior over posterior blastodermal segments might be an influence of the Hox genes. Mutants or RNAi knockdowns of the gap genes *Tc-Krüppel* (*Tc-Kr*) and *Tc-giant* (*Tc-gt*) result in homeotic transformations and segment identity shifts of gnathal and thoracic segments with double-segment periodicity (Bucher and Klingler, 2004; Cerny et al., 2005). These findings were interpreted as evidence for a possible regulation of anterior Hox genes (like *Tc-Deformed* (*Tc-Dfd*), *Tc-Sex-combs reduced* (*Tc-Scr*), and possibly *Tc-Antennapedia* (*Tc-Antp*) and *Tc-Ultrathorax* (*Tc-Utx*)) by the pair-rule genes. For two gap genes (*Tc-gt* and *Tc-knirps*), there is support of pair-rule regulation (Bucher and Klingler, 2004; Peel et al., 2013). Rescueing

(p)PRG expression during transition from blastoderm to germband might (directly or indirectly) influence the expression of anterior Hox genes. These Hox genes could then give the rescued blastodermal segments an anterior identity, regardless of their "original" identity. To examine the possible influence of rescued PRG expression after *Tc-eve* RNAi on anterior Hox gene expression, their expression should be analyzed in hs-treated *Tc-eve* RNAi embryos. This could shed light on a possible homeotic transformation of rescued segments.

Similar to the findings from the pPRG rescue, rescueing of Wnt pathway components showed a much higher degree of rescue for the anterior-most segments (labrum and antennae) than for any other segment (Fig.4.5B and 4.6B). These results, however, are also explainable by the proposed stabilization of established but slowly fading (para-)segmental borders after rescue of Wnt pathway RNAi (as mentioned in section 5.2.1.2). The stabilization of segmental borders (instead of actual rescue of segmentation) is further supported by the *Tc-arrow* RNAi rescue at the later time point at 13-16h which "rescued" more blastodermal segment borders than the earlier time point ("hsVSR, 13-16h" in Fig. 4.5B and C). Only the latest time point at 16-19h seems too late to properly stabilize segmental borders, because cuticles without any segmentation and empty eggs are increasing (Fig. S7.2A). The observation that the hs-tratment at 13-16h increased the amount of stabilized segmental borders compared to hs-treatment at 10-13h was not observed for the Tc-Wnt8/D; *Tc-wls* double RNAi rescue (Fig. 4.6B and S7.3). This might be explained by the fact that *Tc-arrow* is a co-receptor of canonical Wnt signaling, while *Tc-Wnt8/D* is rather specific to the posterior germband. *Tc-wls*, however, is necessary for Wnt ligand secretion (Bänziger et al., 2006; Das et al., 2012), and therefore plays a role in canonical Wnt signaling as well. Why rescue of *Tc-wls* was not comparable to the rescue of *Tc-arr* remains unclear.

The only gene which met the expectation to rescue posterior over anterior segments was the sPRG *Tc-prd*. Here not only the abdominal segments, but also the second thoracic segment were rescued to a higher degree than the more anterior head segments, the mandibles and the labium (Figs. 4.3B and S7.1A).

In conclusion, anterior "blastodermal" segments can be rescued to a higher degree than posterior segments using pPRG RNAi rescue experiments, for as of yet unknown reasons.

Hypothetical influence of anterior Hox genes in this phenomenon were discussed, but would require further studies.

5.2.4 Consequences for current models of *Tribolium*/short-germ insect segmentation

There currently are several, mostly complementary models explaining segmentation in *Tribolium* (described in detail in the introduction). The first model is mainly based on the earlier publications of Choe and colleagues stating a simple pPRG circuit with an activation-based regulation, mainly based on single-gene *in-situ* hybridizations in WT and pPRG RNAi *Tribolium* germbands (Choe and Brown, 2007; Choe and Brown, 2009; Choe et al., 2006). Later, oscillating gene expressions of the pPRGs were shown (El-Sherif et al., 2012; Sarrazin et al., 2012). However, the idea that a segmentation clock-like mechanism might be responsible for *Tribolium* or short-germ insect segmentation is older (Maderspacher et al., 1998; Peel and Akam, 2003). Both the "speed regulator" (Zhu et al., 2017) and "timing factor" (Clark et al., 2019) model are based on inhibition-based regulation of the segmentation clock oscillation. They come to this conclusion by different approaches. The former was concerned with finding a regulatory relationship between genes that could be used to facilitate patterning in both blastoderm- and germband like tissues (Zhu et al., 2017). The latter derived from the regulation of the pPRGs from the *Drosophila* PRG regulatory network, modified to pattern in a sequential segmentation mode, and a limited number of double stainings in PRG RNAi and wild type *Tribolium* germbands and other insects (Clark, 2017; Clark and Peel, 2018; Clark et al., 2019).

In this study I could reveal that *Tc-eve* still showed a weak (and mainly unstriped) expression pattern after RNAi knockdown. I also found that both *Tc-run* and *Tc-odd* were still expressed and even formed some posterior stripes in these *Tc-eve* knockdowns (Figs. 4.14A[iii] and A[iv], 4.16B and C, and 4.17B and C). However, qPCR analysis showed that both *Tc-run* and *Tc-odd* transcripts were slightly reduced after *Tc-eve* RNAi, while the intronic signal of Tc-eve was upregulated (Fig. 4.19 and tbl 4.1). My work therefore provides another data point, that might help to further test the proposed models. In respective simulations, *Tc-eve* RNAi should lead to its own upregulation. It also should separate the germband into a posterior *Tc-eve* and an anterior *Tc-wg* expression domain (Fig. 4.14A[vi]). More importantly, simulations need to reflect the breakdown of segmentation after Tc-eve

RNAi and the re-initiation of the system upon the rescued expression of the pPRGs, but not (posterior) Wnt signaling.

5.2.5 Auto-regulation of *even-skipped* during segmentation

RNAi has proven to be a useful tool for functional gene analysis, but is never 100% efficient in knocking down the targeted gene. In *Tribolium*, however, it has been shown multiple times that RNAi can phenocopy mutants with very high penetrance (compare *itchy* and *scratchy* mutants cuticles (Maderspacher et al., 1998) to *Tc-prd* or *Tc-sloppy-paired* RNAi cuticles (Choe and Brown, 2007) or the *jaws* phenotype to *Tc-Krüppel* RNAi cuticles (Cerny et al., 2005)). Nevertheless, a certain percentage of targeted transcript will always remain (G. Bucher, pers. communication; Kitzmann et al., 2017). Choe and collogues (2006) had previously reported that they did not detect *Tc-eve* transcripts in *Tc-eve* RNAi germbands using NBT/BCIP *in-situ* stainings. Contrary, I did find *Tc-eve* transcripts in *Tc-eve* RNAi germbands (Fig. 4.14A^{i}, 4.15A^{i}, B^{i}) using HCR staining. Enzymatic detection via AP-conjugated secondary α-DIG antibodies (as used in standard *in-situ* stainings) do offer a potentially greater amplification of the initial mRNA "signal". Therefore, such stainings are not well suited for quantification of gene expression, especially since its outcome can vary depending on fixation procedure, RNA probe binding or degradation and the time until ultimate termination of the reaction.

The remaining *Tc-eve* mRNA observed in my stainings could either represent transcripts not yet targeted by RNAi, or nuclear pre-mRNA, not yet accessible by the RNAi machinery. My data indeed indicates that the signal stems from nuclear pre-mRNA. A preliminary analysis using software-based background reduction of the HCR *Tc-eve* signal (using a build-in feature of the LAS-X software from Zeiss) showed that the strongest *Tc-eve* signal was often located in the nucleus in non-heat shocked *Tc-eve* RNAi germbands (not quantified, see Fig S7.13). Further, qPCR revealed a strong upregulation of intronic *Tc-eve* signal after *Tc-eve* RNAi, which returned to normal upon RNAi inhibition (Fig. 4.19, Tbl. 4.1). My controls could also indicate that the hs-treatment itself is not causing this decrease/return to normal of *Tc-eve*-intron signal ("vw, Tc-eve" in Tbl 4.1). Therefore, the increase of *Tc-eve* transcripts and subsequently, Tc-EVE protein, upon RNAi inhibition led to the decrease of transcription (i.e. pre-mRNA). Such negative auto-regulatory behavior could make sense in the light of oscillatory gene expression in the segmentation clock.

Similar negative autoregulatory behavior is for example a known of *hairy* genes (Lewis, 2003; Schröter et al., 2012), which is also proposed to be part of *Tribolium* segmentation (Clark, 2017; Clark and Peel, 2018; Clark et al., 2019)). In contrast, for *Drosophila* a positive autoregulation of *Tc-eve* during segmentation was reported (Harding et al., 1989; Jiang et al., 1991).

The autoregulative behavior of *eve* and the evolved context-dependency (positive vs. negative autoreguation) makes it rather interesting and should be studied in more detail. The suggested negative autoregulation of *Tc-eve* could be interpreted as a way to increase or maintain its oscillation in the segmentation clock, but further work is necessary to untangle its possible involvement in the pPRG oscillation.

5.3 Possible Application of VSRs and hsVSR in developmental biology.

In this work, I have shown that a VSRs (hsVSR, see Ulrich, 2015) can successfully be used to rescue the function of genes after knocked-down during segmentation. This rescue showed that the segmentation clock that patterns the AP axis of *Tribolium* and probably many other arthropods can be re-initiated after RNAi-induced breakdown. The hsVSR system is useful since it is target-gene independent. Theoretically, any gene knocked-down by RNAi could be rescued by hs-treatment in combination with the hsVSR line. Currently, its limitations are mainly the earliest target gene expression time point due to the *Tribolium* heat shock promoter used (Schinko et al., 2012)). However, an actual rescue of its function and any resulting phenotype depends on more criteria, like the context in which the target gene is functioning (e.g. Wnt signaling as a “posterior signaling center”, see section 4.1.2) or possible pleiotropy of the target gene.

Using different genetic methods to express VSR could potentially increase its usefulness and circumvent some of these limitations. One important use of the VSR is overcoming pupal or adult lethality and sterility after parental RNAi. Many genes causing such dramatic effects after pRNAi are known, for example the already mentioned *Tc-cad*. Any work involving Wnt signaling components also often leads to sterility of injected pupa (this work, not shown; G. Bucher, pers. communication), increasing the necessary work load to produce sufficient numbers of individuals for analysis. Further, such collected eggs could originate from inefficiently affected animals reflecting a hypomorphic situation.

Ubiquitous, but low-level expression of the VSR in (homozygous) adult tissue could suppress sterility and other negative effects in the mother by a possible accumulation of the inhibitor over time. In early embryos, no or low-level expression of the inhibitor (due to low number of cells and possibly modulated by heterozygosity) could allow the RNAi to occur. This strategy, however, might only work with genes active very early in development because the VSR will eventually be zygotically expressed by the embryo at some point and show an effect. The VSR system used in this study (CrPV-1A) antagonizes the very last step in the RNAi pathway, Ago2 (Nayak et al., 2010; Nayak et al., 2018). Therefore, the actual processing and spread of dsRNA into the eggs by the injected mother would be unaffected. *Tc-cad*, which could not be tested with the hsVSR system in this study due to the severe sterility its pRNAi causes, would be a good example to test such a system. It would remain to be tested if only its earlier blastoderm function or also the later germband function would be influenced.

Another application could be the disentangling of maternal from zygotic effects. Since pRNAi will disturb the maternal function which often masks any later zygotic function or phenotype, it is difficult to study genes with both maternal and zygotic functions. In a recent publication from our lab, *Tc-germ cell-less* (*Tc-gcl*) was identified as a maternal component necessary in breaking AP axis symmetry by loading *Tc-axin* mRNA into the developing egg (Ansari et al., 2018). This early function and the phenotype caused by its knockdown, hinders the analysis of its possible zygotic function. Inhibition of maternal RNAi by ubiquitous RNAi inhibition in the mother could circumvent such problems. The maternal gene effect can occur, even after pRNAi. The dsRNA, however, is still processed and "inherited" to the offspring. Since there is likely little to no accumulation and, at least during early embryogenesis, also little to no expression of the VSR, embryonic (i.e. zygotic) gene function is inhibited and a phenotype might be recovered after pRNAi. A possibly lower zygotic expression of the VSR in the embryo could further be achieved by heterozygosity.

A more precise and targeted approach would be the expression of the VSR via the GAL4/UAS system (Schinko et al., 2010), that would enable blocking RNAi in specific tissue while RNAi could occur in all other tissues. Tests with GFP and body colour enzymes using the GAL4/UAS system were already successfully performed (Ulrich, 2015). The effectiveness of this approach is depending on the availability of GAL4 (enhancer trap)

lines. In *Tribolium*, the GEKU screen (Trauner et al., 2009) produced a large number of GAL4 enhancer traps lines that can be screened for suitable candidates with expression (or lack of) in specific tissue or over time. A gene with a known and desired expression pattern, could be engineered to a GAL4-line via CRISPR/Cas9 (Farnworth et al., 2020; Gilles et al., 2015). To screen for lines that do show GAL4 expression at a specific time and/or tissue is much more convenient than screening for lines that do not. Therefore a reversal of the above mentioned strategy is currently pursued in our lab. In this (as of yet) theoretical line, ubiquitous expression of the VSR would block RNAi in all tissues during development, including maternal tissues. To enable the removal of the RNAi inhibitor from the genome by tissue-specific expression of the Cre recombinase, the transgenic element could be flanked by LoxP sites (Metzger and Feil, 1999; Nagy, 2000). This would allow RNAi to function in only those cells that express the Cre recombinase while RNAi would remain blocked in all Cre recombinase-negative cells. The tissue-specificity of the Cre recombinase could easily be accomplished by GAL4 enhancer trap lines or engineered via CRISPR/Cas9 (Farnworth et al., 2020; Gilles et al., 2015). Research into the function of *Tc-wingless* (*Tc-wg*) during leg development (or many other processes that involve *Tc-wg* or Wnt signaling for that matter) would greatly benefit from such a system. For example, Grossmann and colleagues (2009) had to resort to embryonic RNAi applied at different time point during embryonic development, which is very time consuming and not applicable to all developmental processes or genes (as demonstrated by the failed application of *Tc-prd* "RNAi pulses", see Ulrich, 2015). Using a system as described above would enable tissue-specific RNAi in *Tribolium*, which has been utilized with great success in *Drosophila* research.

While the expression of the VSR via the endogenous heat-shock promoter of *Tribolium* offers easy and reliable expression, more nuanced ways to express an VSR with less "side effects" could even increase its usefulness. The genetic toolkit available in *Drosophila* is, compared to *Tribolium*, much more sophisticated. Especially the use of optogenetic-like[9] manipulation and photoconversion of proteins, which has only begun to be used in *Tribolium* research (Benton et al., 2013; Kitzmann, 2016), is ideal for rescue experiments.

[9] The word "optogenetic-like" is chosen as a compromise since there is no clear consensus on what "optogenetics" actually encompasses. By choosing this phrase, I hope to highlight the precise nature of optogenetical applications without assuming the mentioned references are using optogenetics.

For example, in a not yet peer-reviewed preprint (Johnson et al., 2019), the terminal patterning system of *Drosophila*, that is lost in Torso signaling mutants and results in loss of both anterior and posterior structures, was rescued by the use of an optogenetically activated Ras/Erk activity (being the intracellular signaling component of Torso signaling) (Johnson et al., 2017). This approach allowed for a more nuanced modification of Torso signaling both temporally and locally. Similar experiments in *Drosophila* using optogentic tools enabled for example a more detailed examination of the concentration dependence of *bcd* targets genes by modulation of *bcd* expression via varying illumination duration (Huang et al., 2017).

I used the hsVSR system in a sort of "all-or-nothing" approach to achieve the maximum amount of VSR expression balanced with survivability of embryos into L1 larvae. The VSR expression and therefore its RNAi inhibition and subsequent rescue effect could be adjusted by modulating length and, to a lesser degree, strength (i.e. temperature) of the heat shock treatment. Our hsVSR system is also applicable for RNAi of any gene (with the few limitations listed above), while many optogenetic approaches are gene specific. With the advancement of light-sheet live-imaging in *Tribolium* (Strobl and Stelzer, 2014; Strobl et al., 2015), an opto-genetically driven RNAi inhibition system, that might even be more "tunable" by light impulses, might b possible. Such a system could be used to directly observe rescue of the segmentation clock and its consequences in a developing germband and would be a much-welcomed tool. This in combination with the other described ideas of modulating VSR expression could increase the precision of gene function studies and the usefulness of *Tribolium* as a model organism.

6 References

Ahlmann-Eltze, C. (2019). *ggsignif: Significance Brackets for "ggplot2."*

Akam, M. (1987). The molecular basis for metameric pattern in the Drosophila embryo. *Development* **101**, 1–22.

Alberts, B., Johnson, A., Lewis, J., Raff, M., Roberts, K. and Walter, P. (2002). Drosophila and the molecular genetics of pattern formation: Genesis of the body plan. In *Molecular Biology of the Cell. 4th edition*, p. Garland Science.

Altschul, S. F., Gish, W., Miller, W., Myers, E. W. and Lipman, D. J. (1990). Basic local alignment search tool. *Journal of molecular biology* **215**, 403–410.

Anderson, L. E. (1954). Hoyer's Solution as a Rapid Permanent Mounting Medium for Bryophytes. *The Bryologist* **57**, 242–244.

Ansari, S., Troelenberg, N., Dao, V. A., Richter, T., Bucher, G. and Klingler, M. (2018). Double abdomen in a short-germ insect: Zygotic control of axis formation revealed in the beetle Tribolium castaneum. *Proceedings of the National Academy of Sciences of the United States of America* **115**, 1819–1824.

Aranda, M. (2006). Functional analysis of a homolog of the pair-rule gene hairy in the short-germ beetle Tribolium castaneum.

Aranda, M., Marques-Souza, H., Bayer, T. and Tautz, D. (2008). The role of the segmentation gene hairy in Tribolium. *Development Genes and Evolution* **218**, 465–477.

Bänziger, C., Soldini, D., Schütt, C., Zipperlen, P., Hausmann, G. and Basler, K. (2006). Wntless, a Conserved Membrane Protein Dedicated to the Secretion of Wnt Proteins from Signaling Cells. *Cell* **125**, 509–522.

Beermann, A., Prühs, R., Lutz, R. and Schröder, R. (2011). A context-dependent combination of Wnt receptors controls axis elongation and leg development in a short germ insect. *Development (Cambridge, England)* **138**, 2793–2805.

Bénazéraf, B. and Pourquié, O. (2013). Formation and segmentation of the vertebrate body axis. *Annual review of cell and developmental biology* **29**, 1–26.

Benton, M. A. (2018). A revised understanding of Tribolium morphogenesis further reconciles short and long germ development. *PLOS Biology* **16**, e2005093.

Benton, M. A., Akam, M. and Pavlopoulos, A. (2013). Cell and tissue dynamics during Tribolium embryogenesis revealed by versatile fluorescence labeling approaches. *Development (Cambridge, England)* **140**, 3210–3220.

Besnard-Guérin, C., Jacquier, C., Pidoux, J., Deddouche, S., Antoniewski, C. and Antoniewsk, C. (2015). The cricket paralysis virus suppressor inhibits microRNA silencing mediated by the Drosophila Argonaute-2 protein. *PLOS ONE* **10**, e0120205.

Bolognesi, R., Beermann, A., Farzana, L., Wittkopp, N., Lutz, R., Balavoine, G., Brown, S. J. and Schröder, R. (2008a). Tribolium Wnts: evidence for a larger repertoire in insects with overlapping expression patterns that suggest multiple redundant functions in embryogenesis. *Development Genes and Evolution* **218**, 193–202.

Bolognesi, R., Farzana, L., Fischer, T. D. and Brown, S. J. (2008b). Multiple wnt genes are required for segmentation in the short-germ embryo of tribolium castaneum. *Current biology : CB* **18**, 1624–1629.

Bolognesi, R., Fischer, T. D. and Brown, S. J. (2009). Loss of Tc-arrow and canonical Wnt signaling alters posterior morphology and pair-rule gene expression in the short-germ insect, Tribolium castaneum. *Development Genes and Evolution* **219**, 369–375.

Boos, A., Distler, J., Rudolf, H., Klingler, M. and El-Sherif, E. (2018). A re-inducible gap gene cascade patterns the anterior–posterior axis of insects in a threshold-free fashion. *eLife* **7**, 273.

Brown, S. J., Patel, N. H. and Denell, R. E. (1994). Embryonic expression of the single Tribolium engrailed homolog. *Developmental Genetics* **15**, 7–18.

Brown, S. J., Shippy, T. D., Miller, S., Bolognesi, R., Beeman, R. W., Lorenzen, M. D., Bucher, G., Wimmer, E. A. and Klingler, M. (2009). The red flour beetle, Tribolium castaneum (Coleoptera): a model for studies of development and pest biology. *Cold Spring Harbor Protocols* **2009**, pdb.emo126-pdb.emo126.

Bucher, G. (2009). *The Beetle Book*. 1.2. self-published.

Bucher, G. and Klingler, M. (2004). Divergent segmentation mechanism in the short germ insect Tribolium revealed by giant expression and function. *Development (Cambridge, England)* **131**, 1729–1740.

Bucher, G., Scholten, J. and Klingler, M. (2002). Parental RNAi in tribolium (coleoptera). *Current biology : CB* **12**, R85-6.

Budd, G. E. (2001). Why are arthropods segmented? *Evol Dev* **3**, 332–342.

Cerny, A. C., Bucher, G., Schröder, R. and Klingler, M. (2005). Breakdown of abdominal patterning in the Tribolium Krüppel mutant jaws. *Development (Cambridge, England)* **132**, 5353–5363.

Chapman, A. D. (2009). *Numbers of living species in australia and the world*.

Chipman, A. D. and Akam, M. (2008). The segmentation cascade in the centipede Strigamia maritima: involvement of the Notch pathway and pair-rule gene homologues. *Dev. Biol.* **319**, 160–169.

Chipman, A. D., Arthur, W. and Akam, M. (2004). A double segment periodicity underlies segment generation in centipede development. *Current Biology* **14**, 1250–1255.

Choe, C. P. and Brown, S. J. (2007). Evolutionary flexibility of pair-rule patterning revealed by functional analysis of secondary pair-rule genes, paired and sloppy-paired in the short-germ insect, Tribolium castaneum. *Developmental biology* **302**, 281–294.

Choe, C. P. and Brown, S. J. (2009). Genetic regulation of engrailed and wingless in Tribolium segmentation and the evolution of pair-rule segmentation. *Developmental biology* **325**, 482–491.

Choe, C. P., Miller, S. C. and Brown, S. J. (2006). A pair-rule gene circuit defines segments sequentially in the short-germ insect Tribolium castaneum. *Proceedings of the National Academy of Sciences of the United States of America* **103**, 6560–6564.

Choi, H. M. T., Schwarzkopf, M., Fornace, M. E., Acharya, A., Artavanis, G., Stegmaier, J., Cunha, A. and Pierce, N. A. (2018). Third-generation in situ hybridization chain reaction: multiplexed, quantitative, sensitive, versatile, robust. *Development (Cambridge, England)* **145**, dev165753.

Clark, E. (2017). Dynamic patterning by the Drosophila pair-rule network reconciles long-germ and short-germ segmentation. *PLOS Biology* **15**, e2002439.

Clark, E. and Akam, M. (2016). Odd-paired controls frequency doubling in Drosophila segmentation by altering the pair-rule gene regulatory network. *eLife* **5**, 1.

Clark, E. and Peel, A. D. (2018). Evidence for the temporal regulation of insect segmentation by a conserved sequence of transcription factors. *Development (Cambridge, England)* dev.155580.

Clark, E., Peel, A. D. and Akam, M. (2019). Arthropod segmentation. *Development (Cambridge, England)* **146**, dev170480.

Cooke, J. and Zeeman, E. C. (1976). A clock and wavefront model for control of the number of repeated structures during animal morphogenesis. *Journal of theoretical biology* **58**, 455–476.

Copf, T., Schröder, R. and Averof, M. (2004). Ancestral role of caudal genes in axis elongation and segmentation. *Proceedings of the National Academy of Sciences of the United States of America* **101**, 17711–17715.

Csorba, T., Pantaleo, V. and Burgyán, J. (2009). RNA Silencing: An Antiviral Mechanism. In *Advances in Virus Research*, pp. 35–230. Elsevier.

Damen, W. G. M., Weller, M. and Tautz, D. (2000). Expression patterns of hairy, even-skipped, and runt in the spider Cupiennius salei imply that these genes were segmentation genes in a basal arthropod. *PNAS* **97**, 4515–4519.

Das, S., Yu, S., Sakamori, R., Stypulkowski, E. and Gao, N. (2012). Wntless in Wnt secretion: molecular, cellular and genetic aspects. *Front Biol* **7**, 587–593.

Davis, G. K. and Patel, N. H. (1999). The origin and evolution of segmentation. *Trends in Cell Biology* **9**, M68–M72.

Davis, G. K. and Patel, N. H. (2002). Short, long, and beyond: molecular and embryological approaches to insect segmentation. *Annual review of entomology* **47**, 669–699.

Davis, G. K., Jaramillo, C. A. and Patel, N. H. (2001). Pax group III genes and the evolution of insect pair-rule patterning. *Development* **128**, 3445–3458.

de Rosa, R., Prud'homme, B. and Balavoine, G. (2005). caudal and even-skipped in the annelid Platynereis dumerilii and the ancestry of posterior growth. *Evolution & development* **7**, 574–587.

Distler, J. (2012). Überexpression von Gapgenen im Kurzkeimembryo von Tribolium castaneum.

Dönitz, J., Schmitt-Engel, C., Grossmann, D., Gerischer, L., Tech, M., Schoppmeier, M., Klingler, M. and Bucher, G. (2015). iBeetle-Base: a database for RNAi phenotypes in the red flour beetle Tribolium castaneum. *Nucleic Acids Res* **43**, D720–D725.

Dray, N., Tessmar-Raible, K., Gouar, M. L., Vibert, L., Christodoulou, F., Schipany, K., Guillou, A., Zantke, J., Snyman, H., Béhague, J., et al. (2010). Hedgehog Signaling Regulates Segment Formation in the Annelid Platynereis. *Science* **329**, 339–342.

El-Sherif, E., Averof, M. and Brown, S. J. (2012). A segmentation clock operating in blastoderm and germband stages of Tribolium development. *Development (Cambridge, England)* **139**, 4341–4346.

El-Sherif, E., Zhu, X., Fu, J. and Brown, S. J. (2015). Caudal regulates the spatiotemporal dynamics of pair-rule waves in tribolium. *PLoS genetics* **10**, e1004677.

Farnworth, M. S., Eckermann, K. N., Ahmed, H. M. M., Mühlen, D. S., He, B. and Bucher, G. (2020). The Red Flour Beetle as Model for Comparative Neural Development: Genome Editing to Mark Neural Cells in Tribolium Brain Development. In *Brain Development: Methods and Protocols* (ed. Sprecher, S. G.), pp. 191–217. New York, NY: Springer.

Farzana, L. and Brown, S. J. (2008). Hedgehog signaling pathway function conserved in Tribolium segmentation. *Development Genes and Evolution* **218**, 181–192.

Fire, A., Xu, S., Montgomery, M. K., Kostas, S. A., Driver, S. E. and Mello, C. C. (1998). Potent and specific genetic interference by double-stranded RNA in Caenorhabditis elegans. *Nature* **391**, 806–811.

Fu, J., Posnien, N., Bolognesi, R., Fischer, T. D., Rayl, P., Oberhofer, G., Kitzmann, P., Brown, S. J. and Bucher, G. (2012). Asymmetrically expressed axin required for anterior development in Tribolium. *Proceedings of the National Academy of Sciences* **109**, 7782–7786.

Gilbert, S. F. (2000). *Developmental Biology*. 6th ed. Sinauer Associates.

Gilles, A. F., Schinko, J. B. and Averof, M. (2015). Efficient CRISPR-mediated gene targeting and transgene replacement in the beetle Tribolium castaneum. *Development (Cambridge, England)*.

Graham, A., Butts, T., Lumsden, A. and Kiecker, C. (2014). What can vertebrates tell us about segmentation? *EvoDevo* **5**, 24.

Green, J. and Akam, M. (2013). Evolution of the pair rule gene network: Insights from a centipede. *Developmental Biology* **382**, 235–245.

Grimaldi, D. A. and Engel, M. S. (2005). *Evolution of the insects*. Cambridge [u.a.]: Cambridge Univ. Press.

Grossmann, D., Scholten, J. and Prpic, N.-M. (2009). Separable functions of wingless in distal and ventral patterning of the Tribolium leg. *Dev Genes Evol* **219**, 469–479.

Haas, S. M., Brown, S. J. and Beeman, R. W. (2001). Pondering the procephalon: the segmental origin of the labrum. *Dev Genes Evol* **211**, 89–95.

Hannibal, R. L. and Patel, N. H. (2013). What is a segment? *EvoDevo* **4**, 10.

Harding, K., Hoey, T., Warrior, R. and Levine, M. (1989). Autoregulatory and gap gene response elements of the even-skipped promoter of Drosophila. *The EMBO Journal* **8**, 1205–1212.

He, X., Semenov, M., Tamai, K. and Zeng, X. (2004). LDL receptor-related proteins 5 and 6 in Wnt/β-catenin signaling: Arrows point the way. *Development* **131**, 1663–1677.

Heemskerk, J., DiNardo, S., Kostriken, R. and O'Farrell, P. H. (1991). Multiple modes of engrailed regulation in the progression towards cell fate determination. *Nature* **352**, 404–410.

Herndon, N., Shelton, J., Gerischer, L., Ioannidis, P., Ninova, M., Dönitz, J., Waterhouse, R. M., Liang, C., Damm, C., Siemanowski, J., et al. (2020). Enhanced genome assembly and a new official gene set for Tribolium castaneum. *BMC Genomics* **21**, 47.

Horikawa, K., Ishimatsu, K., Yoshimoto, E., Kondo, S. and Takeda, H. (2006). Noise-resistant and synchronized oscillation of the segmentation clock. *Nature* **441**, 719–723.

Huang, A., Amourda, C., Zhang, S., Tolwinski, N. S. and Saunders, T. E. (2017). Decoding temporal interpretation of the morphogen Bicoid in the early Drosophila embryo. *eLife* **6**, e26258.

Hubaud, A. and Pourquié, O. (2014). Signalling dynamics in vertebrate segmentation. *Nat Rev Mol Cell Biol* **15**, 709–721.

Ingham, P. W., Taylor, A. M. and Nakano, Y. (1991). Role of the Drosophila patched gene in positional signalling. *Nature* **353**, 184–187.

Janssen, R., Le Gouar, M., Pechmann, M., Poulin, F., Bolognesi, R., Schwager, E. E., Hopfen, C., Colbourne, J. K., Budd, G. E., Brown, S. J., et al. (2010). Conservation, loss, and redeployment of Wnt ligands in protostomes: implications for understanding the evolution of segment formation. *BMC Evolutionary Biology* **10**, 374.

Jiang, J., Hoey, T. and Levine, M. (1991). Autoregulation of a segmentation gene in Drosophila: combinatorial interaction of the even-skipped homeo box protein with a distal enhancer element. *Genes Dev.* **5**, 265–277.

Johnson, H. E., Goyal, Y., Pannucci, N. L., Schüpbach, T., Shvartsman, S. Y. and Toettcher, J. E. (2017). The Spatiotemporal Limits of Developmental Erk Signaling. *Developmental Cell* **40**, 185–192.

Johnson, H. E., Shvartsman, S. Y. and Toettcher, J. E. (2019). Optogenetic rescue of a developmental patterning mutant. *bioRxiv* 776120.

Jouve, C., Palmeirim, I., Henrique, D., Beckers, J., Gossler, A., Ish-Horowicz, D. and Pourquie, O. (2000). Notch signalling is required for cyclic expression of the hairy-like gene HES1 in the presomitic mesoderm. *Development* **127**, 1421–1429.

Kassambara, A. (2020). *ggpubr: "ggplot2" based publication ready plots*.

Kitzmann, P. (2016). Morphogenesis and Genetic Regulation of the Insect Head.

Kitzmann, P., Weißkopf, M., Schacht, M. I. and Bucher, G. (2017). A key role for foxQ2 in anterior head and central brain patterning in insects. *Development (Cambridge, England)* **144**, 2969–2981.

Lewis, J. (2003). Autoinhibition with Transcriptional Delay: A Simple Mechanism for the Zebrafish Somitogenesis Oscillator. *Current Biology* **13**, 1398–1408.

Livak, K. J. and Schmittgen, T. D. (2001). Analysis of Relative Gene Expression Data Using Real-Time Quantitative PCR and the 2−ΔΔCT Method. *Methods* **25**, 402–408.

Lorenzen, M. D., Brown, S. J., Denell, R. E. and Beeman, R. W. (2002). Cloning and characterization of the Tribolium castaneum eye-color genes encoding tryptophan oxygenase and kynurenine 3-monooxygenase. *Genetics* **160**, 225–234.

Maderspacher, F., Bucher, G. and Klingler, M. (1998). Pair-rule and gap gene mutants in the flour beetle Tribolium castaneum. *Development Genes and Evolution* **208**, 558–568.

Maroto, M., Bone, R. A. and Dale, J. K. (2012). Somitogenesis. *Development* **139**, 2453–2456.

Marques-Souza, H., Aranda, M. and Tautz, D. (2008). Delimiting the conserved features of hunchback function for the trunk organization of insects. *Development (Cambridge, England)* **135**, 881–888.

Martin, B. L. and Kimelman, D. (2009). Wnt signaling and the evolution of embryonic posterior development. *Current biology : CB* **19**, R215-9.

Matsumiya, M., Tomita, T., Yoshioka-Kobayashi, K., Isomura, A. and Kageyama, R. (2018). ES cell-derived presomitic mesoderm-like tissues for analysis of synchronized oscillations in the segmentation clock. *Development* **145**,.

McGregor, A. P., Pechmann, M., Schwager, E. E., Feitosa, N. M., Kruck, S., Aranda, M. and Damen, W. G. M. (2008). Wnt8 Is Required for Growth-Zone Establishment and Development of Opisthosomal Segments in a Spider. *Current Biology* **18**, 1619–1623.

McGregor, A. P., Pechmann, M., Schwager, E. E. and Damen, W. G. (2009). An ancestral regulatory network for posterior development in arthropods. *Communicative & integrative biology* **2**, 174–176.

Metzger, D. and Feil, R. (1999). Engineering the mouse genome by site-specific recombination. *Current opinion in biotechnology* **10**, 470–476.

Mohler, J. and Vani, K. (1992). Molecular organization and embryonic expression of the hedgehog gene involved in cell-cell communication in segmental patterning of Drosophila. *Development* **115**, 957–971.

Nagy, A. (2000). Cre recombinase: the universal reagent for genome tailoring. *Genesis* **26**, 99–109.

Nagy, L. M. and Carroll, S. (1994). Conservation of wingless patterning functions in the short-germ embryos of Tribolium castaneum. *Nature* **367**, 460–463.

Nayak, A., Berry, B., Tassetto, M., Kunitomi, M., Acevedo, A., Deng, C., Krutchinsky, A., Gross, J., Antoniewski, C. and Andino, R. (2010). Cricket paralysis virus antagonizes Argonaute 2 to modulate antiviral defense in Drosophila. *Nature Publishing Group* **17**, 547–554.

Nayak, A., Kim, D. Y., Trnka, M. J., Kerr, C. H., Lidsky, P. V., Stanley, D. J., Rivera, B. M., Li, K. H., Burlingame, A. L., Jan, E., et al. (2018). A viral protein restricts drosophila RNAi immunity by regulating argonaute activity and stability. *Cell Host & Microbe* **24**, 542-557.e9.

Nüsslein-Volhard, C. and Wieschaus, E. (1980). Mutations affecting segment number and polarity in Drosophila. *Nature* **287**, 795–801.

Oberhofer, G. (2014). A functional analysis of a signaling center of the insect head.

Oberhofer, G., Grossmann, D., Siemanowski, J. L., Beissbarth, T. and Bucher, G. (2014). Wnt/β-catenin signaling integrates patterning and metabolism of the insect growth zone. *Development (Cambridge, England)* **141**, 4740–4750.

Paese, C. L. B., Schoenauer, A., Leite, D. J., Russell, S. and McGregor, A. P. (2018). A SoxB gene acts as an anterior gap gene and regulates posterior segment addition in a spider. *eLife* **7**, e37567.

Palmeirim, I., Henrique, D., Ish-Horowicz, D. and Pourquié, O. (1997a). Avian hairy gene expression identifies a molecular clock linked to vertebrate segmentation and somitogenesis. *Cell* **91**, 639–648.

Palmeirim, I., Henrique, D., Ish-Horowicz, D. and Pourquié, O. (1997b). Avian hairy Gene Expression Identifies a Molecular Clock Linked to Vertebrate Segmentation and Somitogenesis. *Cell* **91**, 639–648.

Patel, N. H., Condron, B. G. and Zinn, K. (1994). Pair-rule expression patterns of even-skipped are found in both short- and long-germ beetles. *Nature* **367**, 429–434.

Pedersen, T. L. (2019). *patchwork: The composer of plots*.

Peel, A. and Akam, M. (2003). Evolution of segmentation: Rolling back the clock. *Current Biology* **13**, R708–R710.

Peel, A. D., Chipman, A. D. and Akam, M. (2005). Arthropod segmentation: beyond the Drosophila paradigm. *Nature reviews. Genetics* **6**, 905–916.

Peel, A. D., Schanda, J., Grossmann, D., Ruge, F., Oberhofer, G., Gilles, A. F., Schinko, J. B., Klingler, M. and Bucher, G. (2013). Tc-knirps plays different roles in the specification of antennal and mandibular parasegment boundaries and is regulated by a pair-rule gene in the beetle Tribolium castaneum. **13**, 25.

Posnien, N., Schinko, J., Grossmann, D., Shippy, T. D., Konopova, B. and Bucher, G. (2009a). RNAi in the red flour beetle (tribolium). *Cold Spring Harbor Protocols* **2009**, pdb.prot5256-pdb.prot5256.

Posnien, N., Bashasab, F. and Bucher, G. (2009b). The insect upper lip (labrum) is a nonsegmental appendage-like structure. *Evolution & development* **11**, 480–488.

Prpic, N.-M. and Damen, W. G. M. (2008). Arthropod appendages: a prime example for the evolution of morphological diversity and innovation. In *Evolving Pathways: Key Themes in Evolutionary Developmental Biology*, pp. 381–398. Cambridge University Press.

Prud'homme, B., Rosa, R. de, Arendt, D., Julien, J.-F., Pajaziti, R., Dorresteijn, A. W. C., Adoutte, A., Wittbrodt, J. and Balavoine, G. (2003). Arthropod-like Expression Patterns of engrailed and wingless in the Annelid Platynereis dumerilii Suggest a Role in Segment Formation. *Current Biology* **13**, 1876–1881.

Pultz, M. A., Zimmerman, K. K., Alto, N. M., Kaeberlein, M., Lange, S. K., Pitt, J. N., Reeves, N. L. and Zehrung, D. L. (2000). A Genetic Screen for Zygotic Embryonic Lethal Mutations Affecting Cuticular Morphology in the Wasp Nasonia vitripennis. *Genetics* **154**, 1213–1229.

R Core Team (2018). *R: A language and environment for statistical computing*. Vienna, Austria.

Richmond, D. L. and Oates, A. C. (2012). The segmentation clock: inherited trait or universal design principle? *Current Opinion in Genetics & Development* **22**, 600–606.

Riedel-Kruse, I. H., Müller, C. and Oates, A. C. (2007). Synchrony Dynamics During Initiation, Failure, and Rescue of the Segmentation Clock. *Science* **317**, 1911–1915.

RStudio Team (2015). *RStudio: Integrated development environment for r*. Boston, MA.

Sambrook, J. and Russell, D. W. (2001). *Molecular cloning*. CSHL Press.

Sander, K. (1976). Specification of the Basic Body Pattern in Insect Embryogenesis. In *Advances in Insect Physiology*, pp. 125–238. Elsevier.

Sarrazin, A. F., Peel, A. D. and Averof, M. (2012). A segmentation clock with two-segment periodicity in insects. *Science* **336**, 338–341.

Schindelin, J., Arganda-Carreras, I., Frise, E., Kaynig, V., Longair, M., Pietzsch, T., Preibisch, S., Rueden, C., Saalfeld, S., Schmid, B., et al. (2012). Fiji: an open-source platform for biological-image analysis. *Nature Methods* **9**, 676–682.

Schinko, J. B., Kreuzer, N., Offen, N., Posnien, N., Wimmer, E. A. and Bucher, G. (2008). Divergent functions of orthodenticle, empty spiracles and buttonhead in early head patterning of the beetle Tribolium castaneum (Coleoptera). *Developmental biology* **317**, 600–613.

Schinko, J., Posnien, N., Kittelmann, S., Koniszewski, N. and Bucher, G. (2009). Single and double whole-mount in situ hybridization in red flour beetle (tribolium) embryos. *Cold Spring Harbor Protocols* **2009**, pdb.prot5258-pdb.prot5258.

Schinko, J. B., Weber, M., Viktorinova, I., Kiupakis, A., Averof, M., Klingler, M., Wimmer, E. A. and Bucher, G. (2010). Functionality of the GAL4/UAS system in Tribolium requires the use of endogenous core promoters. **10**, 53.

Schinko, J. B., Hillebrand, K. and Bucher, G. (2012). Heat shock-mediated misexpression of genes in the beetle Tribolium castaneum. *Development Genes and Evolution* **222**, 287–298.

Schmidt-Ott, U. and Technau, G. M. (1992). Expression of en and wg in the embryonic head and brain of Drosophila indicates a refolded band of seven segment remnants. *Development* **116**, 111–125.

Schmidt-Ott, U., González-Gaitán, M., Jäckle, H. and Technau, G. M. (1994). Number, identity, and sequence of the Drosophila head segments as revealed by neural elements and their deletion patterns in mutants. *Proc Natl Acad Sci U S A* **91**, 8363–8367.

Schmitt-Engel, C., Schultheis, D., Schwirz, J., Ströhlein, N., Troelenberg, N., Majumdar, U., Dao, V. A., Grossmann, D., Richter, T., Tech, M., et al. (2015). The iBeetle large-scale RNAi screen reveals gene functions for insect development and physiology. *Nature communications* **6**, 7822.

Schmittgen, T. D. and Livak, K. J. (2008). Analyzing real-time PCR data by the comparative Ct method. *Nature Protocols* **3**, 1101–1108.

Schönauer, A., Paese, C. L. B., Hilbrant, M., Leite, D. J., Schwager, E. E., Feitosa, N. M., Eibner, C., Damen, W. G. M. and McGregor, A. P. (2016). The Wnt and Delta-Notch signalling pathways interact to direct pair-rule gene expression via caudal during segment addition in the spider Parasteatoda tepidariorum. *Development (Cambridge, England)* **143**, 2455–2463.

Schoppmeier, M. and Schröder, R. (2005). Maternal torso signaling controls body axis elongation in a short germ insect. *Current Biology* **15**, 2131–2136.

Schröder, R. (2003). The genes orthodenticle and hunchback substitute for bicoid in the beetle Tribolium. *Nature* **422**, 621–625.

Schröder, R., Jay, D. G. and Tautz, D. (1999). Elimination of EVE protein by CALI in the short germ band insect Tribolium suggests a conserved pair-rule function for even skipped. *Mechanisms of Development* **80**, 191–195.

Schröder, R., Eckert, C., Wolff, C. and Tautz, D. (2000). Conserved and divergent aspects of terminal patterning in the beetle Tribolium castaneum. *Proceedings of the National Academy of Sciences of the United States of America* **97**, 6591–6596.

Schröder, R., Beermann, A., Wittkopp, N. and Lutz, R. (2008). From development to biodiversity – Tribolium castaneum, an insect model organism for short germband development. *Development Genes and Evolution* **218**, 119–126.

Schröter, C., Ares, S., Morelli, L. G., Isakova, A., Hens, K., Soroldoni, D., Gajewski, M., Jülicher, F., Maerkl, S. J., Deplancke, B., et al. (2012). Topology and Dynamics of the Zebrafish Segmentation Clock Core Circuit. *PLOS Biology* **10**, e1001364.

Schultheis, D., Weißkopf, M., Schaub, C., Ansari, S., Dao, V. A., Grossmann, D., Majumdar, U., Hakeemi, M. S., Troelenberg, N., Richter, T., et al. (2019). A large scale systemic RNAi screen in the red flour beetle tribolium castaneum identifies novel genes involved in insect muscle development. *G3: Genes|Genomes|Genetics* g3.200995.2018.

Schulz, C., Schröder, R., Hausdorf, B., Wolff, C. and Tautz, D. (1998). A caudal homologue in the short germ band beetle Tribolium shows similarities to both, the Drosophila and the vertebrate caudal expression patterns. *Development Genes and Evolution* **208**, 283–289.

Siemanowski, J., Richter, T., Dao, V. A. and Bucher, G. (2015). Notch signaling induces cell proliferation in the labrum in a regulatory network different from the thoracic legs. *Developmental biology* **408**, 164–177.

Stollewerk, A., Schoppmeier, M. and Damen, W. G. M. (2003). Involvement of Notch and Delta genes in spider segmentation. *Nature* **423**, 863–865.

Strobl, F. and Stelzer, E. H. K. (2014). Non-invasive long-term fluorescence live imaging of Tribolium castaneum embryos. *Development (Cambridge, England)* **141**, 2331–2338.

Strobl, F., Schmitz, A. and Stelzer, E. H. K. (2015). Live imaging of Tribolium castaneum embryonic development using light-sheet-based fluorescence microscopy. *Nature Protocols* **10**, 1486–1507.

Sulston, I. A. and Anderson, K. V. (1996). Embryonic patterning mutants of Tribolium castaneum. *Development* **122**, 805–814.

Suppressor of RNA silencing (2020). *Viralzone*.

Tautz, D. (2004). Segmentation. *Developmental Cell* **7**, 301–312.

Tautz, D. and Sommer, R. J. (1995). Evolution of segmentation genes in insects. *Trends in Genetics* **11**, 23–27.

Tomoyasu, Y. and Denell, R. E. (2004). Larval RNAi in Tribolium (Coleoptera) for analyzing adult development. *Development Genes and Evolution* **214**, 575–578.

Trauner, J., Schinko, J., Lorenzen, M. D., Shippy, T. D., Wimmer, E. A., Beeman, R. W., Klingler, M., Bucher, G. and Brown, S. J. (2009). Large-scale insertional mutagenesis of a coleopteran stored grain pest, the red flour beetle Tribolium castaneum, identifies embryonic lethal mutations and enhancer traps. *BMC Biology* **7**, 73.

Ulrich, J. (2015). Application of RNA interference for the study of lethal genes and dynamic processes.

Ulrich, J., Dao, V. A., Majumdar, U., Schmitt-Engel, C., Schwirz, J., Schultheis, D., Ströhlein, N., Troelenberg, N., Grossmann, D., Richter, T., et al. (2015). Large scale RNAi screen in Tribolium reveals novel target genes for pest control and the proteasome as prime target. *BMC Genomics* **16**, 674.

van Mierlo, J. T., van Cleef, K. W. R. and van Rij, R. P. (2011). Defense and counterdefense in the RNAi-based antiviral immune system in insects. In *Antiviral RNAi. Methods in Molecular Biology (Methods and Protocols)*, pp. 3–22.

Wickham, H. (2007). Reshaping data with the {reshape} package. *Journal of Statistical Software* **21**, 1–20.

Wickham, H. (2016). *ggplot2: Elegant graphics for data analysis*. Springer-Verlag New York.

Wickham, H. and Bryan, J. (2019). *readxl: Read excel files*.

Wickham, H., François, R., Henry, L. and Müller, K. (2020). *dplyr: A grammar of data manipulation*.

Xie, F., Xiao, P., Chen, D., Xu, L. and Zhang, B. (2012). miRDeepFinder: a miRNA analysis tool for deep sequencing of plant small RNAs. *Plant Molecular Biology* **80**, 75–84.

Zhu, X., Rudolf, H., Healey, L., François, P., Brown, S. J., Klingler, M. and El-Sherif, E. (2017). Speed regulation of genetic cascades allows for evolvability in the body plan specification of insects. *Proceedings of the National Academy of Sciences of the United States of America* **128**, 201702478-E8655.

7 Appendix

7.1 Supplementary figures

A

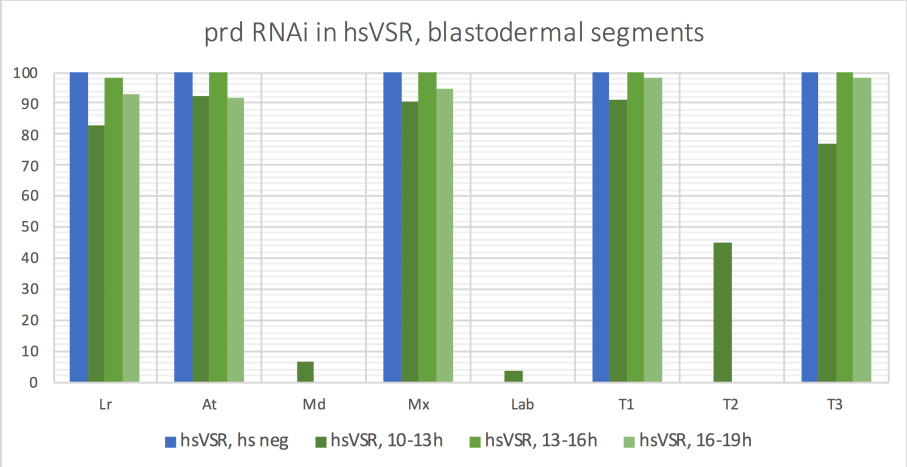

B

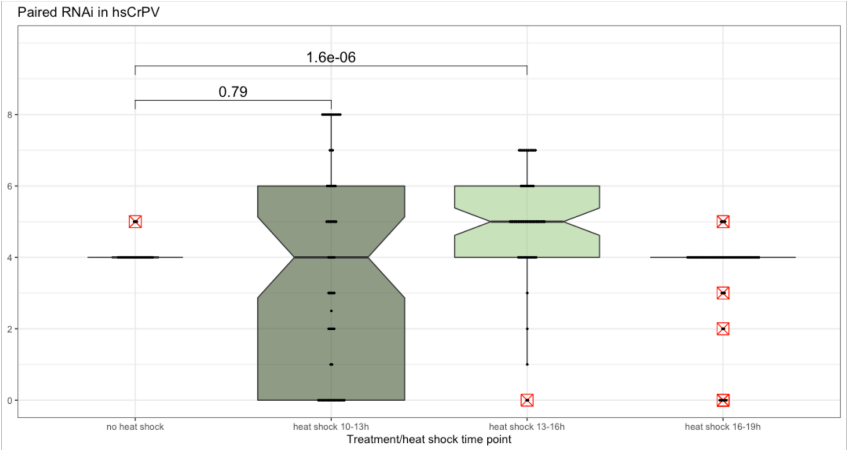

Figure S7.1 – Repetition of Tc-prd RNAi

Repetition of Tc-prd RNAi in hsVSR and hs-treatment at indicated time points. (A) Bar chart of remaining blastodermal segments. (B) Boxplot of remaining abdominal segments. Possible outlier (see material and methods) in red. See text for further details

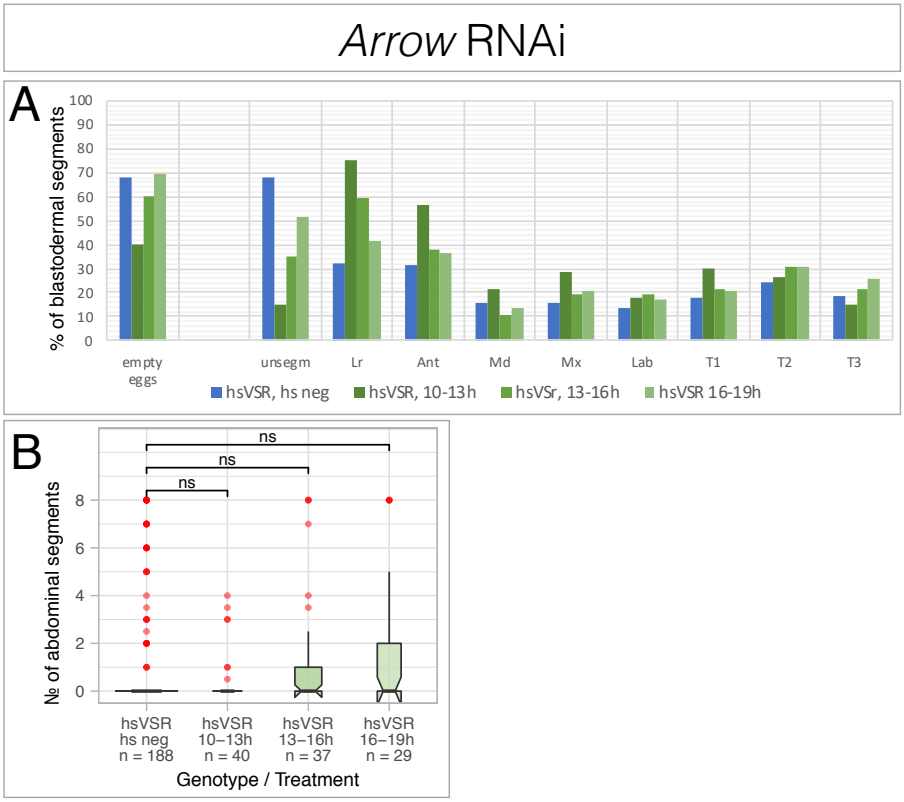

Figure S7.2 – Repetition of Tc-arrow RNAi in hsVSR

Repetition of *Tc-arr* RNAi in hsVSR. Hs-treatment at indicated time points. (A) Bar chart of remaining blastodermal segments. (B) Boxplot of remaining abdominal segments. Possible outlier (see material and methods) in red. See text for further details.

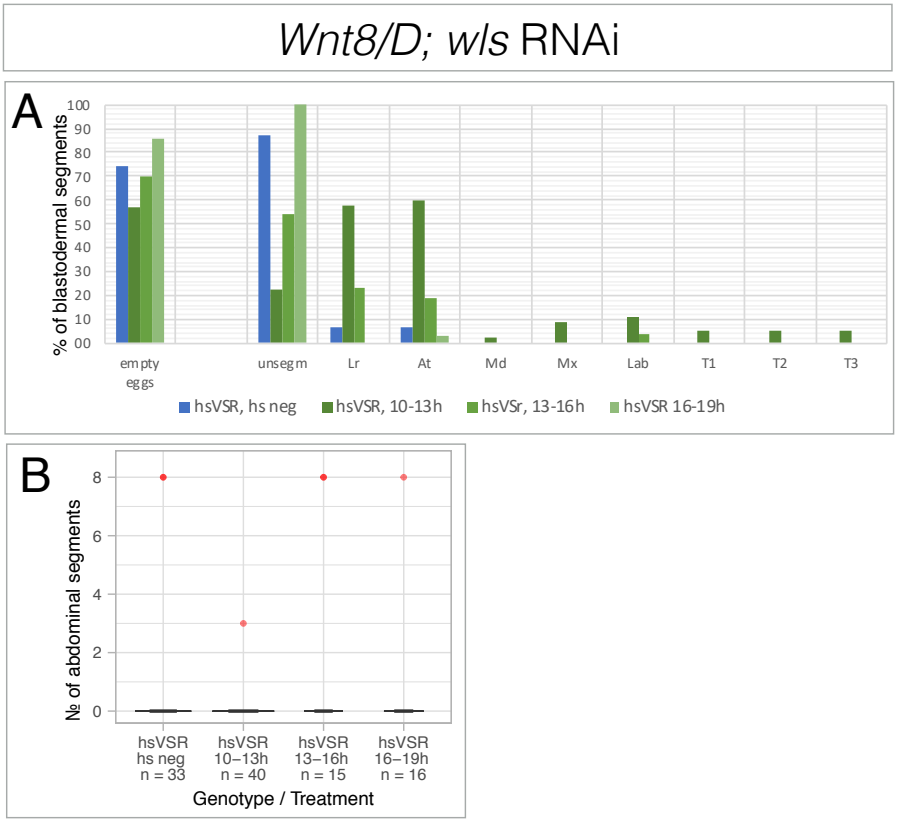

Figure S7.3 – Repetition of Tc-Wnt8/D; Tc-wls RNAi

Repetition of *Tc-Wnt8/D; Tc-wls* RNAi in hsVSR with hs-treatment as indicated. (A) Bar chart of remaining blastodermal segments. (B) Boxplot of remaining abdominal segments. Possible outlier (see material and methods) in red. See text for further details.

A

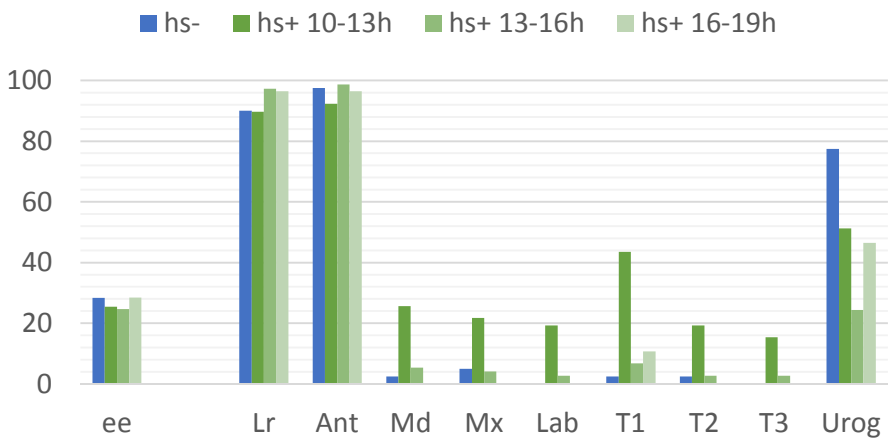

B

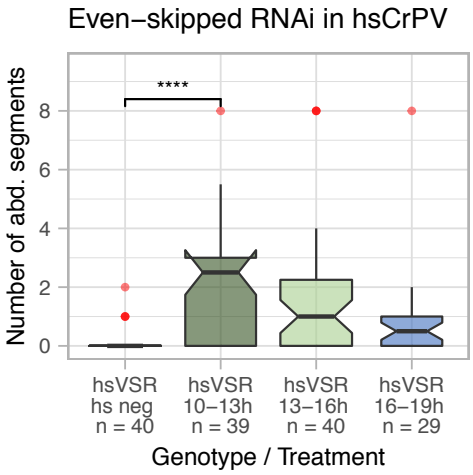

Figure S7.4 – Repetition of Tc-eve RNAi I

Repetition of *Tc-eve* RNAi in hsVSR and hs-treatment as indicated. (A) Bar chart of remaining blastodermal segments. (B) Boxplot of remaining abdominal segments. Possible outlier (see material and methods) in red. See text for further details.

A

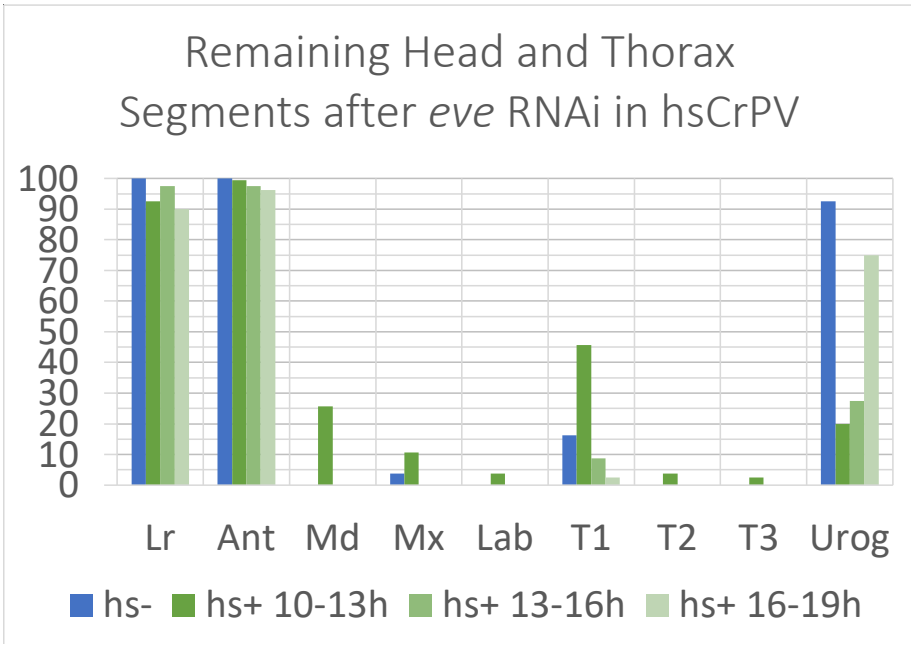

B

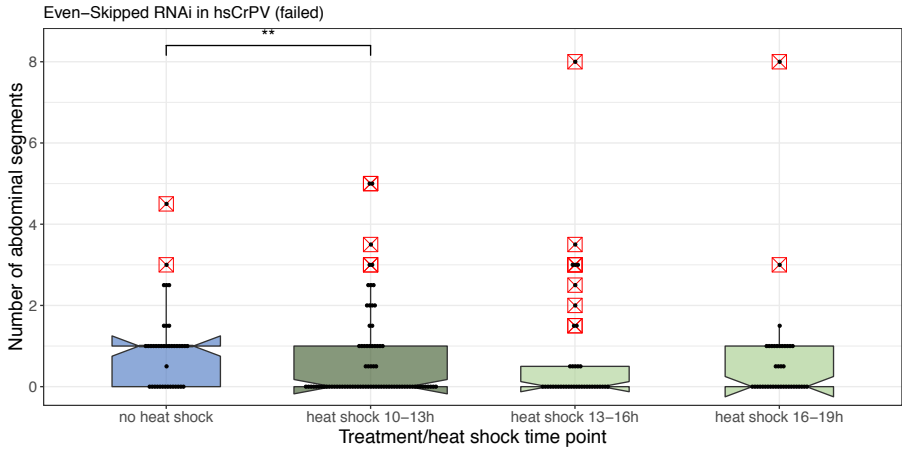

Figure S7.5 – Repetition of Tc-eve RNAi II

Repetition of *Tc-eve* RNAi in hsVSR. (A) Bar chart of remaining blastodermal segments. (B) Boxplot of remaining abdominal segments. Possible outlier (see material and methods) in red. See text for further details.

A

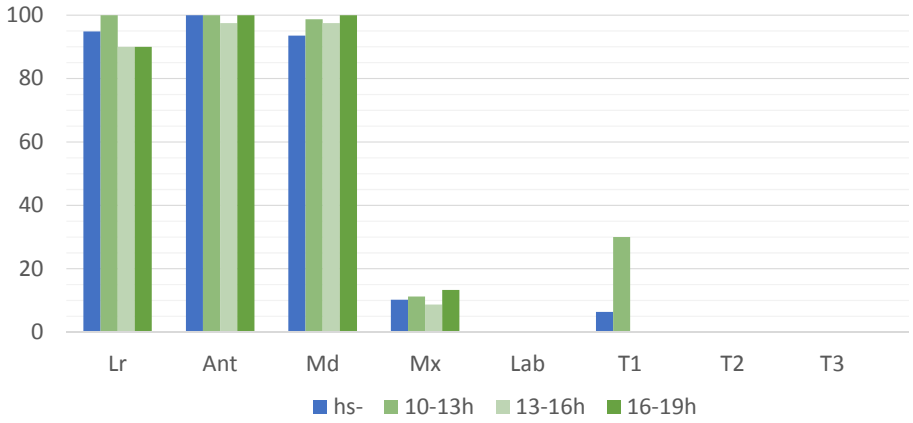

B

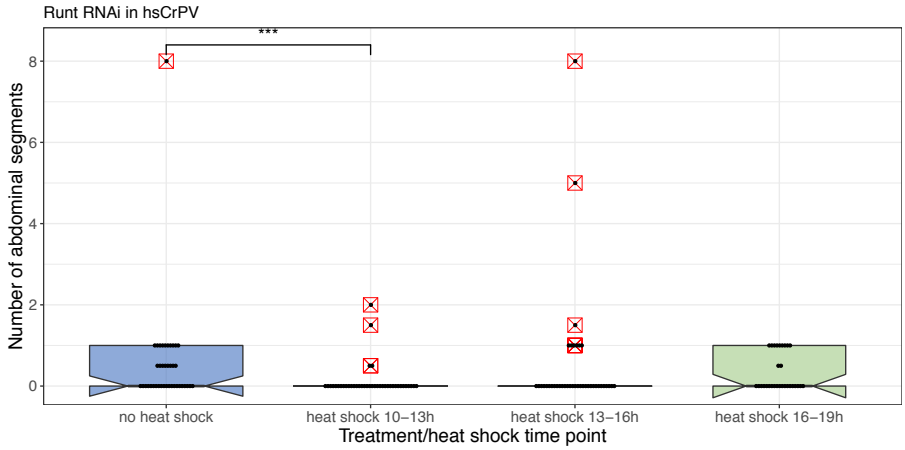

Figure S7.6 – Repetition of Tc-run RNAi I

Repetition of *Tc-run* RNAi in hsVSR and hs-treatment as indicated. (A) Bar chart of remaining blastodermal segments. (B) Boxplot of remaining abdominal segments. Possible outlier (see material and methods) in red. See text for further details.

A

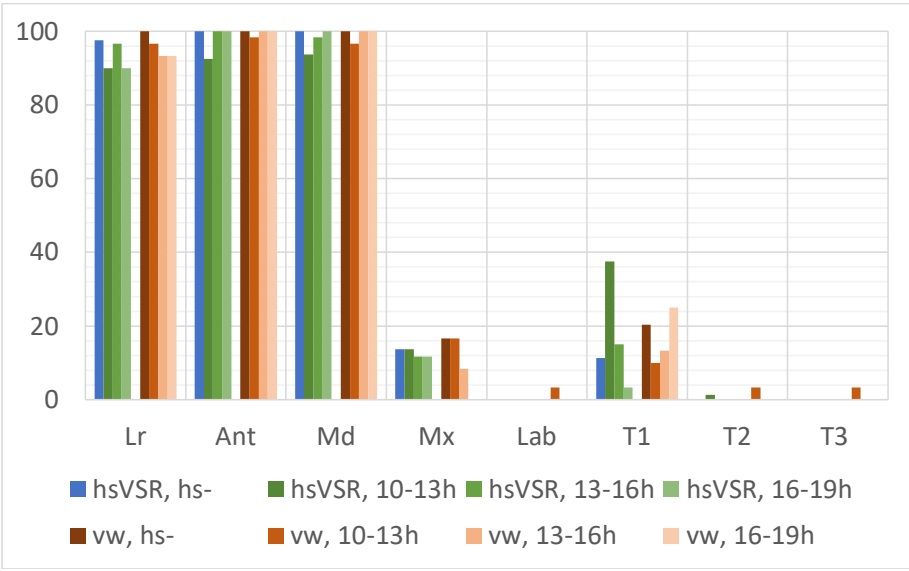

B

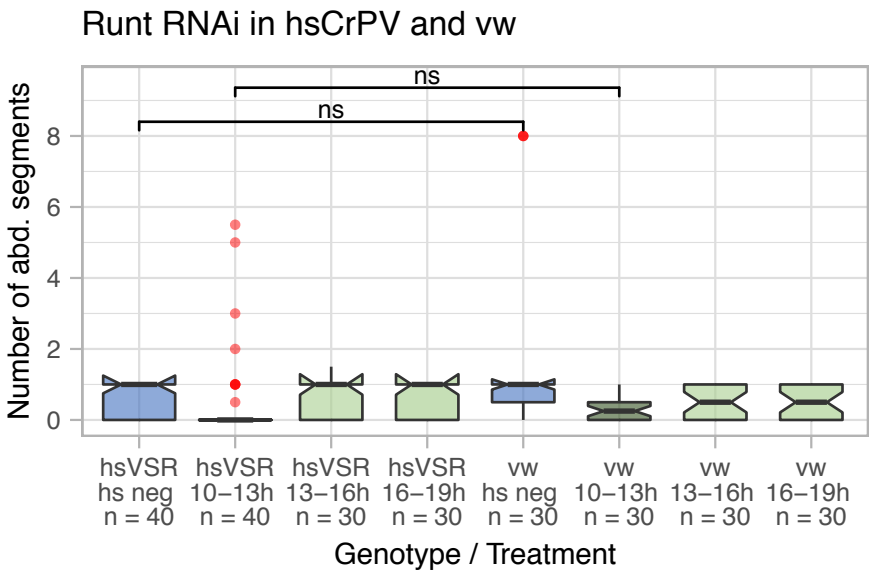

Figure S7.7 – Repetition of Tc-run RNAi II

Repetition of *Tc-run* RNAi in hsVSR and vw, hs-treatment as indicated. (A) Bar chart of remaining blastodermal segments. (B) Boxplot of remaining abdominal segments. Possible outlier (see material and methods) in red. See text for further details.

A

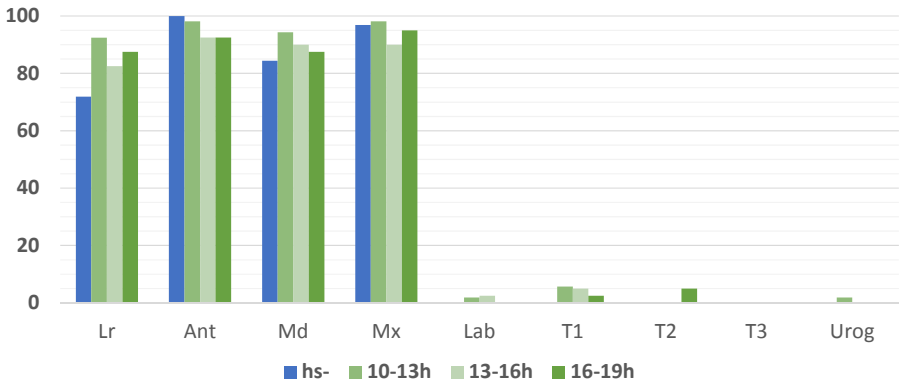

B

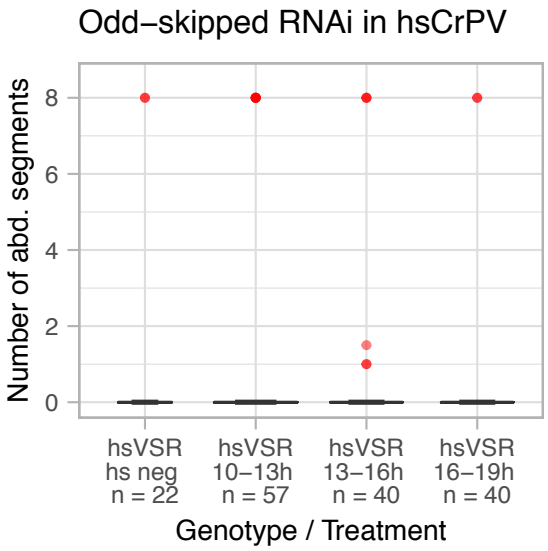

Figure S7.8 – Repetition of Tc-odd RNAi I

Repetition of *Tc-odd* Rnai in hsVSR and hs-treatment as indicated. (A) Bar chart of remaining blastodermal segments. (B) Boxplot of remaining abdominal segments. Possible outlier (see material and methods) in red. See text for further details.

A

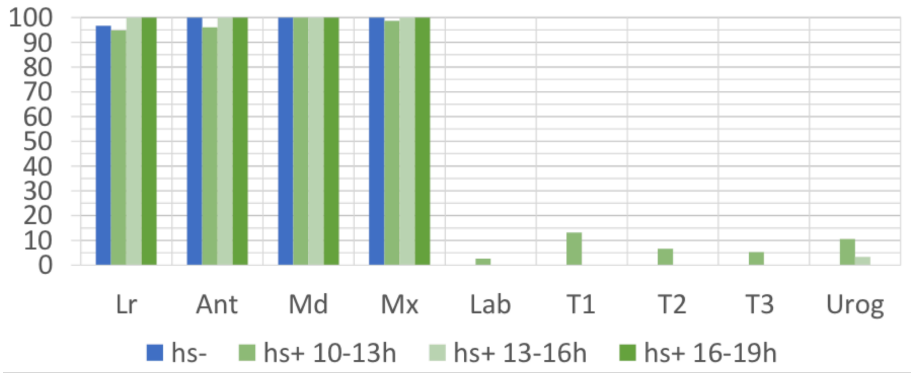

B

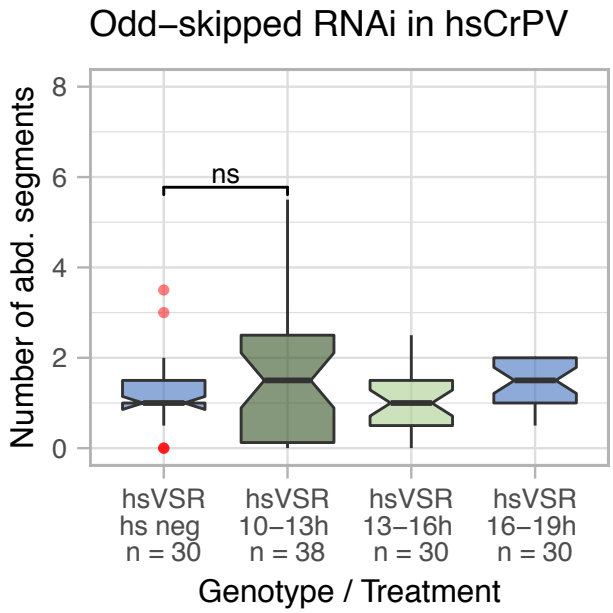

Figure S7.9 – Repetition of Tc-odd RNAi II

Repetition of *Tc-odd* RNAi in hsVSR, hs-treatment as indicated. (A) Bar chart of remaining blastodermal segments. (B) Boxplot of remaining abdominal segments. Possible outlier (see material and methods) in red. See text for further details.

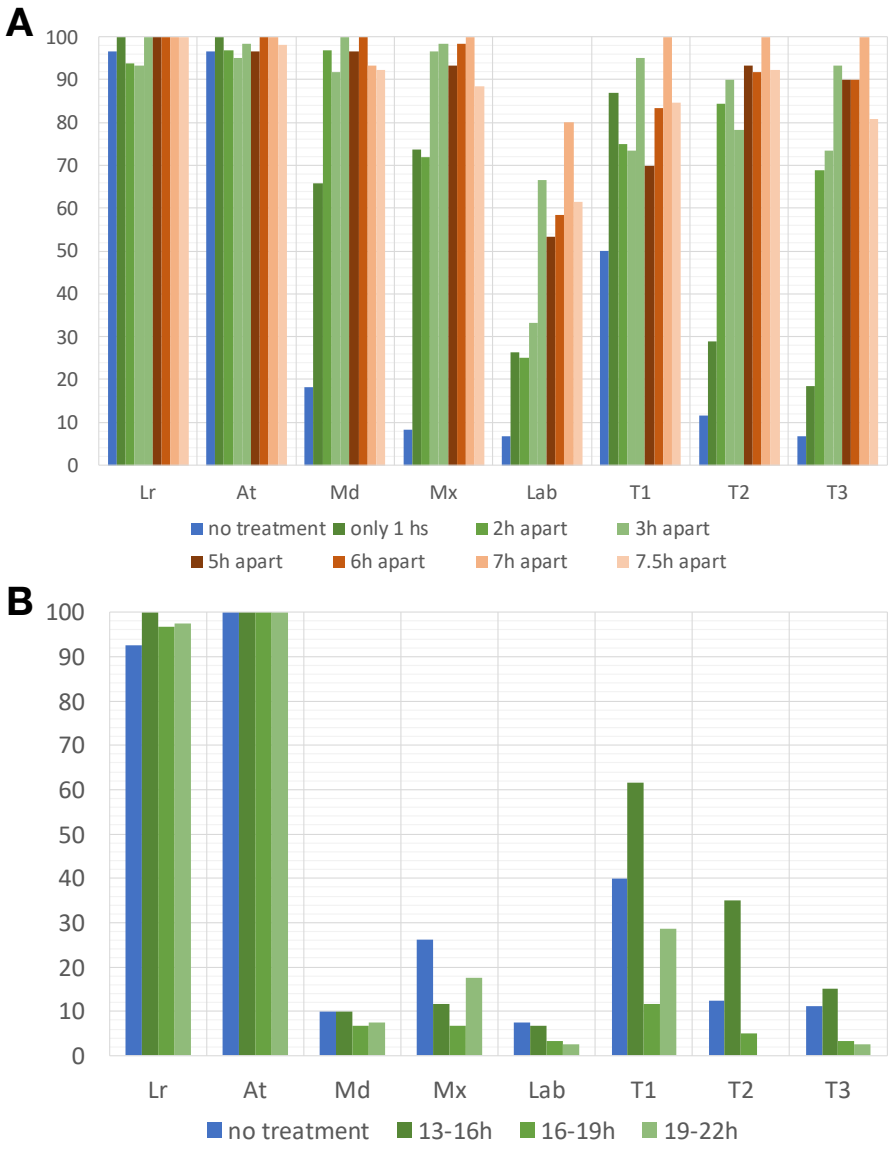

Figure S7.10 – Blastodermal segments after Tc-eve RNAi in hsVSR X hshb

Remaining blastodermal segments after *Tc-eve* RNAi and hs-treatment as indicated (see Fig. 4.20A for experimental procedure related to A; see Fig. 4.20B for experimental procedure related to B). Segments of cuticles in A correspond to abdominal segments shown in Boxplot 4.21A, while Segments of cuticles in B correspond to abdominal segments shown in Boxplot 4.21B.

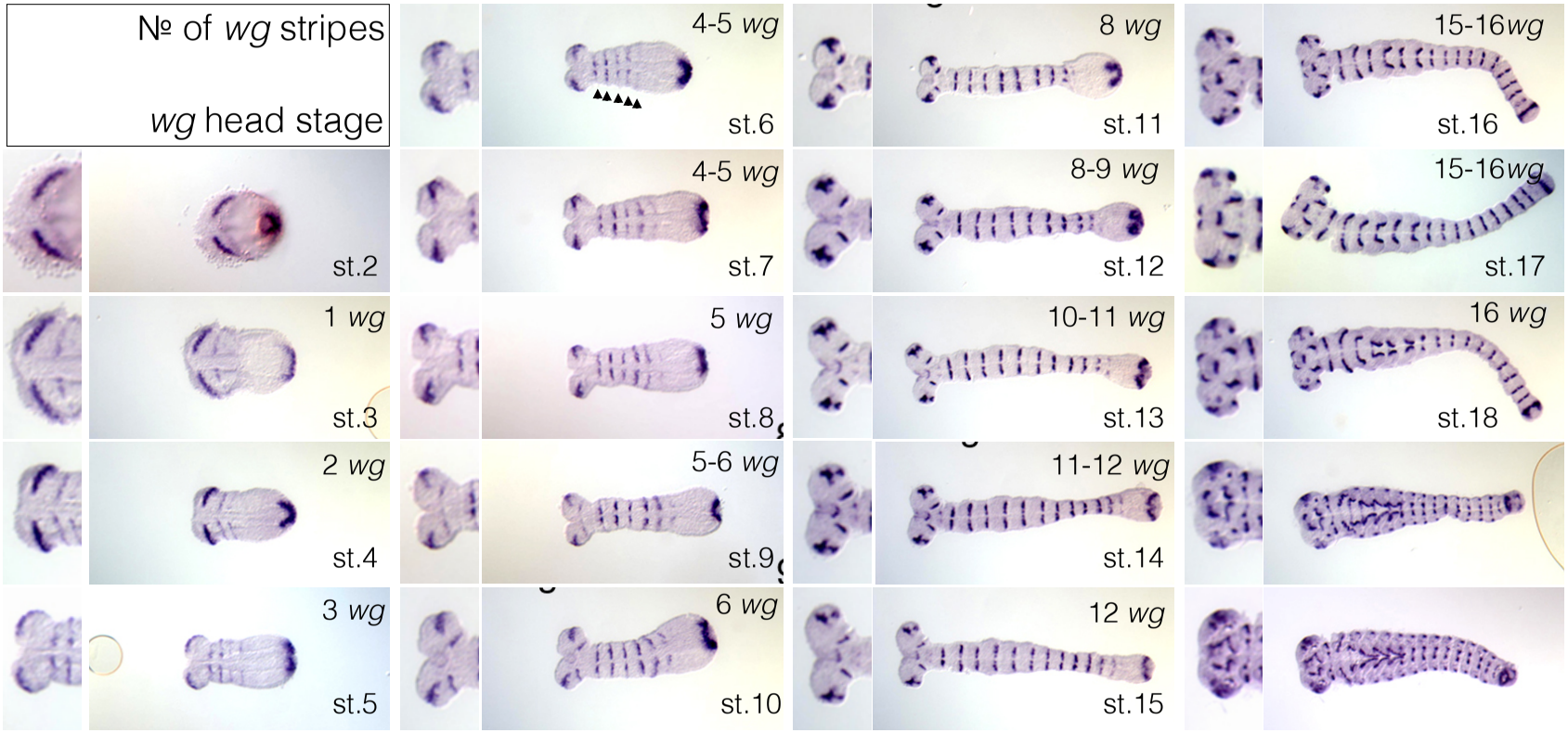

Figure S7.11 – Tc-wg head stages

Anterior to the left. Overview of *Tc-wg* head stages. Germbands are sorted by the increasing number of *Tc-wg* stripes, counted from the mandibular stripe onwards. Magnification of the head region used for head staging to the left of each germband. (Images of *Tc-wg* in-situ hybridization by G. Bucher (unpublished))

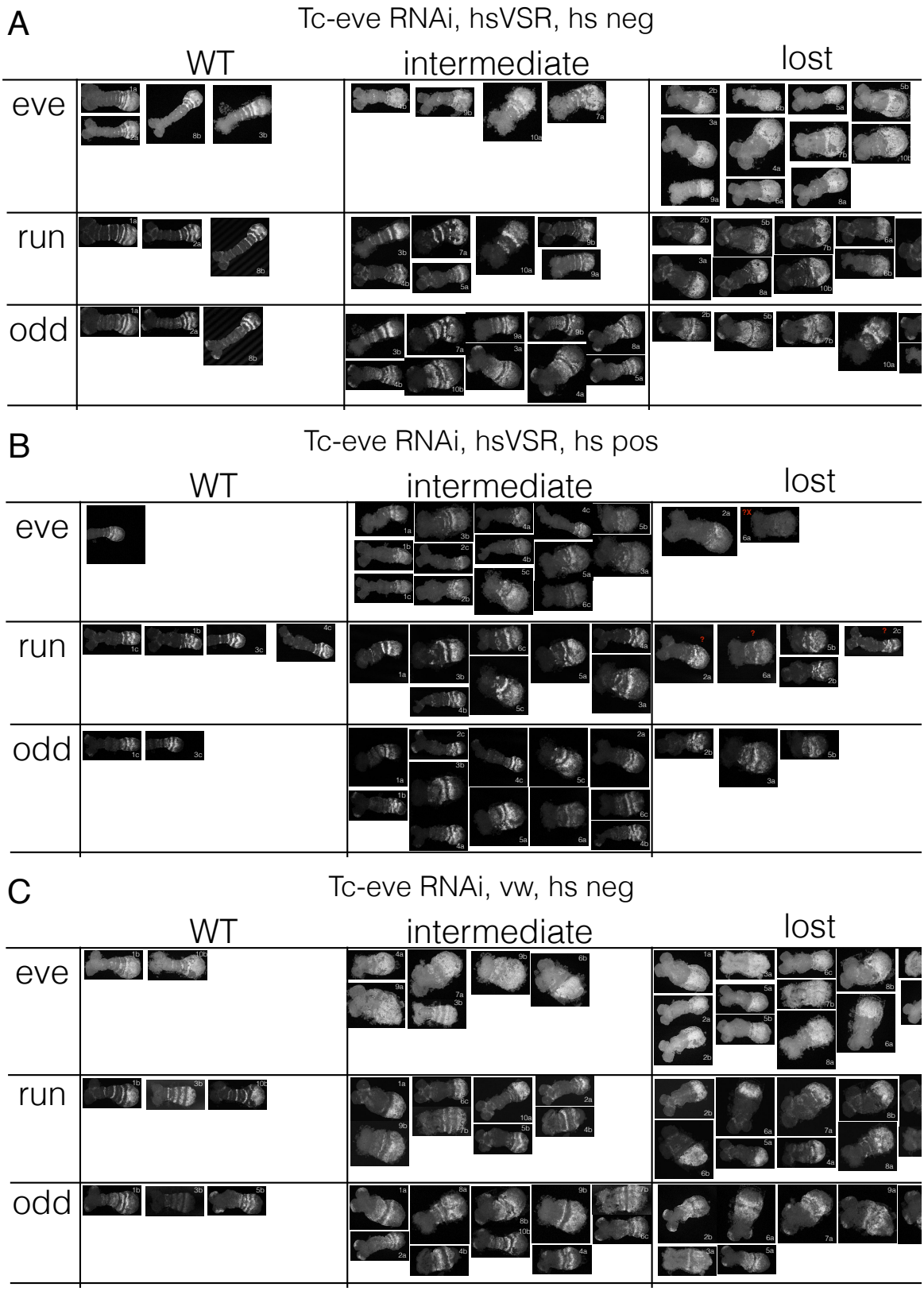
A
Tc-eve RNAi, hsVSR, hs neg
WT
intermediate
lost
eve
run
odd
B
Tc-eve RNAi, hsVSR, hs pos
WT
intermediate
lost
eve
run
odd
C
Tc-eve RNAi, vw, hs neg
WT
intermediate
lost
eve
run
odd

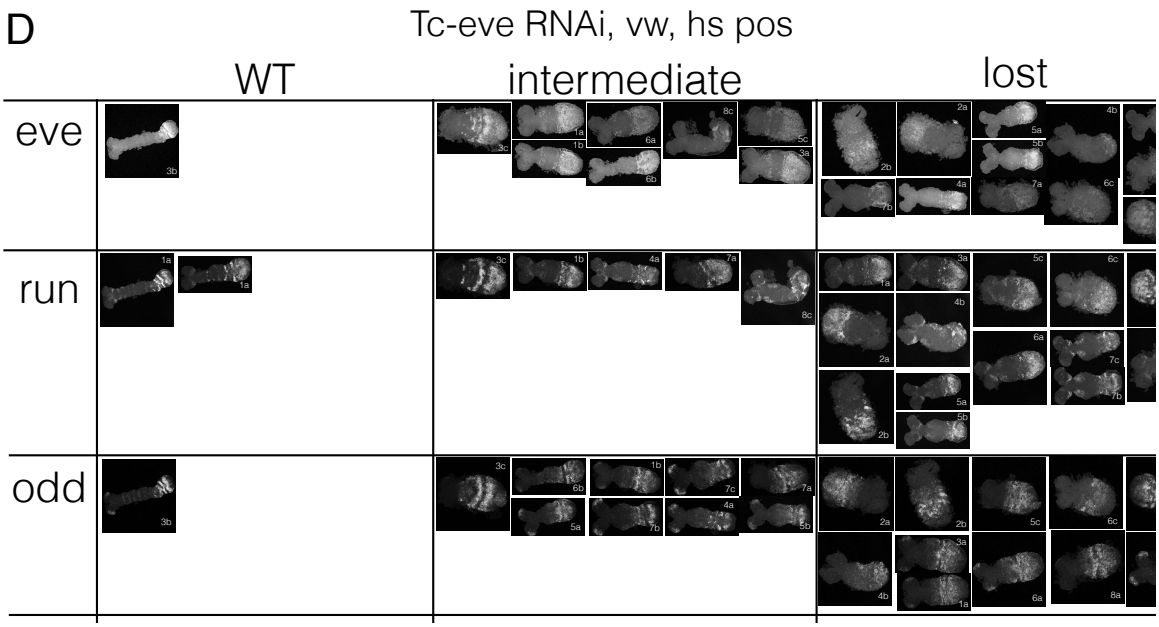

Figure S7.12 – pPRG rescue classes – overview

Images of all documented germbands used for the pPRG stripe and HCR rescue class analyses. Line and hs-treatment status ("hs pos" for heat shocked, "hs neg" for no heat shock) indicated above each panel. For higher quality images, see digital supplementary files.

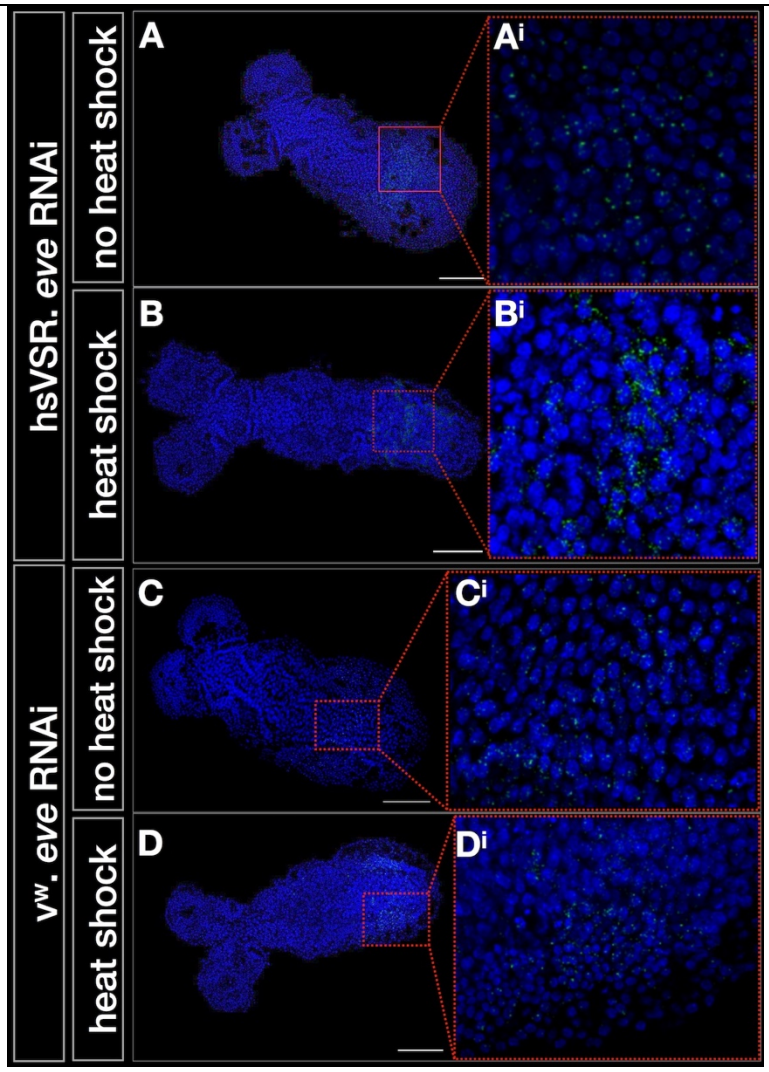

Figure S7.13 - Nuclear signal of Tc-eve transcripts after Tc-eve RNAi

Anterior to the left. Software-based reduction of *Tc-eve* HCR signal revealed a possible nuclear localization of remaining *Tc-eve* transcripts after Tc-eve RNAi. After hs-treatment in the hsVSR line, *Tc-eve* transcripts can be found in the cytoplasm. Scale is 100µm

7.2 Supplementary files

Cuticle analysis and HCR data can be found in Excel file “Cuticles and HCR data.xlsx”. Corresponding Excel file sheet names and figures are indicated in the following table:

Table S7.1 – Supplementary Excel sheet names and corresponding figures

Excel sheet	**Figure**	**Excel sheet**	**Figure**
empty eggs	4.5, 4.6, S7.4	Eve (2018-10)	4.7
Arr (2018-12)	4.5	Prd (2017-09)	S7.1
Arr (2018-04)	S7.2	Prd (2019-10)	4.3
Wnt8d.wls (2018-03)	S7.3	Eve (hsVSR+vw, 2019-07) cuticle	
Wnt8d.wls (2018-12)	4.6	EveRNAi HCR (2019-07) stripe#	4.13, 4.16
Tor (2017-09)	4.4	EveRNAi HCR (2019-07) HCR class	4.17
Odd (2019-10)	4.9	hsVSR, uninj hs_neg + hs_pos	
Odd (2018-06)	S7.9	Eve (hshb x hsVSR, 2019-06)	4.21A and S7.10A
Odd (2016-09)	S7.8	Eve (hshbXhsVSR 2019-10)	4.21B and S7.10B
Run (2018-08)	S7.7	Dev-delay-wg	4.11A
Run (2018-03)	S7.6	Dev_delay_HCR data	4.11B
Runt (2019-12)	4.8		
Eve (2018-07)	S7.5		
Eve (2018-04)	S7.4		

Higher quality images of all HCR data germbands (as shown in Fig. S7.12) are attached (“hcr classes all embryos_high.pdf”, (158MB))